Universidade de Aveiro Departamento de Química
Ano 2011

Tânia Sofia Rodrigues de Melo

ESTUDO DE ALTERAÇÕES EM LÍPIDOS ASSOCIADOS À DOENÇA DE ALZHEIMER.

STUDY OF LIPID ALTERATIONS RELATED WITH ALZHEIMER DISEASE.

Universidade de Aveiro Departamento de Química
Ano 2011

Tânia Sofia Rodrigues de Melo

ESTUDO DE ALTERAÇÕES EM LÍPIDOS ASSOCIADOS À DOENÇA DE ALZHEIMER.

STUDY OF LIPID ALTERATIONS RELATED WITH ALZHEIMER DISEASE.

Dissertação apresentada à Universidade de Aveiro para cumprimento dos requisitos necessários à obtenção do grau de Mestre em Bioquímica, realizada sob a orientação científica da Doutora Maria do Rosário Gonçalves Reis Marques Domingues, Professora Auxiliar do Departamento de Química da Universidade de Aveiro e da Doutora Maria Manuel Silva Oliveira, Professora Auxiliar da Universidade de Trás-os-Montes e Alto Douro.

Apoio financeiro da FCT ao projecto FCT/SAU-NMC/115865/2009, Financiado no âmbito do Programa Operacional Temático Factores de Competitividade (COMPETE) E Comparticipado pelo Fundo Comunitário Europeu (FEDER).

Dedico este trabalho aos meus pais e irmã pelo incansável apoio.

o júri

Presidente

Prof. Doutor Mário Manuel Quialheiro Simões
professor auxiliar do Departamento de Química da Universidade de Aveiro

Prof. Doutor Romeu António Videira
investigador auxiliar da Universidade de Trás-os-Montes e Alto Douro

Prof. Doutora Maria do Rosário Gonçalves Reis Marques Domingues
professora auxiliar do Departamento de Química da Universidade de Aveiro

Prof. Doutora Maria Manuel Silva Oliveira
professora auxiliar da Universidade de Trás-os-Montes e Alto Douro

Agradecimentos

Gostaria de agradecer em primeiro lugar às minhas orientadoras Professora Rosário Domingues e Professora Maria Manuel Oliveira pelos seus ensinamentos, orientação, disponibilidade, incansável ajuda, motivação, confiança depositada, apoio ao longo da realização deste trabalho e acima de tudo por terem acreditado em mim e nas minhas capacidades.

Às minhas colegas de mestrado, e incansáveis companheiras de bancada, pelo incentivo, permanente disponibilidade, ajuda constante no laboratório, e principalmente por todos os bons momentos de convívio e descontracção.

Às meninas de doutoramento pela orientação e ajuda, assim como a todo o grupo de espectrometria de massa que me recebeu da melhor forma, em especial à Cristina Barros pela disponibilidade, ajuda, ensinamentos e principalmente pela sua sempre boa disposição.

A todos os meus amigos e família pela paciência, apoio e por terem acreditado em mim.

Agradeço também o apoio da FCT ao projecto FCT/SAU-NMC/115865/2009, Financiado no âmbito do Programa Operacional Temático Factores de Competitividade (COMPETE) E Comparticipado pelo Fundo Comunitário Europeu (FEDER).

palavras-chave

Fosfolípidos, esfingolípidos, espectrometria de massa, stresse oxidativo, mitocôndria, tacrina.

resumo

A doença de Alzheimer é caracterizada por defeitos na sinalização mediada pela acetilcolina. A tacrina foi anteriormente utilizada como inibidor da acetilcolinesterase (AChE) aprovado para o tratamento da doença de Alzheimer. Contudo, o tratamento com tacrina apresentava alguns efeitos tóxicos associados à disfunção mitocondrial, produção de ROS e peroxidação lipídica. Alterações no metabolismo de esfingolípidos também estão associadas com o desenvolvimento e progressão desta doença.

Neste estudo, a espectrometria de massa foi utilizada para identificar o perfil fosfolipídico das membranas mitocondriais não-sinápticas de cérebro de ratos, antes e após o tratamento com a tacrina, e seus análogos (amostras T1 e T2). Os resultados obtidos com este estudo permitiu-nos perceber que o tratamento com tacrina induz alterações no conteúdo dos fosfolípidos mitocondriais, parece aumentar a susceptibilidade da PS mitocondrial à oxidação, e afecta a bioenergética mitocondrial. O tratamento com os análogos T1 e T2 parece induzir menores alterações nos parâmetros avaliados, quando em comparação com a tacrina. O análogo T1 mostrou ser o mais eficiente na capacidade de inibir a actividade da AchE. Este trabalho contribui para uma melhor compreensão dos efeitos da tacrina na função mitocondrial cerebral, e para a pesquisa de novos análogos da tacrina, com mais eficiência inibitória e com menos efeitos toxicológicos.

Para melhor compreender as alterações de esfingolípidos induzidas por stresse oxidativo, um possível processo subjacente à doença de Alzheimer, estudaram-se as modificações oxidativas específicas de SM (d18:1/16:0), SPC (d18:1) e Cer (d18:1/18:0) induzidas pelo radical hidroxilo gerado sob condições da reacção de Fenton (H_2O_2 e Fe^{2+}), utilizando a espectrometria de massa. Os resultados obtidos com este estudo permitiram-nos identificar, pela primeira vez, vários produtos de oxidação produzidos durante a oxidação da SPC e SM. Este trabalho contribui para uma melhor compreensão do comportamento de alguns esfingolípidos sob condições de stresse oxidativo, fundamental para a sua possível detecção em sistemas biológicos.

keywords

Phospholipids, sphingolipids, mass spectrometry, oxidative stress, mitochondria, tacrine.

abstract

Alzheimer disease is characterized by defects in the signaling mediated by acetylcholine. Tacrine was used as acetylcholinesterase (AChE) inhibitor approved for the treatment of Alzheimer's disease. However, tacrine treatment has some toxicological effects associated with mitochondrial dysfunction, ROS generation and lipid peroxidation. Deregulation in sphingolipid metabolism is also associated with establishment and progression of this disease.

In this study, mass spectrometry was used to identify the membrane phospholipid profile of rats brain non-synaptic mitochondria, before and after treatment with tacrine and its analogues (samples T1 and T2). The results obtained with this study allowed us to understand that treatment with tacrine induces changes in mitochondrial phospholipid content, seems to increase the susceptibility to oxidation of mitochondrial PS, and affects mitochondrial bioenergetics. O tratamento com os análogos T1 e T2 parece induzir menores alterações nos parâmetros avaliados, quando em comparação com a tacrina.

Treatment with T1 and T2 analogues seems to induce less change in evaluated parameters, comparing with tacrine. T1 analogue was shown to be the most efficient of all in its inhibitory capacity for AchE activity.

This work contributes to a better understanding of the effects of tacrine in brain mitochondrial function, and to research of new tacrine analogues with more inhibitory efficiency and with lower toxicological effects.

To better understand the changes in sphingolipid-induced oxidative stress, a possible process underlying Alzheimer's disease, we studied the oxidative modification of specific SM (d18:1/16:0), SPC (d18:1) and Cer (d18:1/18:0) induced by hydroxyl radical generated under conditions of Fenton reaction (H_2O_2 and Fe^{2+}), using mass spectrometry. The results of this study allowed us to identify for the first time, several oxidation products produced during the oxidation of SM and SPC. This work contributes to a better understanding of the behavior of some sphingolipids under conditions of oxidative stress, important for its possible detection in biological systems.

Index

Figure Index

Charpter I

Table Index

Charpter I

Charpter III

Scheme Index

Charpter II

Charpter III

Abbreviations

Aβ - β-amyloid peptide

Ach - Acetylcholine

AChE - Acetylcholinesterase

AD - Alzheimer Disease

ADP - Adenosine Diphosphate

ApoE - Apolipoprotein E

APP - Amyloid Precursor Protein

ATP - Adenosine Triphosphate

BChE - Butyrylcholinesterase

Cer - Ceramide

ChEs - Cholinesterases

CL - Cardiolipin

Complex I - NADH-quinone oxidoreductase

Complex III - Cytochrome bc1 complex

Complex IV - Cytochrome c oxidase

Complex V – ATP synthase

DNA - Deoxyribonucleic Acid

EDTA - Ethylenediaminetetraacetic acid

ETC - Electron Transport Chain

ESI - Electrospray

FT-ICR - Cyclotron Resonance of Fourier /Fourier Transform ion Cyclontron

GSH – Glutathione

HPLC - High Performance Liquid Chromatography

HHE - 4-hydroxy-2-hexanal

HNE - 4-hydroxy-2-nonenal

LC – Liquid Chromatography

LH - Polyunsaturated Lipid

$LOO^{\bullet}$ - lipid peroxyl radical

LOOH - Lipid hydroperoxide

MALDI - Desorption/Ionization Matrix-Assisted Laser

MDA - Malonildialdehyde

MIB - Mitochondria isolation medium

MS - Mass Spectrometry

MS/MS - Tandem Mass Spectrometry

mtDNA – Mitochondrial DNA

m/z - mass/charge

PA – Phosphatidic Acid

PC - Phosphatidylcholine

PE - Phosphatidylethanolamine

PG - Phosphatidylglycerol

PI - Phosphatidylinositol

PS - Phosphatidylserine

Q - Quadrupole

RNA - Ribonucleic Acid

RNS - Reactive Nitrogen Species

$RO^{\bullet}$ - Alcoxil radical

ROS - Reactive Oxygen Species

SM - Sphingomyelin

SPs – Sphingolipids

SPC -Sphingosylphosphorylcholine

SOD - Superoxide Dismutase

THA - Tetrahydroaminoacridine

TLC - Thin Layer Chromatography

TOF - Time-of-flight

Tris - 2-Amino-2-hydroxymethyl-propane-1,3-diol

UV - Ultra-violet

2D - Two-dimensional

CHAPTER I

Introduction

Introduction

Alzheimer disease is a progressive neurodegenerative disorder characterized by dementia, cognitive impairment, memory loss [1,2], and defects in the signaling mediated by acetylcholine [3,4]. Tacrine was used as acetylcholinesterase (AChE) inhibitor approved for the treatment of Alzheimer's disease. However, several evidences suggest that Tacrine have toxicological effects, namely neuro [5] and hepatotoxic effects [6,7], and is associated with mitochondrial dysfunction [8,9], ROS generation and lipid peroxidation [10]. Alzheimer disease has been also associated with sphingolipid metabolism deregulation [11].

Phospholipids and sphingolipids are important structural components of cellular and subcellular membranes, and thus they are essential in maintaining the integrity and functions of cell. It has been suggested that changes in phospholipid structure namely triggered under oxidative stress conditions have been associated with toxicological effects of some drugs and inflammatory processes.

Oxidative stress occurs due to a change in the redox balance of cells, as a result of increased of ROS and RNS production and/or decreased of antioxidant defenses, leading to cell damage and progressive decrease of physiological functions. It is well known that oxidative stress causes structural and functional damage to cell components such as lipids, proteins, nucleic acids (DNA and RNA) and carbohydrates [12]. These toxic effects have been associated to aging and development of various diseases, including neurodegenerative diseases, diabetes and other diseases related to aging [13].

Mitochondria are the primary site of ROS production as a result of electron transfer process that occurs during oxidative phosphorylation. Brain contains at least two major populations of mitochondria, based on cellular localization [14], which include the synaptic mitochondria, which primarily originate from the synaptic bouton of neurons, and non-synaptic mitochondria, originate from neuronal and glial cell bodies [15]. Mitochondrial membrane phospholipids can influence various functions such as mitochondrial activity of the electron transport chain, properties of membrane fluidity and permeability, and ATP synthesis [15].

1. Alzheimer Disease and Tacrine treatment

Neurodegenerative diseases include a group of diseases in which occurs destruction of brain cells, including neurons, which is a natural process, but in this case, this occurs at a faster pace and causes the malfunction of brain. When it happens, depending on the disease, there is a loss of motor functions, physiological and/or cognitive ability. Examples of neurodegenerative diseases are Parkinson's disease, multiple sclerosis, Alzheimer's disease, among others. The pathophysiology of neurodegenerative diseases is multi-factorial, encompassing processes such as oxidative stress, mitochondrial alterations, protein aggregation, endosomal stress, inflammation, among others.

1.1 Alzheimer Disease

Alzheimer's disease (AD), was first described by Alois Alzheimer in 1906, and is a progressive neurodegenerative disorder characterized by dementia, progressive, selective and irreversible loss of specific populations of neurons which affects the regions that control memory and cognitive functions [1,2], such as the hippocampus, amygdala and cortical regions, resulting in the reduction of its functions. Brain regions involved in this process are reduced in size due to loss of neurons and synapses. During normal aging process, a decrease in brain weight, which is accelerated over the years, changes in neurons number, and a significant reduction in brain cells volume are also observed, but never to the extreme seen in neurodegenerative diseases. Alzheimer's disease is generally classified into two groups: Alzheimer's disease with early onset (occurring before 65 years of age), which represents between 5-10% of cases of Alzheimer's disease and late-onset Alzheimer's (occurring after 65 years of age), which represents about 90-95% of cases. Age is therefore considered a dominant risk factor in development and progression of AD, largely as a direct consequence of increased life expectancy. The progressive nature of neurodegenerative process suggests an age-dependent process, which culminates with synaptic failure and neuronal damage in brain regions critical to memory and mental functions, as a result of an increase in oxidative, metabolic and inflammatory processes. The aging process is associated with an increased production of ROS and formation of radicals in mitochondria during energy metabolism, especially in

the central nervous system due to its high oxygen demand and high metabolic rate; a concomitant decrease in antioxidant defense ability, and consequent increase in oxidative processes affecting lipids, proteins and nucleic acids. Hence, there is a progressive loss in body's ability to combat environmental and physiological stress, and for repairing the cellular constituents successively, several oxidative changes occurs which increase the susceptibility of individuals to develop this disease.

Genetic factors are also considered high risk factors; however, its implications needs be better understood. To date only four genes have been implicated in the pathophysiology of AD, in spite of other genes can be associated with this disease. Nevertheless it represents only a small percentage of cases, early onset Alzheimer's disease is considered the most severe form of the disease, being the majority of cases caused by mutations in one of these three genes: amyloid precursor protein (APP) gene located in chromosome 21, and presenilin 1 and presenilin 2 genes located on chromosomes 14 and 1, respectively. Late onset Alzheimer's disease represents the majority of cases of AD, which have very complex patterns, and the apolipoprotein E (ApoE) gene on chromosome 19 is the only one consistently associated with disease, because a common polymorphism in this gene (e4) confers an increased risk of AD.

Physiological changes thought to play significant roles in the pathology of AD are degeneration and neuronal death in brain regions involving memory and learning; and include changes in redox status and oxidative stress; mitochondrial dysfunction and consequent decrease of ATP production and increased excitotoxicity mediated by calcium (Ca^{2+}); presence of pathologic markers associated with this disease: accumulation of extracellular senile plaques, mostly formed by β-amyloid peptide deposits, and formation of intracellular neurofibrillary tangles formed by hyperphosphorylated tau protein aggregation [16]; dysfunction and loss of synapses; neurotransmission failures; defects in the cholinergic system, such as defects in the signaling mediated by acetylcholine [3,4].

Since changes in signaling mediated by neurotransmitters has been considered as one of the processes involved in AD development, current therapeutic approaches used in AD treatment focuses on increasing cholinergic neurotransmission in brain through the use

of drugs that act as inhibitors of cholinesterase (ChEs) activity. One of these drugs is tacrine.

1.2 Tacrine

Tacrine or 1,2,3,4-tetrahydroacridin-9-amine (THA, also known as Cognex®) (figure 1) was the first drug approved for the treatment of Alzheimer Disease [17]. Tacrine is a centrally acting reversible cholinesterase inhibitor, which blocks the degradation of acetylcholine in the neurons of cerebral cortex by suppression AChE and BChE [18] and thereby increasing cholinergic transmission [19]. However, this drug is no longer used due of severe side effects [20]. Prolonged use of tacrine has proven to be hepatotoxic [6,7] with liver cell necrosis [17] and to induce mitochondrial dysfunction [8,9]. Tacrine accumulation within mitochondria induces severe mtDNA depletion, enhances p53, and induces mitochondrial permeability transition and Bax protein leading to cell apoptosis, after several weeks of treatment [17]. Oxidative stress and lipid peroxidation, evidenced by enhanced ROS production and glutathione (GSH) depletion [10,17] are supposed to increase during tacrine treatment, and being associated with it toxic effects.

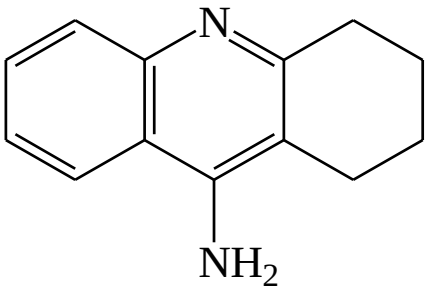

Figure 1. Chemical structure of tacrine (1,2,3,4-tetrahydroacridin-9-amine).

Although side effects of tacrine treatment, the search for tacrine analogues is still of interest. Modifications on the tacrine structure have been performed, either by increasing the number of rings or changing their size or introducing heteroatoms [21].

Recently Campos and collaborators have proposed new tacrine analogues [21], and two of them were studied and analyzed in this work (figure 2).

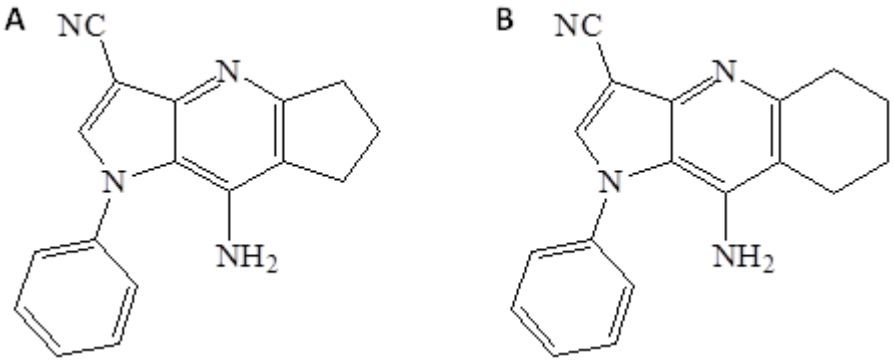

Figure 2. Chemical structure of tacrine analogues; (A) T1, 8-Amino-1,5,6,7-tetrahydro-1 phenylcyclopenta[e]pyrrolo[3,2-b]pyridine-3-carbonitrile; (B) T2, 9-Amino-5,6,7,8-tetrahydro-1-phenyl-1H-pyrrolo[3,2-b]quinoline-3-carbonitrile.

1.3 Tacrine and Phospholipids

Tacrine possesses a hydrophobic aromatic ring system, together with a short side chain containing a protonating amino group (figure 1), characteristic of a large number of drugs [22], which could binds to phospholipids and in membrane, probably, interacts with their negatively charged phosphate group, whereas the aromatic moiety resides either in the interfacial region, because tacrine is an amphipathic molecule, or deeper within the membrane [22]. In fact, Lehtonen and co-authors (1996) demonstrates that tacrine preferential binds by electrostatic interaction to acidic phospholipid-containing membranes and located in the interfacial region of the lipid bilayer, may be followed by penetration of the drug into the bilayer [22].

Considering the essential role of mitochondria in cell function, particularly in energy production, and also in the generation of free radicals during oxidative phosphorylation, is particularly important to explore and study the mitochondrial changes and its constituents, including lipid after tacrine treatment in order to understand their side effects.

2. Mitochondria, Oxidative Stress and Lipid Peroxidation

2.1 Mitochondrial Dysfunction

Mitochondria are involved in a number of cellular functions and are key components in the development, aging and cell death. The many functions of mitochondria include the production of cellular ATP, participation in the synthesis of key metabolites, cellular health monitor for intervening in the initiation and regulation of cell death by apoptosis, calcium buffering and homeostasis, and the primary source of endogenous reactive oxygen species [23], as well as in cell signaling, degradation of neurotransmitters, detoxification of aldehydes, nucleotide transport, mitochondrial protein import, among others.

The intracellular distribution of mitochondria is essential for cell physiology, so mitochondria are localized in subcellular regions with high metabolic needs [23,24]. Brain cells have high metabolic needs since they are highly differentiated cells which require large amounts of ATP for its normal function and neurotransmission. Since the neuronal ATP is produced by oxidative metabolism, neurons are highly dependent on the mitochondrial function and energy providing to various activities. In neurons, mitochondria are involved in synaptic transmission, Ca^{2+} homeostasis regulation, axonal/dendritic transport, ion channels and ion pump activity, maintenance of membrane potential, release or uptake of neurotransmitters [23,25]. Neurons are particularly sensitive to changes in mitochondrial function since they are extremely energy dependent with many neuronal activities [23]. Not surprisingly, mitochondrial injury can have severe consequences for neuronal function and survival. Mitochondrial dysfunction and the resulting energy deficit triggers the onset of neuronal degeneration and death, which is observed in brains with AD [26,27].

Changes in mitochondrial function, namely in electron transport chain, are associated with a decreased rate of production of ATP (adenosine triphosphate), an increase of ROS levels and consequent increase in cellular oxidative stress, altered homeostasis and Ca^{2+} influx, with consequent excitotoxicity [28], since mitochondria serves as Ca^{2+} high-capacity compartment, but over-abstraction and increased Ca^{2+} in mitochondria has been associated with an increased ROS production, inhibition of ATP synthesis, induction of

permeability transition, cytochrome c release [26], mitochondrial membrane depolarization and apoptosis [29].

Mitochondrial dysfunction has been linked to AD [30], because once the mitochondrial oxidative phosphorylation is the major source of ROS, there may be an intrinsic link between the mitochondrial alterations in neurodegenerative diseases and the involvement of oxidative stress. In fact, evidences indicate that mitochondrial abnormalities and oxidative damage are early events in AD [31], and oxidative stress originating in mitochondria is a primary event associated with neurodegeneration. Increased neuronal oxidative stress may result from mitochondrial dysfunction, or may lead to this phenomenon. However, it is often difficult to distinguish whether the mitochondrial defects are a primary cause of toxicity or instead reflect secondary collateral damage, or is likely to have a contribution from both. In both cases, this increased oxidative can exacerbate mitochondrial dysfunction.

Since increase of ROS and oxidation has been associated with side effects of tacrine and their new chemically analogues, is particularly important to explore and study functional and structural changes in mitochondrial phospholipids that may occur due tacrine treatment, considering that phospholipids are one the main target of ROS.

2.2 Oxidative Stress

Oxidative stress has been currently defined as a change in the redox balance of cells, as a result of increased production ROS and RNS and/or decreased of antioxidant defenses. However, oxidative stress may be better defined as a disruption of redox signaling, rather than as an imbalance of pro-oxidants and antioxidants [32], which leads to an excess of free radicals in the body and, consequently, cellular damage and gradual reduction of physiological functions occurs.

ROS, key players in the process of oxidative stress, can be divided into radical species (as superoxide anion and hydroxyl radical) and non-radical species (as hydrogen peroxide), and are produced by a series of cellular oxidative metabolic processes, the most important being oxidative phosphorylation of mitochondrial respiratory chain [33]. Mitochondria is the major site of ROS production because the pumping of protons (H^+)

across the membrane during oxidative phosphorylation leads to accumulation of electrons, which when in excess can be transferred directly to oxygen (especially complexes I and III), forming superoxide anion radical ($O_2^{\bullet-}$) which is more polar than oxygen and cannot easily cross through membranes by simple diffusion, hence not a particularly reactive molecule. Its deleterious effects are related to its ability to generate secondary species; $O_2^{\bullet-}$ can be reduced to hydroxyl radical ($^{\bullet}OH$) or undergo spontaneous or catalytic dismutation by superoxide dismutase (SOD) to form hydrogen peroxide (H_2O_2), which has the ability to cross lipid membranes by diffusion because it is soluble and relatively nonpolar, acting in regions far from their places of synthesis, making this molecule relatively dangerous and toxic to the cells. $O_2^{\bullet-}$ can also react with nitric oxide to form peroxynitrite ($ONOO^-$), which is a powerful oxidizing agent [34]. However, transition metals may also be sources of oxidant species [12]. In fact, H_2O_2 can be converted to $^{\bullet}OH$ via the Fenton reaction, which occurs through the reaction of iron ions (Fe^{2+}) and H_2O_2, with the consequent production of $^{\bullet}OH$ (equation 1), which is the most reactive oxygen species generated in living systems, being responsible for the oxidation of biomolecules, including lipids.

$$Fe^{2+} + H_2O_2 \longrightarrow Fe^{3+} + {}^{\bullet}OH + OH^- \text{ (equation 1)}$$

$O_2^{\bullet-}$ can also react with H_2O_2 in the presence of metals such as Cu^{2+} and Fe^{2+}, featuring the call of Haber-Weiss reaction, which also culminates in the formation of $^{\bullet}OH$ (equation. 2).

$$H_2O_2 + O_2^{\bullet-} \xrightarrow{Fe2+} O_2 + {}^{\bullet}OH + OH^- \text{ (equation 2)}$$

Despite being a relatively small body mass, brain needs high oxygen consumption due to their high need for ATP, thus increasing mitochondrial activity and thus the production of a relatively high level of ROS. Increased neuronal oxidative stress resulting from excessive production of ROS causes damage to neuronal membranes as lipid peroxidation and protein oxidation. The central nervous system is particularly susceptible to oxidative damage because it has a high energy requirement, high consumption of oxygen, a deficit in antioxidant defenses compared with other organs, high concentrations of lipids rich in polyunsaturated fatty acids [35], particularly arachidonic acid (20:4) and docosahexaenoic

acid (22:6), which are the main targets of oxidation [36], and high content of transition metals that can act as potent pro-oxidants [35]. Given these characteristics, it is expected that the oxidative damage in brain manifests predominantly in the form of lipid peroxidation, as described by Praticò (2002) [37] as result of physiopathological processes or due treatment with drugs.

2.3 Lipid Peroxidation

Oxidative stress causes changes in a diversity of native phospholipids found in living species which results in a vast number of structurally different oxidation products, which may have different biological activities that depends not only on the location, but also on the nature of the changes. Oxidized phospholipids are the result of a series of radical catalyzed chemical reactions and their presence in biological membranes induces changes in physical properties such as fluidity and acyl packing, which can have an impact on the integrity of the membrane, causing apoptotic events [35].

Lipid peroxidation has been defined as the cascade of biochemical events that include a cyclic series of reactions, with different phases (initiation, propagation and termination cyclic), resulting from the action of ROS on lipid membrane.

It is known that is initiated by the attack of reactive chemical species such as $^{\bullet}OH$, capable of abstracting a hydrogen atom from a reactive methyl group of a polyunsaturated lipid (LH), with the formation of lipid alkyl radical ($L^{\bullet}$), which was the key factor for the onset of lipid peroxidation. The presence of a double bond in the fatty acid weakens the C–H bonds on the carbon atom nearby to the double bond and thus facilitates the hydrogen abstracting. The lipid alkyl radical ($L^{\bullet}$) resulting from the initiation reacts with oxygen to form a lipid peroxyl radical ($LOO^{\bullet}$) which can abstract a hydrogen atom from adjacent polyunsaturated fatty acid in membrane to produce a lipid hydroperoxide (LOOH) and a second lipid radical [39]. The resulting peroxide may be cleaved, by reduced metals, such as Fe^{2+}, producing alkoxyl ($RO^{\bullet}$) or epoxiperoxil ($OROO^{\bullet}$) radicals, and both stimulate the chain reaction of lipid peroxidation by abstracting additional hydrogen atoms. Therefore, the formation of lipid peroxyl radical initiates the called “lipid peroxidation chain”, which has as main product the lipid hydroperoxide

(LOOH) [36]. It should be emphasized that the chain propagation is carried by lipid peroxyl radicals independent of the type of chain-initiating free radicals. The sequence of reactions shown in Figure 3 illustrates the phenomenon.

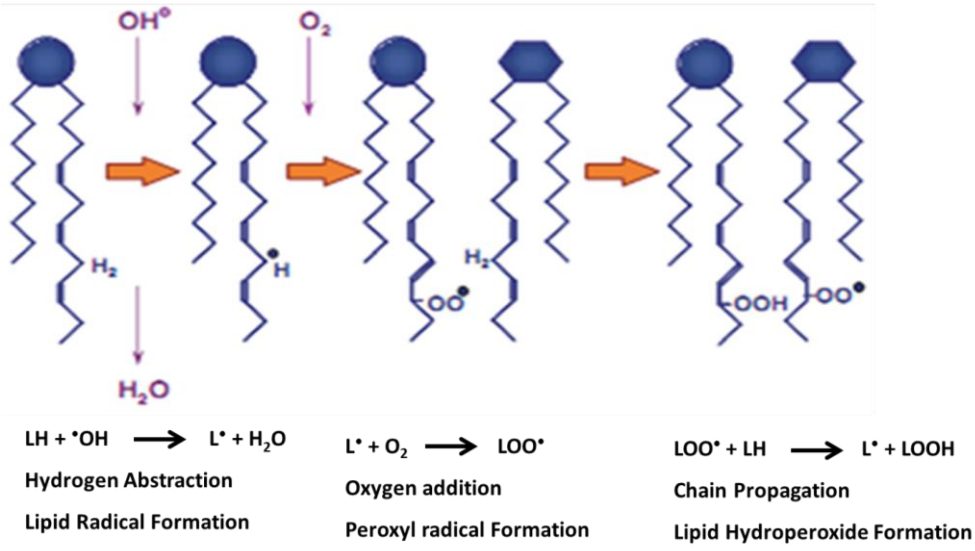

Figure 3. Steps of membrane lipid peroxidation [53].

It became evident recently that lipid peroxidation as well as ROS/RNS exert various biological functions in vivo such as regulators of gene expression, signaling messengers, activators of receptors and nuclear transcription factors, and inducers of adaptive responses [40]. Lipid oxidation products also change the properties of biological membranes, because their polarity and shape may differ significantly from the structures of their parent molecules. Thus, lipid peroxidation is associated with disruption of hydrophobic interactions in biological membranes leading to loss of structural and functional characteristics, such as lipid-lipid and lipid-protein interactions, selective permeability, phospholipid asymmetry, decreased fluidity and membrane potential and increased permeability [36,40,41] leading to cell death. Injure to mitochondria induced by lipid peroxidation can direct to further ROS generation [40] and be associated with mitochondrial dysfunction.

Taking this into account, will be of high importance to research early (oxidative) changes in cellular and subcellular biomolecules, namely in lipids.

3. Lipids

Lipids can be defined based on their solubility in organic solvents or by presence of long hydrocarbon chains. Thus lipids comprise a vast number of chemical molecules, structurally and functionally distinct, resulting from combinations of fatty acids with different structures. Species can be nonpolar (sterols), neutral (triacylglycerides) and polar (phospholipids) [42].

Cellular lipids form a membrane bilayer and are therefore essential for their structural integrity and functionality; allow protein trafficking and anchoring to the membrane; provide an appropriate hydrophobic environment for membrane proteins function and interactions; serve as storage of energy, which can be rapidly and easily accessed; membrane lipids are involved in intra and intercellular signaling since a variety of bioactive lipids can be produce by enzymatic reactions [43].

Currently, based on their chemical structure and biosynthesis, lipids are classified into eight categories - fatty acids, glycerolipids, glycerophospholipids, sphingolipids, sterol lipids, prenol lipids, saccharolipids and polyketides - which contain different classes and subclasses of molecules [42,56]. In most mammalian cells, phospholipids represent approximately 60% of total lipids, the sphingolipids comprise roughly 10% of total fat and the remaining percentage corresponds to the non-polar lipids.

Fatty acids are the most simple and one of the most important lipid classes. Structurally, the natural fatty acids have a saturated or unsaturated hydrocarbon chain with 14 to 24 carbon atoms and 0 to 6 double bounds. The difference of polyunsaturated fatty acids of less unsaturated, is the presence of repeated units $=CH\text{-}CH_2\text{-}CH=$, which defines its significantly role in the membrane, producing a highly flexible structure [44,53]. Functionally, they are precursors of a variety of bioactive lipid molecules [42]. The glycerolipids include monoacylglycerides, diacylglycerides and triacylglycerides, which are very important in cell energy storage and as mediators in metabolic processes and disease. Sterol lipids which include cholesterol are important components of lipid membrane and are involved in signaling regulation and cellular fluidity modulation [45].

3.1 Phospholipids

Phospholipids are the major building blocks of biological membranes, where they play an important structural role as part of the lipid bilayer, modulate membrane trafficking, are indispensable as precursors for various regulators of intra-and extracellular metabolism and the function of organelles. Metabolites derived from their degradation are important intracellular signaling molecules involved in processes such as proliferation and apoptosis [46]. They are therefore involved in the regulation and control of cellular functions in health and disease. There are two major groups of phospholipids: glycerophospholipids and the sphingolipids.

Glycerophospholipids are the major components of biological membranes, and have inherent biological activities by acting as second messengers themselves or as precursors for the generation of second messengers. Glycerophospholipids consist of a glycerol backbone to which are attached two fatty acid chains at *sn*-1 and *sn*-2 by ester linkages, and at least one phosphate group at position *sn*-3. The phosphate group can bind to a polar molecule by phosphodiester bonds [47], forming the so-called polar head group of phospholipids [48]. They are amphipathic molecules, i.e., the head comprising the phosphate group is polar or hydrophilic and the tail formed by chains of fatty acids is nonpolar or hydrophobic. Phospholipids contain a high number of species with different polar head groups, different linkages at *sn*-1 positions and different combinations of fatty acyl chains in the *sn*-1 and *sn*-2 which may also vary in length and degree of unsaturation, making them high complex molecules.

Seven classes of glycerophospholipids are commonly recognized based in the chemical structure of head group that are linked to the phosphate: phosphatidic acid (PA), phosphatidylcholines (PC), phosphatidylethanolamine (PE), phosphatidylserine (PS), phosphatidylglycerol (PG), phosphatidylnositol (PI). Figure 4 represents the general structure of glycerophospholipids.

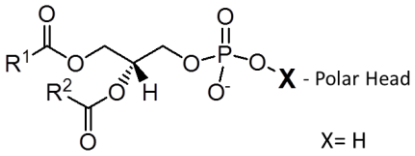

X= H (**PA**) X= $CH_2CH(COO^-)NH_3^+$ (**PS**)
X= $CH_2CH_2N^+(CH_3)_3$ (**PC**) X= $CH_2CHOHCH_2OH$ (**PG**)
X= $CH_2CH_2NH_3^+$ (**PE**) X= $C_6H_{12}O_6$ (**PI**)

Figure 4. General structure of glycerophospholipids. R^1 and R^2 represent the fatty acyl chains esterified to glycerol backbone [53]. PA – Phosphatidic acid, PC – Phosphatidylcholine, PE – Phosphatidylethanolamine, PS – Phosphatidylserine, PG – Phosphatidylglycerol, PI – Phosphatidylinositol.

Due to the different chemical bonds of the aliphatic chains at the *sn*-1 position of glycerol backbone in phospholipids, each class is further divided into three subclasses, i.e., phosphatidyl, plasmenyl and plasmanyl (figure 5), corresponding to the ester, vinyl ether, and alkyl ether linkages, respectively [43]. In mammalians, ether linkages occur predominantly in PCs and PEs. Plasmanyl species typically exist as PC species, whereas plasmenyl species mainly exist as PE species with the exception of the heart where plasmenyl PC species predominate. The main significance of ether species relate to the production of platelet activating factor (1-alkyl-2-acetyl-PC) and its concomitant implication in blood coagulation and inflammatory responses. In most cellular membrane lipids, the phosphatidyl subclass of phospholipids is predominant; however in electroactive cellular membrane such as neuronal cells, plasmenyl subclasses are major components of phospholipids [43].

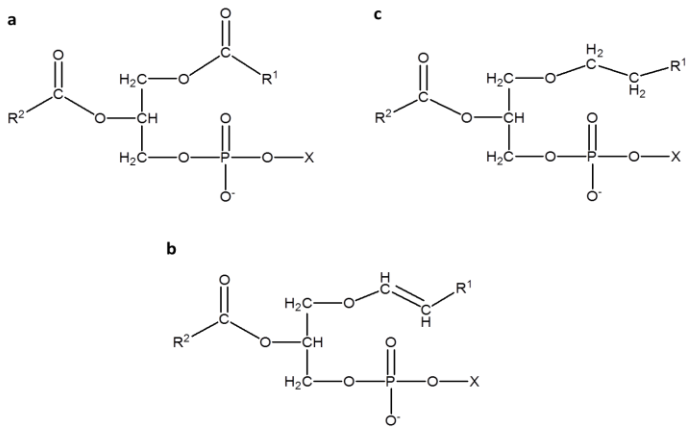

Figure 5. Glycerophospholipids subclasses based on the linkage of aliphatic chain at the *sn*-1 position of glycerol backbone; (a) phosphatidyl, (b) plasmenyl and (c) plasmanyl. R^1 and R^2 represent the fatty acyl chains esterified to glycerol backbone [53] and X represents the head group.

Lysospecies exist having only one fatty acyl or fatty alcohol moiety attached to the glycerol phosphate backbone. Lysospecies occur as intermediates in glycerophospholipid biosynthesis, and act as second messengers.

Cardiolipin (CL, 1,3-bis(*sn*-3-phosphatidyl)-*sn*-glycerol) is a dimeric phospholipid containing two phosphatidic acids linked by a central glycerol group that holds two more molecules of glycerol in its structure, and has four fatty acyl chains. The relationship between the three glycerol molecules creates a unique environment for each ester linkage [49]. The fact that the headgroup alcohol is shared by two phosphate moieties is a feature with important implications regarding the overall physical properties of CL within the context of a lipid bilayer, namely in their mobility and conformational flexibility [50]. Figure 6 represents the general structure of cardiolipin.

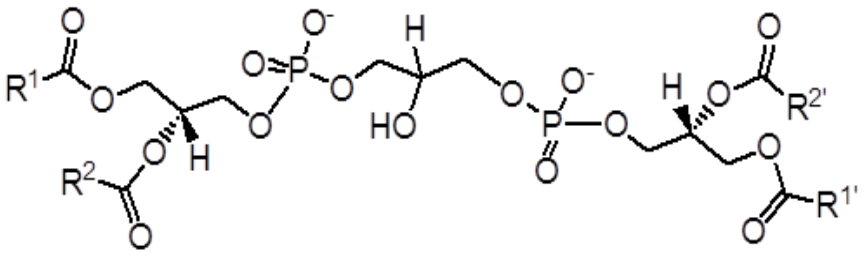

Figure 6. Structure of cardiolipin. R^1, R^2, $R^{1'}$ and $R^{2'}$represent the fatty acyl chains esterified to glycerol backbone.

Sphingolipids (SPs) are amphipatic lipids which share a common structural feature: a sphingosine backbone as the main chain (Figure 7). SPs are known bioactive compounds playing important roles in diverse cellular processes, as proliferation, differentiation, signaling, apoptosis, inflammation [51,52], biological recognition, cell growth, membrane organization, among others, in addition to its role in membrane structure. They are classified into different classes, such as ceramide (Cer), which contain a fatty acid linked via an amide bond to sphingosine backbone (Figure 7); sphingomyelins (SM) which contain an amide linked fatty acid, as well as a polar head group (phosphocholine) attached to the *sn*-1 hydroxyl group in the sphingosine backbone; sphingosylphosphorylcholine, a lyso sphimgomyelin which has a phosphocholine polar head attached to the *sn*-1 hydroxyl group in the sphingosine backbone but don't have any

fatty acyl chain; cerebroside and other glycosphingolipids (gangliosides, sulfatide, among others) based on a polar head group linked to the *sn*-1 position of sphingosine [43]. Phosphorylation of sphingosine or ceramide results in sphingosine-1-phosphate and ceramide-1-phosphate, respectively.

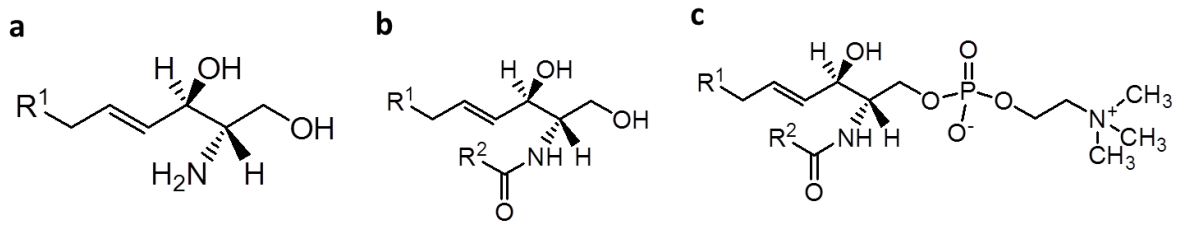

Figure 7. General structure of sphingosine (a), ceramide (b) and sphingomyelin (c). R^1 represents the sphingosine backbone; R^2 represents the fatty acyl chain esterified to sphingosine backbone.

3.2 Lipids and Brain

Lipids, particularly phospholipids, are fundamental to the architecture and function of the central nervous system, being essential as structural components, and this is evident based on lipid content and dry weight of nerve tissue, with a high concentration of lipids, similar to adipose tissue [53,54].

Nerve tissue contains a variety of lipids including neutral lipids such as cholesterol, glycolipids such as galactosylceramide and gangliosides, and phospholipids such as PC, PE, PS, several species of CL, sphingolipids, among others. The glycerophospholipids are important in the structure and functioning of the brain membranes and sphingolipids are important in many cellular processes including differentiation, proliferation and apoptosis, in the nervous system [55].

Main of fatty acids esterified to glycerol in brain phospholipids [56,57] are presented in Table 1. These fatty acids have varying degrees of unsaturation, and brain polyunsaturated fatty acids are present in higher percentage.

Neuronal membranes are highly specialized on the reception, processing and transmission of information, functions that are dependent on the balance between the amounts of membrane phospholipids, neutral lipids and glycolipids. However, the composition and lipid metabolism both change with brain development and anatomic

region [53] and cellular and subcellular localization. In addition, differences in phospholipid classes, diversity within each class and susceptibility to oxidation must be considered. The homeostasis of membrane lipids, especially those of mitochondrial membrane in neurons, and myelin, are essential to prevent the loss of synaptic plasticity, cell death and neurodegeneration [55].

Table 1. Fatty acyl chains more common in brain phospholipids and its nomenclature.

12:0	Dodecanoic	Lauroyl	Saturated	Non-oxidizable
14:0	Tetradecanoic	Myiristoyl	Saturated	Non-oxidizable
16:0	Hexadecanoic	Palmitoyl	Saturated	Non-oxidizable
18:0	Octadecanoic	Stearoyl	Saturated	Non-oxidizable
18:1 (n-9)	9-Octadecanoic	Oleoyl	Monounsaturated	Non-oxidizable
18:2 (n-6)	9,12-Octadecadienoic	Linoleoyl	Polyunsaturated	Oxidizable
20:4 (n-6)	5,8,11,14-Eicosatetraenoic	Arachidonoyl	Polyunsaturated	Oxidizable
22:5	7,10,13,16,19-Docosapentaenoic	Docosapentaenoyl	Polyunsaturated	Oxidizable
22:6 (n-3)	4, 7,10,13,16,19-Docosahexenoic	Docosahexaenoyl	Polyunsaturated	Oxidizable

Fatty acyl is designated as 18:1, where 18 indicates the summed number of carbon atoms and 1 designates the number of double bonds at both positions.

3.3 Mitochondrial Membrane Phospholipids

Brain contains at least two major populations of mitochondria, based on cellular localization [14], which include the non-synaptic mitochondria, originate from neuronal and glial cell bodies, and the synaptic mitochondria, originate from the synaptic bouton of neurons [15].

The mitochondrial membrane phospholipids, which include PC, PE, PI, PS, PA, PG and CL, can influence various functions such as mitochondrial activity of the electron transport chain (Electron Transport Chain, ETC), the transport of nucleotides, the mitochondrial protein import, the properties of membrane fluidity and permeability and ATP synthesis [15, 58].

Phosphatidylcholine and phosphatidylethanolamine are the most abundant phospholipid in membrane cells [59] and higher proportions are found in mitochondria, where they are obviously a key building block of membrane bilayers. Phosphatidylinositol plays an important role as a key membrane constituent and appear to have crucial roles

in interfacial binding of proteins, regulation of proteins at the cell interface, cell growth and differentiation, motility, calcium mobilization and oncogenesis [60,61] as a participant in essential metabolic processes as cellular signaling, both directly and via a number of metabolites. Phosphatidylserine are present in low abundance in mitochondria, but may enhance mitochondrial function because they are precursors to mitochondrial phosphatidylethanolamine. Phosphatidic acid has the simplest polar head group, and serves as a precursor and metabolite in the biosynthetic and catabolism pathways of phospholipids [60]. Phosphatidylglycerol is synthesized only in mitochondria of non-photosynthetic eukaryotes, where it is used as the precursor for cardiolipin [60].

Cardiolipin is a specific inner mitochondrial membrane phospholipid, which is responsible for about 25% of all mitochondrial lipids [62]. In the brain, CL containing long unsaturated fatty acid chains like arachidonic (20:4), docosatetraenoic (22:4) and docosahexaenoic (22:6) [63], which are highly susceptible to oxidative damage [62,63] by ROS [62], beside its close association with ECT, in the inner mitochondrial membrane, which are known to be a major source of ROS in mitochondria [64]. CL are very susceptible to oxidative damage [63,64] being suggested as the preferred substrate to undergo oxidation in neuronal diseases [38,63].

CL has been proposed to play a central role in mitochondrial function, energy metabolism and apoptosis since as an integral part of the inner mitochondrial membrane where is essential for maintenance of membrane fluidity and osmotic stability [64] and is associated with many mitochondrial proteins, namely respiratory complexes I, III, IV, V, and ADP-ATP carrier [65]. CL contribute to association of complexes III and IV, and consequently for development, assembly and stabilization of the mitochondrial respiratory chain supercomplexes [66], improving the efficiency of oxidative phosphorylation, by elimination the need for diffusion of substrates and products between the individual components of the ETC [67]. Besides its role in mitochondrial bioenergetics, CL electrostatically anchors cytochrome c to the inner mitochondrial membrane [68] and can therefore play an important regulatory role in the release of cytochrome c, which triggers the events of apoptosis being a key role in programmed cell death [69]. Decrease in mitochondrial CL content [62,64,70] or alteration in CL structure,

namely due to an increase in CL peroxidation [62,64,71] or changes in fatty acyl profile [64], have been associated with mitochondrial dysfunction [64], namely ECT dysfunction and release of cytochrome c from mitochondria. Since oxidized CL has a considerable lower affinity for cytochrome c [70] and subsequent tissue degeneration [62] and cell death, and several pathological conditions, particularly neurodegenerative diseases such as AD since CL an is important component of mitochondrial membrane.

3.4 Lipids and Alzheimer Disease

These essential roles of lipids are evidenced by the specific brain lipid disorders that are associated with multiple neuronal diseases, and changes in brain lipid levels due to increased or decreased synthesis, or altered metabolism may result in their homeostatic deregulation and culminate in neurodegeneration. It has been suggested that sphingolipids loss, changes in the composition of phospholipids and their fatty acids and/or the formation of lipid peroxidation products may lead or accelerate the neurodegeneration and pathogenesis of AD [55].

Loss of neuronal membrane phospholipids and fatty acyl chains has been hypothesized to be an early metabolic event in amyloid plaques and neurofibrillary tangles formation, and synapses and neurons loss, resulting in neurodegeneration [55]. Phospholipids changes in AD include increase in degradation products as lysoPC, gliceroPC and gliceroPE [72] and decrease in PE [73]. ROS are generated under oxidative stress in AD, so phospholipids oxidation of biological membranes is also associated with progression of this disease. AD has been associated with loss of docosohexaenoic and araquidonic acid [74]. Decreases of polyunsaturated fatty acids in neurons are associated with lower fluidity and apoptosis.

Deregulation of sphingolipid metabolism also leads to the establishment and progression of diseases such as neurodegenerative diseases, including Alzheimer [11]. Sphingomyelins are reported to decrease Aβ production [75], while gangliosides seem to increase its production [76]. Evidences demonstrate that ceramide accumulates in many tissues, including in brain, during aging [77], inducing cell dysfunction, ROS production, disruption of the respiratory chain membrane and apoptosis [78,79], leading to

neurodegeneration. Han and colleagues (2002) [80] reported increases in ceramide levels in AD patients.

Since AD is associated to sphingolipid metabolism alterations, and on the other hand to oxidative stress, there are no studies that correlate these two factors. The lack of knowledge in this area leads us to propose as one main goal of this work the study of the behavior and changes that occur in sphingolipids under oxidative stress.

Mass spectrometry has recently been used as the main analytical technique for analysis of lipid/phospholipid oxidation products and also in profile in cells or tissues, an approach that often involves preparative chromatography techniques, generically known as Lipidomic.

4. Lipidomic

Lipidomics can be defined as the systematic and large-scale study of structure, function and interactions of lipids with other lipids, proteins and other molecules in biological samples (biological fluids, tissues, cells, among many others), as well as the study of lipid changes that occur during pathophysiological disturbances [81], in response to different stimuli or situations through the integration of multiple modern technologies as mass spectrometry, being an emerging field of research and rapidly expanding [82]. It is considered a branch belonging to a broader field known as metabolomics, since the lipids are biological metabolites. But is itself a distinct discipline due to the unique and specific functions of lipids in relation to other metabolites.

Lipidomic usually involve several steps, beginning with the extraction of lipids from tissues or cells by methods that exploit the high solubility of the hydrocarbon chains of lipids in organic solvents, and include the method of Bligh and Dyer [83], their separation, usually by chromatography, identification and quantification of each molecular species [84] using phosphorous assay that measures the inorganic phosphate present in the sample, and additional analysis of the lipid profile by mass spectrometry (figure 8). This methodology is also applied in the analysis of lipid peroxidation products that are generated in in vivo conditions, named as oxidative lipidomic.

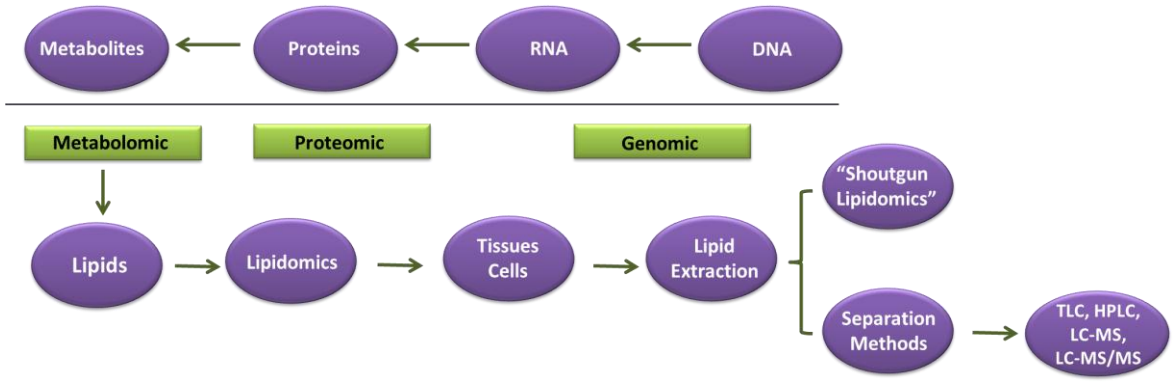

Figure 8. Lipidomics, techniques employed in the analysis of lipids.

4.1 Lipid Extraction

The lipid extraction methods exploit the high lipid solubility of the hydrocarbon chains of lipids in organic solvents, and include the Bligh and Dyer method [83], which will be used during this study, and is based on lipid extraction using a mixture of chloroform/methanol (1:2), getting the lipids in the hydrophobic phase of lower density. Methanol breaks down the lipid-protein bonds and inactivates the lipase, while the chloroform dissolves fat. The success of phase extraction of lipids from cells, tissues or biological fluids is fundamental to the success of subsequent analysis.

4.2 Lipid Separation

Since the lipids obtained from extracts of biological samples include species of different classes, it is necessary their separation, which usually requires a multi-step chromatography to allow identification and quantification of each molecular species [84]. All the systems consist of a chromatographic stationary phase (liquid or solid) and a mobile phase (liquid or gas). The sample components are separated based on their physical and chemical characteristics, and according to the different affinity for the two phases. The separation of lipids from biological samples can be conducted using HPLC (High Performance Liquid Chromatography), that has the advantage of being coupled to MS or by TLC which is nowadays an important technique used for the separation of different classes of phospholipids in biological samples.

4.2.1 Thin Layer Chromatography (TLC)

TLC is used to separate the components of a mixture, but can also be used to quantify, identify and purify components in the mixture.

In TLC, separation of complex mixtures is achieved on a stationary phase due to polarity differences of the analytes with the mobile and stationary phases [85]. Since TLC uses a mobile phase consisting of a liquid (eluent) and a solid stationary phase, is a solid-liquid adsorption technique, in which the solvent molecules compete with the analyte molecules for binding sites on the stationary phase. In lipidomics, TLC has the advantage that it can be used at a preparative scale and allows the separation of different lipid classes from total lipid extracts, and also achieves separation even within the phospholipid classes, in an easy, quick and relatively inexpensive, so it is often used prior to detection by mass spectrometry [86]. This technique has been used for analysis of oxidized phospholipids and is also a useful method to separate headgroup-modified phospholipids [85].

For separation of phospholipids are usually used glass plates which have a stationary phase applied, being the most common coating silica gel (SiO_2). On the surface of silica gel, the oxygen atoms are linked to protons forming hydroxyl groups which make the surface of silica gel highly polar. Thus, the polar portion of the analyte interacts strongly with the surface of the gel particle and nonpolar portion interacts more weakly. Analyte molecules can bind to silica in two ways: by hydrogen bonding and dipole-dipole interactions. There are several chemical modifications that can be made to the silica gel to improve separation of phospholipids classes, as coating the plate with boric acid [86].

For silica gel chromatography, the mobile phase is an organic solvent or mixture of organic solvents ranging in polarity. Using appropriate mixtures of solvents is possible to separate and quantify different classes of lipids [87]. As the mobile phase moves along the surface of the silica gel it transports the analyte particles of the stationary phase. However, the analyte molecules are only free to move with the solvent if they are not bound to the surface of the silica gel. Thus, the fraction of time that the analyte is bound to the surface of the silica gel relative to the time it spends in solution determines the retention factor of the analyte. The ability of an analyte to bind to the surface of the silica

gel in the presence of a particular solvent or mixture of solvents can be viewed as a the sum of two competitive interactions. First, polar groups in the solvent can compete with the analyte for binding sites on the surface of the silica gel. Therefore, if a highly polar solvent is used, it will interact strongly with the surface of the silica gel and will leave few sites on the stationary phase free to bind with the analyte. The analyte will, therefore, move quickly past the stationary phase. Similarly, polar groups in the solvent can interact strongly with polar functionality of the analyte and prevent interaction of the analyte with the surface of the silica gel. This effect also leads to rapid movement of the analyte past the stationary phase [88]. So, phospholipids will migrate on the stationary phase a certain distance based upon their composition and affinity for the mobile phase [86].

In normal phase TLC, the stationary phase (normally silica gel) is polar and the mobile phase is quite apolar [85], so the more non-polar components have more affinity with apolar mobile phase and elute in front of the more polar components, which have higher affinity to the stationary phase. Normal phase chromatography is the standard method of phospholipid class separation according to polarity differences caused by differences of the headgroups of the PL of interest [85]. In reverse phase TLC, the stationary phase consists at linked carbon chains, usually with 18 carbons, and the mobile phase consists of polar solvents; the elution order of phospholipids is the inverse of the normal phase TLC.

The separated lipid fractions can be easily visualized by binding to a dye. This is a critical step when the lipids are then analyzed by mass spectrometry because the staining methods are necessary that do not result in alterations of the molecular weight of the analyte. One very useful dye is primuline because it binds non-covalently to the apolar fatty acyl residues of lipids can be easily removed from the lipid, and does not affect a subsequent MS analysis [89]. The separated and identified species can be removed from the spots on the TLC plates and lipids re-extracted with chloroform and methanol, and analyzed by mass spectrometry.

4.3 Mass Spectrometry

Mass spectrometry (MS) is a powerful analytical technique which has high sensitivity, specificity, selectivity and speed, that can be used to identify unknown compounds. It is

based on the detection of ions (charged molecules) after their separation according to both their total atomic mass (m) and electrical charge (z) by electric and magnetic fields [36,46]. Data generated by the mass spectrometer is represented by the ration of mass of the ion and it charge (as *m/z*) versus their relative abundance (as a relative intensity) [46].

The components of a mass spectrometry instruments are: a system to introduce the sample into the source of ionization, in which is produced in a beam of ions in gas phase resulting from ionization of analyte molecules from the sample, the mass analyzer, where the ions are selected and separated according to the ratio mass/charge (*m/z*) and detector, in which the separated ions are collected and characterized by producing a signal whose intensity is related to the number of detected ions (Figure 9). The detector is connected to a computer that allows to integrate the information received and transformed it into a mass spectra, according to the relative abundance in function of the *m/z* of each ion [46]. The mass spectrometers are complex instruments which allow obtain the mass of small molecules, and having a special characteristic: they need a high vacuum (10^{-5}-10^{-7} Torr) [46] to allow unperturbed transmission and detection of the gas phase ions without simultaneous reactions.

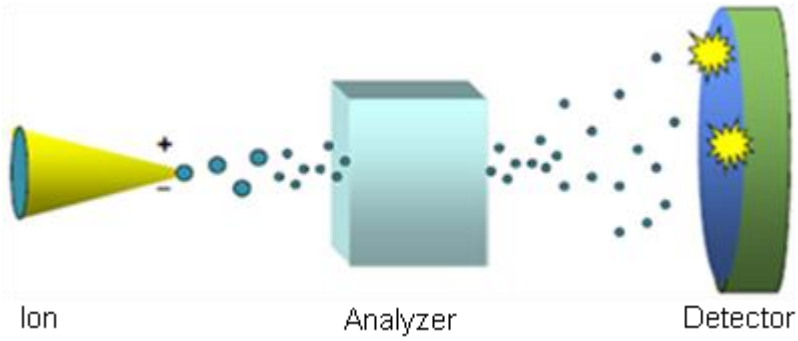

Figure 9. Mass spectrometer components.

Mass spectrometry has been used to identify, as well as the elucidation of relations between structure-activity of different membrane lipids. The combination of sensitivity, specificity, selectivity and speed of mass spectrometry are the ideal technique for the analysis of lipids [46].

Mass spectrometry has been highly used in lipidomic analysis to identify, quantify and characterize the chemical and functional properties of lipids. Lipidomic progress has been

improved by the development of new mass spectrometric techniques, particullary soft ionization techniques [90] and new more robust instruments. For analysis of phospholipids two ionization methods are commonly used: Electrospray Ionization (ESI) and Desorption/Ionization Matrix-Assisted Laser (MALDI). These soft ionization techniques allows the analysis of biomolecules of high molecular weight, nonvolatile and thermolabile, without excessive degradation and with a high probability of detection of the molecular ion, and the study of intact lipid molecular species from very small amounts of samples, with minimal sample preparation (without derivatization) [43].

4.3.1 Ionization Source

Electrospray Ionization (ESI)

Electrospray ionization generates molecular ions at atmospheric pressure by passing stream containing a sample solution through a small capillary at a low flow rate [103]. In ESI a solution containing the analyte of interest dissolved in a solvent more volatile than the analyte, such as methanol is continuously infused into the source through a metallic needle using in a continuous flow a syringe pump. A high voltage is applied to the metallic needle creating a significant amount of charge at the end of the needle, producing a fine spray of highly charged droplets [91,92].

This high voltage will charge the molecules of the solvent, in which the sample is mixed, as well as the sample molecules, producing ions primarily via protonation (in positive ion mode) such as $[M+H]^+$ or deprotonation (in negative ion mode) as $[M-H]^-$ or via formation of cations adduct (e.g. Na^+) or anions adduct (e.g. Cl^-), depending on the chemical properties of the molecules.

Once they are charged, with the same charge, the molecules will repel one another forcing the liquid to exit trough the tip, initially forming a cone of liquid, known as Taylor cone, after which the droplets form the final spray. After release of the droplets, they undergo further division and solvent will gradually evaporate, through a flowing stream of heated inert gas, usually nitrogen, producing a decrease in the volume of the drop until it reaches a value close to the limit of Rayleigh instability, in which the unstable drop undergoes fission in smaller drops. When the ions become close enough together their

electric charges will make them repel each other, because of the Coloumb force. This will force the droplets to divide into smaller droplets until each droplet corresponds to a single charged molecule and the solvent is completely evaporated (Figure 10) [91,92].

The major advantages of ESI-MS are high accuracy, sensitivity, reproducibility, applicability to complex phospholipid solutions without prior derivatization [47], and as soft ionization technique molecules are not broken apart, instead they remain intact. ESI-MS of lipids represents one of the most sensitive, discriminating, and direct methods to assess alterations in cellular lipidome directly from lipid extracts of biological samples [43,91].

The charged ions formed by ESI are then transported to the analyzer. ESI sources can be combined with distinct types of mass analyzers such as quadrupole (Q), ion trap, time-of-flight (TOF), cyclotron resonance of Fourier / Fourier transform ino cyclontron (FT-ICR) and orbitrap [46].

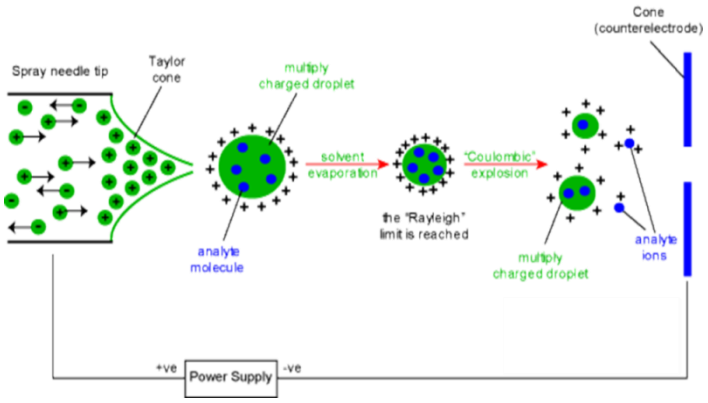

Figure 10. Schematic representation of ion formation by ESI (http://www.chm.bris.ac.uk/ms/theory/esi-ionisation.htm)

4.3.2 Analyzers

After being ionized, sample is sent to the mass spectrometer and is then separated by a component of the mass spectrometer, referred to as analyzer, according to their ratio *m/z*, and independently of their chemical conformation. If different ionization methods require that samples can be analyzed, the different mass analyzers can determine the minimum difference in mass values that can be distinguished and identified as individual species of analyte.

Several analyzers are used in mass spectrometers, as quadrupolo, ion trap, time-of-flight. These analyzers can be used individually in mass spectrometers, or can be combined into complex instruments, the most commonly used Q-TOF, Q-Trap, and triple quadrupoles. They all differ in accuracy (the error in determining the precise mass compared with the theoretical value), resolution (mass divided by the value of the difference in mass between two ions with a small difference in mass) [47], dynamic range and capability to perform tandem mass spectrometry.

Quadrupole, the most used mass analyzers, are ion beam analyzers. The quadrupole is composed by two pairs of parallel rolls connected at the same potential to which is applied a direct and an alternate current between each pair of rolls that affects the trajectory of the ions and allows the transmission of ions through the quadrupole mass analyzer. Only the ion with a certain *m/z* value will reach the detector, while the rest will collide with rods and lose charge or will be ejected. By varying the electrical signals from one quadrupole, one can vary the range of the m/z transmitted. They are relatively inexpensive, small size, easy to use and maintain, and able to provide good accuracy in the measured mass values. However, the resolution is limited, have limited capacity in terms of range and resolving power, and have limited suitability for analysis of tandem mass spectrometry. Moreover, there is a great waste of information since the ions to pass through the quadrupole, are selected according to their mass, so only one value of mass reaches the detector.

Triple quadrupole mass spectrometer is a tandem mass spectrometer consisting of two quadrupole mass spectrometers in series, with an only quandrupole between them to act as a collision cell. The first (Q1) and third (Q3) quadrupoles serve as mass filters, whereas the middle (q2) quadrupole serves as a collision cell, which using an inert gas such as Ar, He, or N2 gas provide fragmentation of a selected precursor ion (selected in Q1). Subsequent fragments are passed through to Q3 where they may be filtered or scanned. This configuration is often abbreviated QqQ.

Linear Ion Trap is a multipole ion-dimensional where the ions are confined radially by a two-dimensional (2D) radio frequency (RF) field, and axially by stopping potentials applied to end electrodes, for long periods of time, can act as a source of ions, ion-

chamber reactions molecule and analyzer. As the ions are trapped and accumulate over the time and can be combined with other mass analyzers and used to isolate ions of selected mass to charge ratios, to perform tandem mass spectrometry experiments, and to study ion molecule chemistry [93]. However, it has several disadvantages such as low accuracy and low dynamic range.

Time-of-flight (TOF) instruments are simple, relatively inexpensive, with high sensitivity and accuracy, and unlimited masses analyzable, but have limited resolution. The operating principle of TOF involves measuring the time differences that generated and accelerated ions take to travel from the ion source and reach to the detector. These ions are accelerated through a flight tube of variable length by an electric field pulse. Based on difference in obtained velocity, ions will be separated according to *m/z*. All the ions are accelerated with the same kinetic energy; their velocities are inversely proportional to the square root of their mass, so the ions hit the detector sequentially in order of increasing value of *m/z* and therefore the lighter ions gain higher speeds and reach the detector before the ions with higher mass and low speed. Thus, the detection sensitivity is lower for heavier ions than for lighter ions. To increase the sensitivity of detection, the ions are accelerated before reaching the detector.

In this work we used three different spectrometers, ESI-Ion Trap, ESI-Q-TOF2 and ESI-QqQ which combines several types of analyzers, making them significantly more sensitive. These instruments use the same method of ionization (ESI), however, different mass analyzers, which allow to obtain different types of information. The Ion Trap allows for tandem mass spectrometry (MS^n). These instruments can be used as complementary analytical techniques.

4.3.3 Tandem Mass Spectrometry

The main characteristics of mass spectra obtained with soft ionization methods are the absence of fragmentation, which allows the accurate determination of molecular masses of constituents of mixtures. However, in these conditions is obtained little information about its molecular structure.

Tandem mass spectrometry is based on selection and isolation of interest ions, with specific *m/z* in a first mass analyzer, followed by fragmentation in collision cell by interaction with a gas, resulting ionic products that are separated in terms of *m/z* values and characterized by a second mass analyzer (Figure 11). Usually several analyzers are coupled in series, however, in some instruments, like the linear ion trap, only one analyzer is able to perform multiple mass spectrometry becoming efficient instruments in structural identification of molecules as phospholipids [60]. This technique is identified as MS/MS, however, the number of steps can increase in order to perform MS^n (n represents the number of generations of ions to be analyzed).

There are several ways in MS/MS: precursor ion scanninig, in which masses of the precursor are checked at the first analyzer, sequentially transmitted to collision cell and the product ion is selected in the second mass analyzer that transmits only a *m/z*, informing on the precursors of an ion fragment; product ion scanning, in which a precursor ion with a given *m/z* is selected in the first mass analyzer, followed by its fragmentation in collision cell and then all the resulting masses are scanned in second mass analyzer, reporting the fragments of a precursor ion; and neutral loss scanning, which ions are sequentially separated at the first analyzer, transmitted to collision cell, and second analyzer reports the same ions that lose a predetermined neutral molecule [81,94].

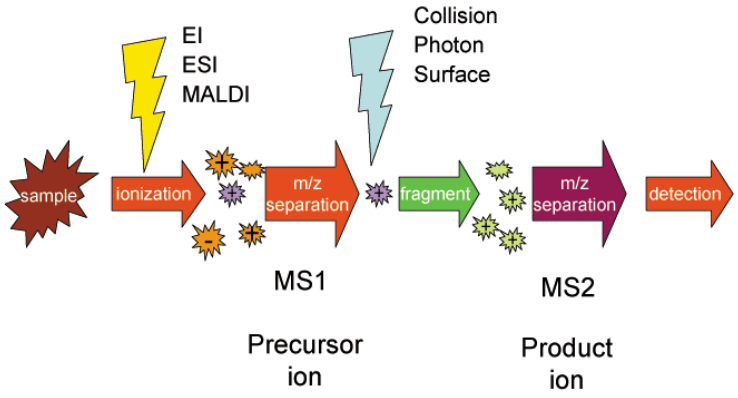

Figure 11. Schematic representation of tandem mass spectrometry.

Using this technology, we can draw several conclusions about the structure of molecules and analyzed the spectra obtained give us not only the forms of molecular

break more often, as the most favorable. Mass spectrometry MS/MS has been used for detailed study and characterization of several molecules, including amino acids and phospholipids.

4.4 Mass Spectrometry in phospholipids analysis

Mass spectrometry is the most powerful contemporary analytical approach in lipidomics [54]. Due the combination of sensitivity, specificity, selectivity and speed, mass spectrometry is the ideal technique for the analysis of lipids; has been used to identify, quantify and characterize the chemical and functional properties of each lipid component, as well as the elucidation of relations between structure-activity of different membrane lipids and providing information about the molecular identity, composition and oxidative state. Tandem mass spectrometry provides detailed information necessary for the structural characterization of new lipid, and the selectivity required to determine the lipid species present in complex mixtures [95]; precursor ion scan and neutral loss of polar head groups or fatty acids are widely used in the detection and identification of structural lipids [96], but a knowledge of the fragmentation patterns is required. Either ESI- or MALDI-MS can analyze phospholipid positively or negatively charged, as described in table 1, because each class of lipids has the ability to acquire positive or negative charges, while in solution, under an ionization source of high energy [46], and the resulting spectra of lipids appears to be considerably different in different modes.

Table 2. Phospholipid classes that can be analyzed by ESI or MALDI in positive (species easily protonated forming $[M+X]^+$ ions) and negative (species easily deprotonated forming $[M-X]^-$ ions) modes. Some species are easily analyzed in both modes.

Positive Mode $[M+X]^+$, X= H, Na, Li, etc	Negative Mode $[M-H]^-$
PC	**PI**
PS	**PG**
PE	**PA**
SM	**PS**
	PE
	CL
	Cer

In negative mode, phospholipids can form $[M-H]^-$ ions or $[M-2H+X]^-$ (X=Na, Li, K) adduct ions; in positive mode can form $[M+H]^+$ ions or $[M+X]^+$, $[M+2X-H]^+$ or $[M+3X-2H]^+$ (X=Na, Li, K) adduct ions [97].

Phosphatydilcholines are characterized by the presence of a quaternary nitrogen atom whose positive charge is neutralized by the negative charge of the phosphate group. The quaternary nitrogen atom readily forms protonated ions $[MH]^+$ under ionization because the phosphate anion can be protonated [60]. The product ion spectra of $[MH]^+$ ions show an abundant product ion at m/z 184 correspondent to the choline polar head $[H_2PO_4(CH_2)_2N(CH_3)_3]^+$ (figure 12). Other product ions with low relative abundance include those formed from loss of $HPO_4(CH_2)_2N(CH_3)_3$ (183 Da) and loss of fatty acyl chains placed at *sn*-1 (R_1COOH and R_1=C=O) and *sn*-2 (R_2COOH and R_2=C=O) [38]. The formation of $[M+H-R_2CH_2CH=C=O]^+$ is more favorable than the $[M+H-R_1CH_2CH=C=O]^+$ ion, arising from losses of the fatty acyl substituents at *sn*-2 and *sn*-1 as ketenes, respectively, while the formation of R_1CO_2H is more favorable than R_2CO_2H, arising from losses of the fatty acyl substituents at *sn*-1 and *sn*-2 as acids. Therefore, the position of the fatty acyl on the glycerol backbone can be assigned [97].

Ionization of PC also produced cationized molecules, such as $[M+Na]^+$ [60], and the product ion spectra show neutral loss of trimethylamine (59 Da), polar head $HPO_4(CH_2)_2N(CH_3)_3$ (−183 Da) and sodiated polar head $NaPO_4(CH_2)_2N(CH_3)_3$ (−205 Da) (figure 12), loss of fatty acyl chains at *sn*-1 (R_1COONa and R_1COOH) and *sn*-2 (R_2COONa and R_2COOH), the product ion at *m/z* 147 (cyclophosphane group), and acyl product ions R_1CO^+ and R_2CO^+ [38]. Tandem MS analysis of plasmalogen phosphocholines shows fragment ions involving loss of polar head and the loss of alkenyl or alkyl chains (*sn*-1 or *sn*-2 fatty acids) as alcohols and ketene/acid (R_1OH and R_2=C=O/R_2COOH) [35]. The higher relative abundance of the product ions resultant from loss of *sn*-2 acyl chains (1-acyl-2-lysophosphatidylcholine), which is a more favorable fragmentation pathway, allows identifying the relative position of fatty acyl chains [38,60]. Since the PC class has a positive charge in the nitrogen, there are few MS studies in the negative mode.

Due to their common choline head group, both PC and SM ionize similarly (figure 12). However, PC and SM can be easily discriminated, since protonated PC molecules appear

at even m/z values, whereas protonated molecules of SM exhibit odd *m/z* values. This is due to the presence of an additional nitrogen atom in SM [98].

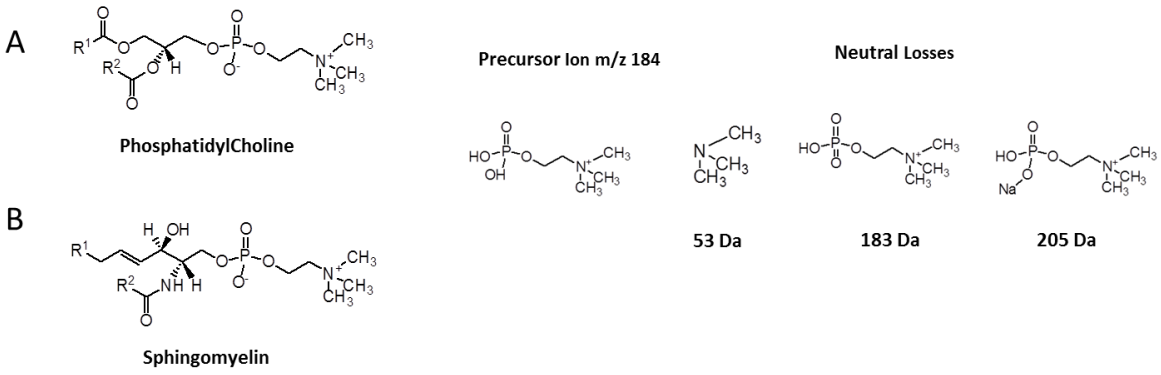

Figure 12. Typical structure of phosphatidylcholine (A), sphingomyelin (B) and their fragments ions and neutral losses. R^1 and R^2 represent the fatty acyl chains esterified to glycerol backbone (A). R^1 represents the sphingosine backbone and R^2 represents the fatty acyl chain esterified to sphingosine backbone(B).

Phosphatydilethanolamine may ionize either in positive or negative mode. Tandem mass spectra of the $[M+H]^+$ ions undergo loss of 141 Da which corresponds to neutral loss of the polar head ($HPO_4(CH_2)_2NH_3$) [60]. Ionization of PE also produced cationized molecules, such as $[M+Na]^+$. The fragmentation pathway of these ions include, apart from loss of 141 Da, the loss of aziridine (-43 Da, CH_2CH_2NH) (figure 13). Fragmentation of $[M-H]^-$ ions of PE [38] leads to abundant carboxylate anion of *sn*-1 (R_1COO^-) and *sn*-2 (R_2COO^-) acyl residues. The relative abundance of R_2COO^- is usually higher than the R_1COO^- anion. Other product ions corresponding to neutral loss of *sn*-1 and *sn*-2 fatty acyl residues (RCOOH and $RCH_2CH=C=O$) are also detected [38]. The loss of fatty acyl as ketene/acid at *sn*-2 position is more favorable [97].The product ion produced by loss of 141 Da is absent.

In positive mode, tandem MS analysis of plasmalogen phosphoethanolamines shows fragment ions involving loss of polar head, aziridine and the loss of alkenyl or alkyl chains (*sn*-1 or *sn*-2 fatty acids) as alcohols and ketene/acid (R_1OH and $R_2=C=O/R_2COOH$). $[M-H]^-$ ions spectra only give one carboxylate anion from *sn*-2 [97].

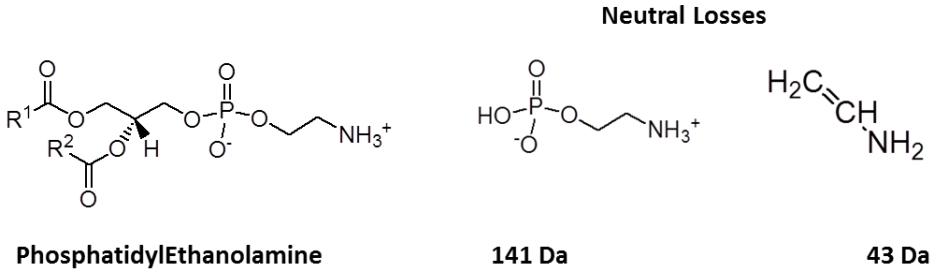

Figure 13. Typical structure phosphatidylethanolamine and its neutral losses. R^1 and R^2 represent the fatty acyl chains esterified to glycerol backbone.

Phosphatydilserine class ionize preferentially in the negative mode with formation of $[M-H]^-$ or $[M-2H+X]^-$ (X= Na, Li, K) ions [38]. The $[M-H]^-$ PS product ion spectra typically shows major loss of serine group (−87 Da) (figure 14) and carboxylate anions (R_1COO^- and R_2COO^-) allows discovering structural features of PS [38]. The *sn*-1 carboxylate anion is typically more abundant than the *sn*-2 [60]. Fatty acyl chains may also be lost as ketene ($[R_xCH_2CH=C=O]^-$) or as acid ($[M-H-R_xCO_2H]^-$); loss of fatty acyl at *sn*-2 position is more favorable [60,97].

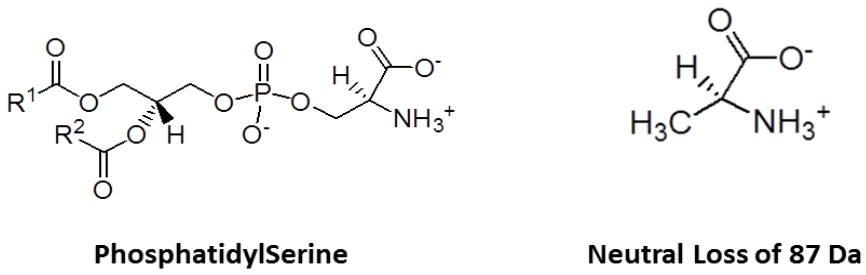

Figure 14. Typical structure of phosphatidylserine and its neutral loss. R^1 and R^2 represent the fatty acyl chains esterified to glycerol backbone.

Phosphatidic acid class (figure 15 A) ionizes preferentially in the negative mode [60]. The *sn*-1 carboxylate anion (R_1COO^-) was typically more abundant than the *sn*-2 carboxylate anion (R_2COO^-) [60]. There are also ions that corresponds to a neutral loss of *sn*-1 and *sn*-2 fatty acyl groups as ketenes ($[M-H-RCH_2CH=C=O]^-$) or carboxylic acids ([M-

H-RCOOH]$^-$) [38], being the last one more favorable [97]. In these cases, the loss of fatty acyl at *sn*-2 position, as acid or ketene, is more favorable than at *sn*-1 [97].

Phosphatdydilinositol class also ionize preferentially in negative mode [60] and shows a characteristic fragment corresponding to phosphoinositol at *m/z* 241 [43] (figure 15 B). Fatty acyl chains are preferentially losses as acid ([M-H-R_xCO_2H]$^-$) in a more favorable way from *sn*-2 position. The relative intensity of carboxylate anions (R_1COO^- and R_2COO^-) is close [97]; however tandem mass spectrometry allows identifying specific fatty acyl substituents and R_1COO^- was typically a little more abundant than R_2COO^-.

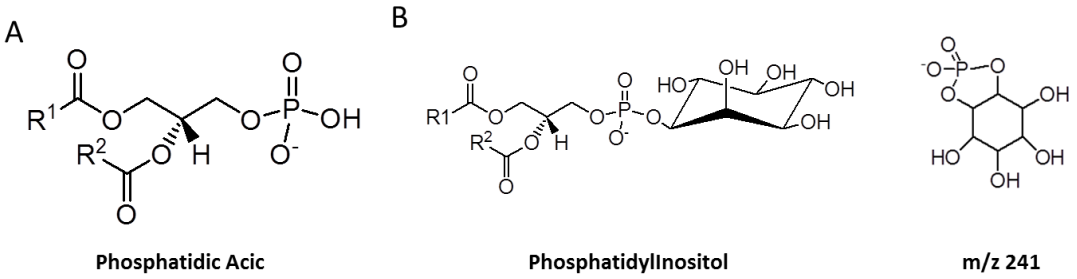

Figure 15. Typical structure of phosphatidic acid (A), phosphatidylinositol (B), and its fragment ions. R^1 and R^2 represent the fatty acyl chains esterified to glycerol backbone.

Phosphatidylglycerol (figure 16) ionize preferentially in negative mode as [M-H]$^-$ ions and shows a characteristic fragment at *m/z* 153 correspondent to glycerophosphate and at *m/z* 171 which are the neutral loss of glycerol polar head group. The loss of fatty acyl at *sn*-2 position as ketene ([M-H-R_2CH_2CH=C=O]$^-$), acid ([M-H-R_2CO_2H]$^-$) or carboxylate anion (R_2COO^-) are the most favorable; loss of *sn*-1 fatty acyl is more favorable as acid (R_1CO_2H) than as ketene (R_1CH_2CH=C=O) [97].

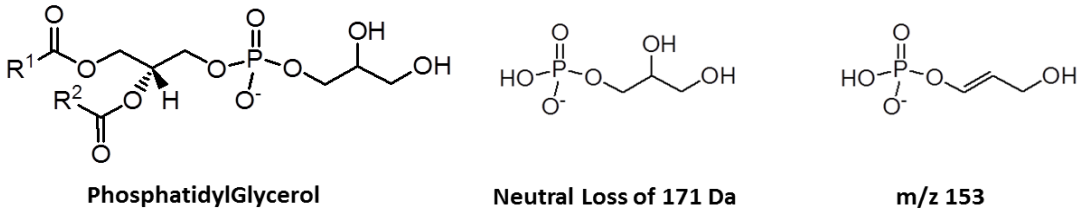

Figure 16. Typical structure of phosphatidylglycerol, and its fragment ion and neutral loss. R^1 and R^2 represent the fatty acyl chains esterified to glycerol backbone.

CL ionize in the form of mono or double charge species ($[M-H]^-$ or $[M-2H]^{2-}$) [35,112] and sodium adducts ($[M+Na-2H]^-$) preferentially in negative mode [38]; however can also be analyzed in positive mode ($[M+Na]^+$ or $[M-2H+3Na]^+$). Fragmentation of the $[M-2H+Na]^-$ ions yield abundant product ions from loss of monoacylphosphatidylglycerol and diacylglycerol groups, and loss of fatty acyl chains [38,99].

Ceramide (figure 17) can ionize in both positive and negative mode, as $[M+H]^+$ and $[M+X]^+$ (X= Na, Li, K) species or $[M-H]^-$ and $[M+X]^-$ (X= Cl^-, $CH_3CO_2^-$, $CF_3CO_2^-$) species, respectively. Ceramide fragmentation results in the formation of two interesting ions corresponding to loss of 30 and 32 Da, which corresponds to loss of HCHO and CH_3OH. The loss of fatty acyl moiety may be in the form of ketene as $RCH_2CH=C=O$, amide as $RCONH_2$ or carboxylate anion (RCO_2^-). Several others ions corresponding to loss or cleavage of sphingosine backbone may be also present in both modes [100].

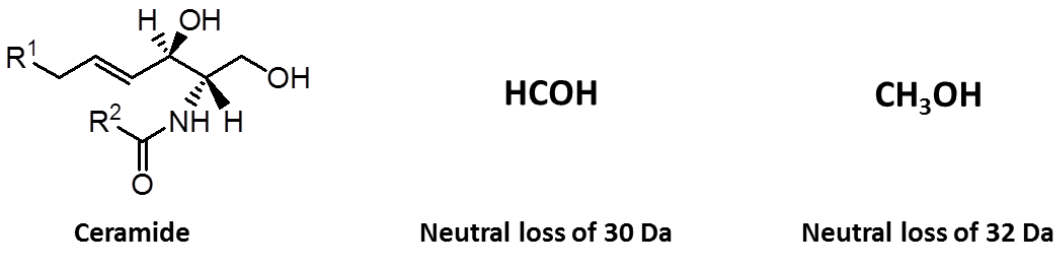

Figure 17. Typical structure ceramide and its neutral losses. R^1 represents the sphingosine backbone and R^2 represents the fatty acyl chain esterified to sphingosine backbone.

Several studies reporting the analysis of brain lipids using mass spectrometry (ESI-and MALDI-MS and MS/MS) were carried out in recent years by Kiebish and co-authors (2008). They used a lipidomic approach for the study of lipids from non-synaptic and synaptic brain mitochondria of C57BL/6J (B6) rats [15]; in the discovery of new species of brain lipids [101]; in the study of the profile of phospholipids and in lysophospholipids of rat brains after ischemic stroke [102]; to quantify lysophosphatidic acid in rat brain tissue [103], among others.

Mass spectrometry (MS) has been used to identify both non-oxidized and oxidized phospholipids [38,97,101] and the specific structures of oxidation products generated during distinct oxidative processes [38]. Product ion in tandem mass spectra of oxidized

phospholipids allow identifying changes in the fatty acyl chain and specific features such as presence of new functional groups in the molecule and their location along the fatty acyl chain [38]. The different oxidation products may be responsible for distinct biological effects and are very likely to modify the properties of biological membranes, because their polarity and shape may differ significantly from the structures of native molecules, thus increasing the relevance of identifying each specific oxidation product in order to understand their specific biological significance and effects [62].

Glycerophosphocholines (PC) are the most studied class of oxidized phospholipids by mass spectrometry and oxidized products have been identified by MS in biological fluids and tissues [38]. Khaselev and Murphy (1999) reported the results of the oxidation by Fenton reaction of PE from bovine brain [104]. Maskrey and collaborators (2007) used LC-MS and MS/MS to recognize the role of oxidation products of arachidonic acid esterified to glycero-phosphatidylethanolamines as contributors or mediators in inflammatory response [105]. Several studies identified and studied phosphatidylserine hydroperoxy and hydroxy species using ESI-MS and ESI-MS/MS in negative mode. Tyurina et al. identified mono-hydroperoxy derivatives of PS generated by gama-irradiation to induce intestinal injury [106]. Bayir and collaborators also propose the presence of PS hydroperoxides derivatives in traumatic brain injury after controlled cortical impact [63]. The hydroperoxy and hydroxyl PS derivates also identified by Tyurin and collaborators during apoptosis induced in neurons by staurosporine [107] and in cells and tissues after pro-apoptotic and pro-inflammatory stimuli [108]. The same group, using oxidative lipidomics approach, showed that the pattern of phospholipid oxidation during apoptosis is nonrandom and that phosphatidylserine (PS) is one of the preferred peroxidation substrates [109]. Kagan and collaborators studied cardiolipin oxidation induced by different conditions in several biological samples by ESI-MS and MS/MS, in the negative mode $[M-H]^-$ and $[M-2H]^{2-}$ [63, 106, 109]. Shadyro and collaborators showed oxidative modification of cardiolipin using MALDI–MS [110,111].

However, sphingomyelins and sphingolipids oxidative modifications have not been a subject of interest by researchers.

5. Aims

AD onset and development have been correlated either with increasing in ROS production and also in changes in sphingolipid metabolism. However there is a lack of knowledge about the effect of ROS in sphingolipids. One of the aims of this work is to study the induced changes of sphingolipids under oxidative stress conditions, and which may help to understand the changes that occur in sphingolipids during the pathological process associated with AD, since deregulation in sphingolipid metabolism has been associated with establishment and progression of this disease [11]. All oxidation products resulting from sphingolipids oxidation are identify and characterized by mass spectrometry.

Alzheimer disease has several aspects that remain unclear, related to pathophysiological process and treatment. Tacrine was used for the treatment of AD [17], however, some toxicological effects has been reported for tacrine [6-10, 17] and also associated with cell apoptosis.

Considering the lipid changes in mitochondria due to oxidative stress has been considered key intermediates in apoptosis, another aim of this study is to evaluate the changes in phospholipid profile of brain mitochondria of rats treated with tacrine and also with two analogues proposed [21], by mass spectrometry coupled with separation techniques, in order to better understand the side effects associated with tacrine treatment.

CHAPTER II

Study of sphingolipids oxidation by electrospray tandem mass spectrometry

Study of sphingolipids oxidation by electrospray tandem mass spectrometry

Tânia Melo[a], Elisabete Maciel[a], Maria Manuel Oliveira[b], Pedro Domingues[a], M. Rosário M. Domingues[a]*

[a]Mass Spectrometry Centre, Chemistry Department, University of Aveiro, 3810-193 Aveiro, Portugal

[b]CQ-VR, Chemistry Department, University of Trás-os-Montes e Alto Douro, 5001-801 Vila Real, Portugal

* Author to whom correspondence should be addressed:

M.Rosário M. Domingues

e-mail: mrd@ua.pt

Phone:+351 234 370 698

Fax:+ 351 234 370 084

Abstract

Sphingolipids are involved in several biological processes namely proliferation, differentiation, migration, intra- and extracellular signaling, senescence, apoptosis, inflammation, among others, some have been associated with oxidative stress conditions. So in the present study, different sphingolipids ((d18:1/16:0) N-palmitoyl-Derythro-sphingosylphosphorylcholine (SM), (d18:1) sphingosylphosphorylcholine (SPC) and (d18:1/18:0) ceramide (Cer) were oxidized by the hydroxyl radical, generated under Fenton reaction conditions, and the oxidation reaction was monitored by ESI-MS in positive mode. Analyisi of ESI-MS spectra allow to see that ceramide does not oxidized while SPC and SM show some oxidation products that were analyzed by ESI-MS/MS. This approach allowed identifying hydroxyl and keto derivatives of SPC and acetaldehydephosphorylcholine derivative (*m/z* 226). SM oxidation occurs exclusively in sphingosine backbone with formation of SPC, hydroxyl and keto derivatives of SPC and the oxidation product at *m/z* 226. This study may give new insight and could help to understanding the behavior and biological roles of the sphingolipids under oxidative stress conditions.

Keywords (3): sphingolipids, oxidation, mass spectrometry

Introduction

Sphingolipids are a class of lipids that play important cellular roles both as structural components of membranes, for example, as components of raft lipids, and as signaling molecules that mediate a diverse set of cellular events [51,52]. This class of lipids includes a range of structurally related compounds, such as sphingosylphosphorylcholine (SPC), ceramides (CM), sphingomyelin (SM), among others. Despite sharing a common sphingoid backbone, these sub-classes have distinct properties and functions.

Ceramides (Figure 1a) exert a wide range of biological functions in relation to cellular signaling and cellular responses to stress, including cell cycle arrest, differentiation, apoptosis, senescence and immune responses [112-118]. Ceramide (Cer) can be formed through sphingomyelinases (SMase)-dependent catabolism of SM and by *de novo* synthesis. Sphingomyelin can be synthesized by transferring phosphocholine to ceramide by sphingomyelin synthase (Scheme 1).

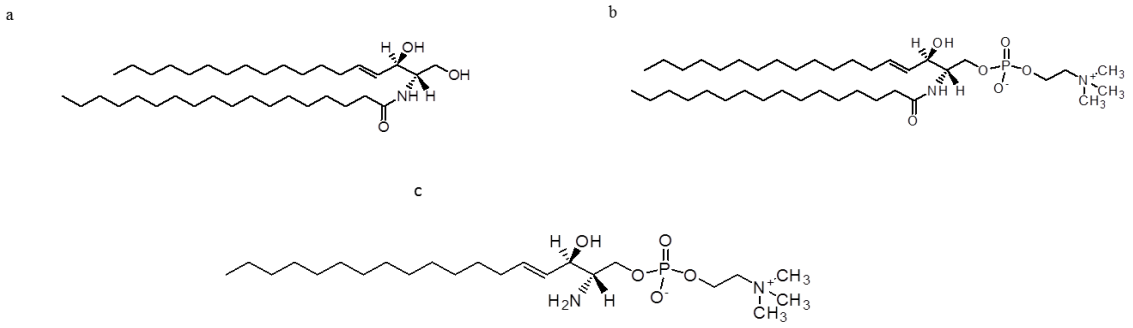

Figure 1. Structure of ceramide d18:1/18:0 (a), sphingomyelin d18:1/16:0 (b) and sphingosylphosphorylcholine d18:1 (c).

Sphingomyelins (SM) (Figure 1b) are structural components of membranes and key components of lipid rafts and lipoproteins. These lipids can be enzymatically converted to ceramide and to sphingosylphosphorylcholine (SPC) as shown in Scheme 1. Sphingosylphosphorylcholine (Figure 1c) affects diverse biological processes such cell growth [119], proliferation [120], cell migration [121], apoptosis [122], among others, acting as a signaling molecule.

Although SM and Cer have been extensively studied, studies involving SPC are limited, although it has been suggested that this class of sphingolipids plays an important role in signaling pathways.

A few studies have implied that SPC may be involved in inflammation and ROS production, and may, therefore, be related to apoptosis and cell death [123,124]. Deregulation of sphingolipid metabolism leads to the onset and progression of various diseases such as neurodegenerative diseases, cardiovascular diseases, chronic inflammation or cancer [125,126]. Oxidized phospholipids have been postulated to be involved in many pathophysiological processes such as those mentioned above, as reviewed recently [127]. In recent years, most studies on oxidized phospholipids have focused on the changes induced in phosphatidylcholines, phosphatidylethanolamines, phosphatidylserines and cardiolipin [38,128]. However, no studies were conducted to investigate the effect of oxidative stress, at the molecular level, on sphingolipids in general or in sphingomyelins in particular, although recently, it has been reported that myeloperoxidase induces oxidation of SM [129].

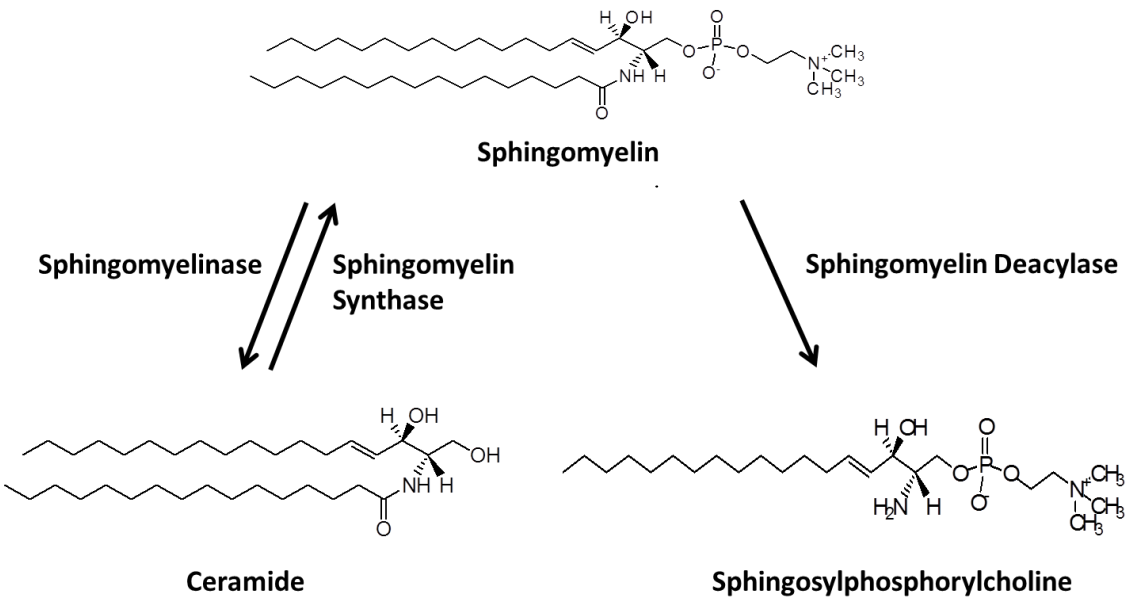

Scheme 1. Alternative metabolic pathways to produce either SPC or ceramide enzymatically from sphingomyelin.

In the present work, we have studied the effect of oxidative stress, using hydrogen peroxide (H_2O_2/Fe^{2+}) as ROS inducing agent, on sphingolipids. We have selected as models of sphingolipids, a ceramide (Cer), a sphingomyelin (SM), and a sphingosylphosphorylcholine (SPC), which is a lysosphingomyelin, as represented in Figure 1. These sphingolipids contain the same sphingosine as backbone and SM and Cer contain a C16 and C18 saturated fatty acyl chain, respectively. Previous studies have shown that saturated fatty acyl chains in phospholipids are not likely to be oxidized under Fenton conditions [38]. In recent years, electrospray mass spectrometry has become an important tool in the structural characterization of sphingolipids [51,52], and oxidized phospholipids [38]. The aim of this paper is perform the structural characterization of oxidative products of sphingolipids, using electrospray ionization mass spectrometry (ESI-MS), tandem mass spectrometry (ESI-MS/MS) and by exact mass measurements.

Experimental

Materials

Sphingomyelin (d18:1/16:0) N-palmitoyl-D-erythrosphingosylphosphorylcholine (SM) and lyso sphingomyelin (d18:1) sphingosylphosphorylcholine (SPC) were purchased from Sigma-Aldrich (Madrid, Spain) and ceramide (d18:1/18:0) was purchased from Avanti Polar Lipids, Inc. (Alabama, USA).

$FeCl_2$ and H_2O_2 (30%, w/v) used for the peroxidation reaction were acquired from Merck (Darmstadt, Germany) and ammonium hydrogencarbonate was purchase from Riedel-de Haën (Germany). All solvents used were HPLC grade.

All standards and reagents were used without further purification.

Oxidation of sphingolipids by Fenton reaction

The SM (d18:1/16:0), SPC (d18:1) and ceramide (d18:1/18:0) were subjected to oxidation under the conditions described for the Fenton reaction. Both sphingolipids were diluted to concentration of 1.42 mM using $CHCl_3$ and dried under nitrogen flow. Then, 223 µL of ammonium hydrogenocarbonate buffer 5mM (pH 7.4) was added to the sphingolipids, vortex well for 2 minutes, placed in water bath ultasons (Selecta Ultrasons)

for 1 minute, and vortex well again, to form the lipid vesicles. The oxidation was performed by adding 25 µL of H_2O_2 50mM and 2 µL of $FeCl_2$ 40µM to a final volume of 250 µL. The mixture was vortex well and incubated at 37ºC in the dark for several days. The extent of oxidation was monitored by electrospray mass spectrometry (ESI-MS). Controls were performed by replacing H_2O_2 with water.

Q-TOF 2 conditions

Analysis of the oxidation products was carried out by positive mode ESI-MS and MS/MS, using a Q-TOF2 mass spectrometer (Micromass, Manchester, UK), with the following electrospray conditions: a flow rate of 10 µL.min^{-1}, the voltage applied to the needle with a 3kV, a cone voltage at 30 V, source temperature at the source of 80ºC, solvation temperature of 150ºC. The resolution was set to about 9,000 (FWHM). Mass spectra were acquired for 1 minute. Tandem mass spectra (MS/MS) were acquired by collision-induced decomposition (CID), using argon as the collision gas (measured pressure in the penning gauge ~ 6x10^{-5} mBar). The collision energy used was between 25 to 30 eV. Tandem mass spectra were acquired for 1 minute. Data acquisition was carried out with a MassLynx 4.0 data system. For the accurate mass measurements, the lock mass in each mass spectrum was the calculated monoisotopic mass/charge of the native sphingolipid (non-modified phospholipid) and the empirical formula, observed and calculated mass/charge ratio, the double bond equivalent and mass error were determined for the ions observed in the MS spectra and correspondent to the new oxidation products.

Results and Discussion

The ESI-MS spectra of non-modified SM, SPC and Cer, acquired in the positive mode, show prominent peaks corresponding to $[M+H]^+$ ions at *m/z* 703.6, 465.4, and 566.6, respectively (Figure 2). The MS spectra of non-modified ceramide also show peaks at *m/z* 588.6 ($[M+Na]^+$) and at *m/z* 548.6 (loss of water from the protonated molecular ion).

The ESI-MS analysis of oxidized samples shows the formation of oxidation products from SPC and SM, while no oxidation products were observed from ceramide (Figure 2).

These last results were confirmed after seven days of oxidation (Figure 2 C2), revealing that, under these experimental conditions, ceramide is not susceptible of being oxidized. Comparison of ESI-MS spectra between control (Figure 2 A1) and oxidation reactions (Figure 2 A2) of SPC, shows new peaks at *m/z* 481.4, 495.4, 493.4 and 226. The ions located at higher m/z than the unmodified SPC were identified as protonated molecules formed by addition of one and two oxygen atoms: at *m/z* 481.4 (SPC+O), 495.4 (SPC+2O-2Da) and 493.4 (SPC+2O-4Da). These species presumably correspond to hydroxyl and keto derivatives, as observed during oxidation of phospholipids [38].

Comparison of ESI-MS spectra of SM between control (Figure 2 B1) and oxidation reactions (Figure 2 B2), shows new peaks at *m/z* 465.4, identified as SPC, and also at *m/z* 481.4 (SPC+O), 495.4 (SPC+2O-2Da) and 493.3 (SPC+2O-4Da) and 226.1. It is important to note that the same peaks are observed after SM and SPC oxidation. No oxidation products due to addition of oxygen atoms (SM+nO) were observed, contrary to that observed in phospholipids oxidation [38,128]. Subsequently, accurate mass measurements were determined and presumed oxidation species were further analyzed by tandem mass spectrometry. Analyses of these samples were also performed in negative mode, but no additional oxidation products were identified (data not shown).

The mass measurement accuracy of positively ionized species, using the QTOF mass spectrometer, was consistently < 20.8 ppm (-3.7-9.7mDa), which is adequate to determine the elemental composition of the oxidation products. The ion peak at *m/z* 481.5 corresponds to $[SPC+O+H]^+$, with an elemental formula of $C_{23}H_{50}N_2O_6P$ (error of 1.6 ppm for SPC and 11.5 ppm for SM); The ion peak at *m/z* 493.5 corresponds to $[SPC+2O-2Da+H]^+$ ($C_{23}H_{46}N_2O_7P$, error of 1.7 ppm for SPC and -6.2 ppm for SM); The ion peak at *m/z* 495.5 corresponds to $[SPC+2O-4Da+H]^+$ ($C_{23}H_{48}N_2O_7P$ error -3.7 ppm for SPC and -7.5 ppm for SM); The ion peak at *m/z* 226.1 corresponds to acetaldehydephosphatidylcholine ($C_7H_{17}NO_5P$, error -10.3 ppm for SPC); And the ion peak at *m/z* 465.4 corresponds to $[SPC+H]^+$ ($C_{23}H_{50}N_2O_5P$, error 20.8 ppm for SM). These results confirm that the oxidation products observed in oxidation of SM have the same molecular formula as those observed for SPC oxidation. This is indicative that oxidation of SM involves the sphingosine backbone and elimination of the acyl chain.

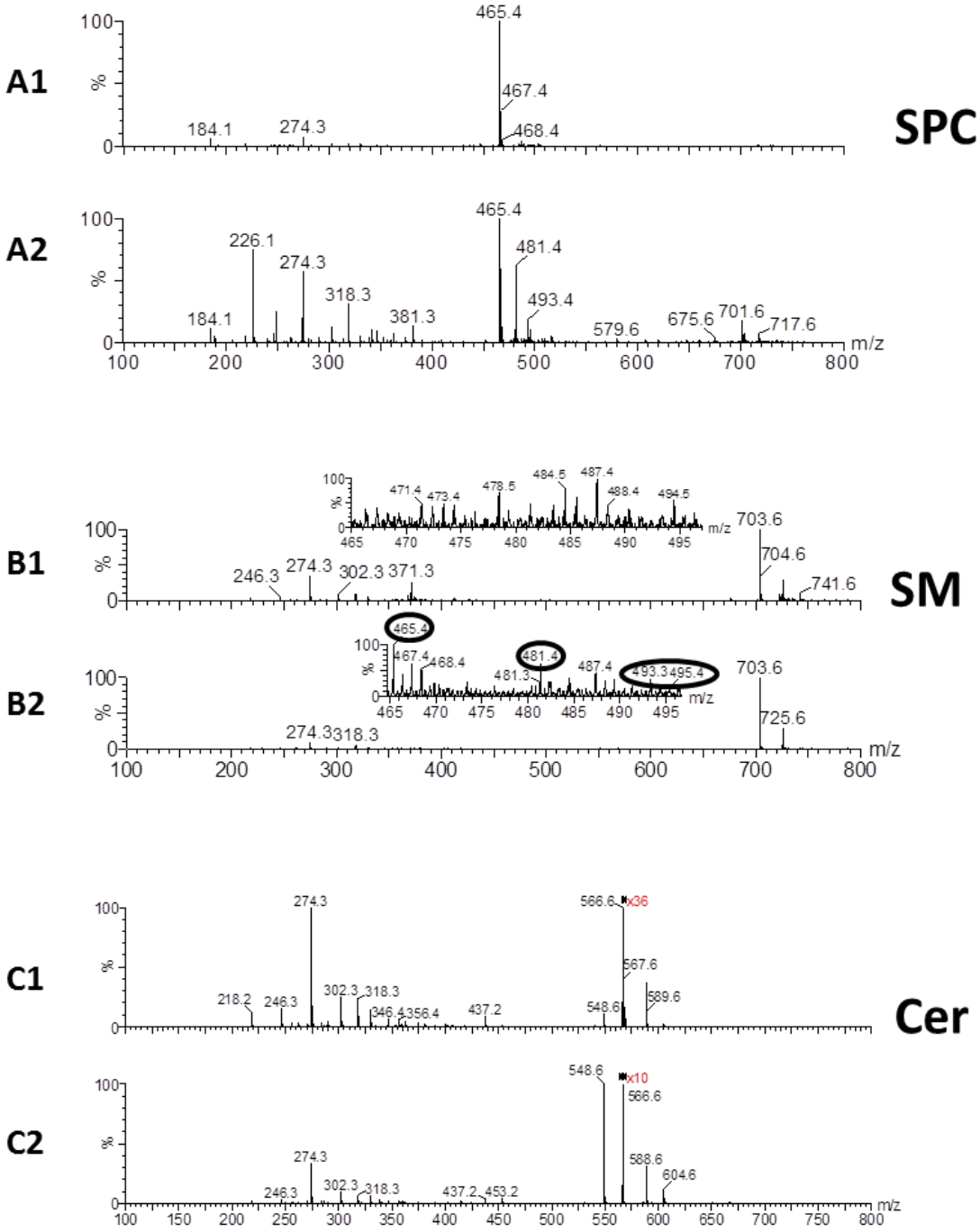

Figure 2. ESI-MS spectra of non-oxidized (A1) and oxidized (A2) SPC after one day of oxidation; non-oxidized (B1) and oxidized (B2) SM after seven days of oxidation; non-oxidized (C1) and oxidized (C2) Cer after seven days of oxidation.

Tandem mass spectra were used to identify the structures of the oxidation products observed for SPC and SM (Figure 3). Interpretation of the MS/MS spectra showed that the species observed at the same *m/z* were identical, providing further evidence that the oxidation products observed in oxidation of SM have the same structure as those observed for SPC oxidation. The MS/MS spectra of SM and SPC standards show a product ion at *m/z* 184.2, which is consistent with a phosphatidylcholine polar head group. Figure 3A-D shows the MS/MS spectra of the oxidation products observed in the ESI-MS spectra of oxidized SPC and SM. The tandem mass spectra of these oxidation products also show the product ion peak at *m/z* 184.2, confirming that they also have the phosphatidylcholine polar head group. The MS/MS spectrum of oxidation product observed at *m/z* 481.5 $[M+H+O]^+$, identified as the hydroxyl derivative of the SPC, show a product ion at *m/z* 298.4 (Figure 3A). This product ion is formed by cleavage of the sphingosine chain in the vicinity of the hydroxyl group, thus confirming the location of this group in C5 of sphingosine. In fact, phospholipid hydroxyl derivatives show typical fragmentation pattern due to cleavage of the C-C bonds next to the oxidation site, as observed in studies of oxidation of phosphatidylcholines, phosphatidylethanolamine and fatty acids, which allows to determine the location of the hydroxyl group [130-132].

The oxidation product observed at *m/z* 495.5 (SPC+2O-2Da), was identified as the oxidation product with additional keto and hydroxyl groups in the SPC moiety. It was not possible to identify the location of the keto moiety since the MS/MS spectrum of this ion only shows the product ion at *m/z* 184.2 (Figure 3B). We propose that C6 is most favorable oxidation site, since this leads to a conjugation system with the double bond of sphingosine, although alternative oxidation sites cannot be excluded. In that case, the hydroxyl group should be present on C2 (Figure 3B, Scheme 2). The tandem mass spectra of the oxidation product at *m/z* 493.5 ($[M+H+2O-4Da]^+$) shows the product ion peak at *m/z* 184.2 and a product ion at *m/z* 226.1 (acetaldehydephosphatidylcholine) (Figure 3C). Similarly, we propose that this oxidation product has a keto group present on C6, a hydroxyl group on C2 and an additional double bond, most probably due to oxidation of the hydroxyl group of the sphingosine to a keto group (Figure 3C, Scheme 2).

In the mass spectra of oxidized SPC, the major peak attributed to an oxidation product is observed at *m/z* 226.1 (Figure 2 A2). This peak is also present, with the low relative abundance, in the mass spectra of oxidized SM samples (Figure 2 B2).

The elemental formula of $C_7H_{17}NO_5P$ (error -1.5 ppm) was deduced from accurate mass measurements of molecular ion peak at *m/z* 226.1. The MS/MS spectrum of this oxidation product shows product ions at *m/z* 184.2 (choline polar head group), and at *m/z* 104.1 ($-N(CH_3)_3(CH_2)_2OH$), 86.1 ($-N(CH_3)_3CHCH_2$), 123.0 ($-COHCH_2HPO_3$) and 167.0 ($-N(CH_3)_3$) (Figure 3D).

Altogether, this information suggests that the oxidation product observed at *m/z* 226.1 was produced by the oxidative cleavage of C2-C3 bond of the sphingosine backbone (Scheme 2). The C2 carbon is a tertiary carbon, allowing the formation of a tertiary radical, in consequence by abstraction of a sphingosine hydrogen atom by the hydroxyl radical, which seems to be stabilized by the presence of a free primary amine group [133-135]. This intermediary leads to the formation of alkoxyl radical, which may induce cleavage of the sphingosine backbone and further loss of NH_2 *termini*.

Interestingly, it was possible to detect the presence of SPC oxidation products just after one day of oxidation, while for SM, oxidation products were only detected after seven days of oxidation. This observation suggests that SPC is more susceptible to oxidative modification compared to SM. Curiously, a recent study found that SPC induces apoptosis of endothelial cells through reactive oxygen species-mediated activation [124].

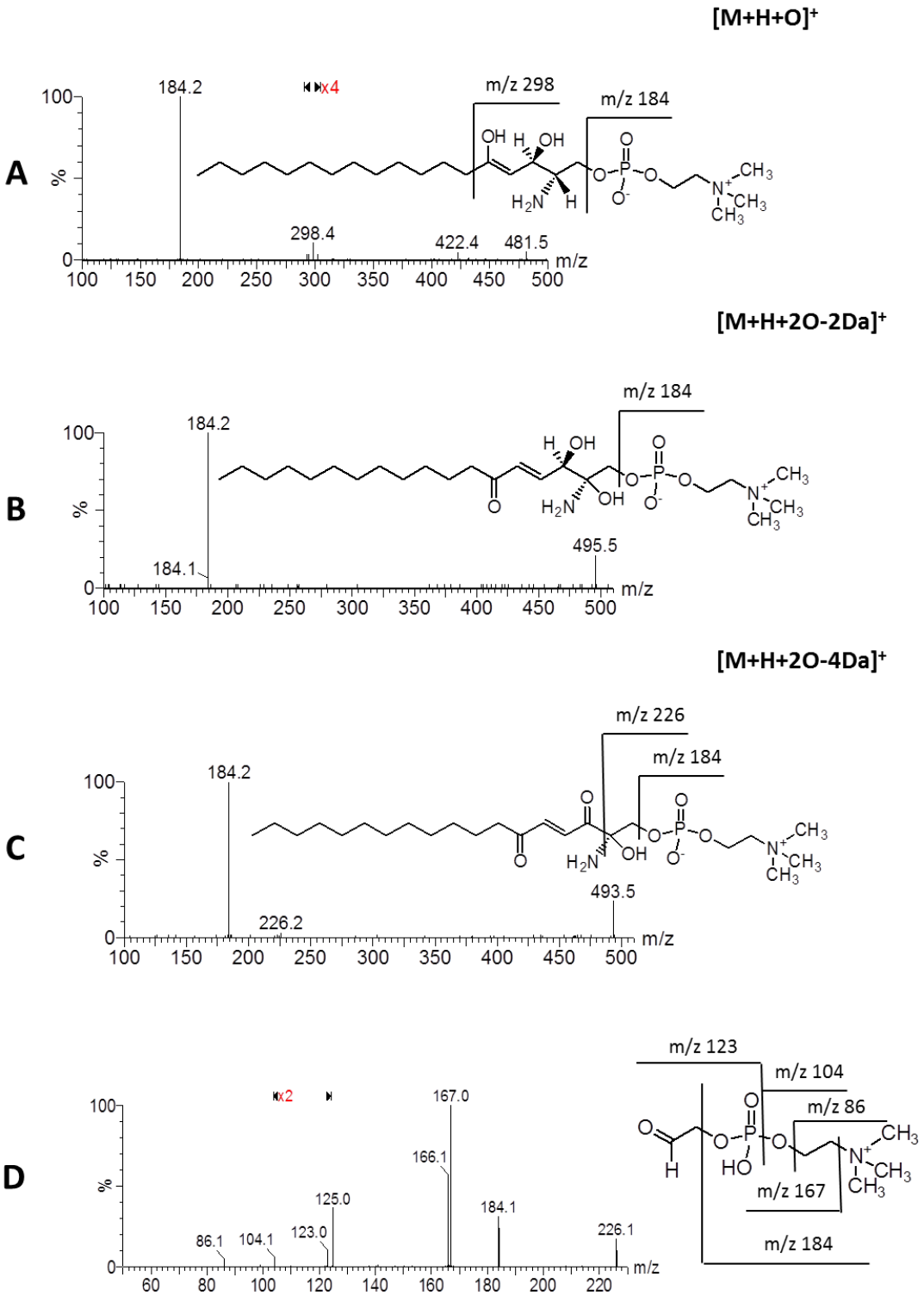

Figure 3. ESI-MS/MS spectrum of oxidation products of SPC by hydroxyl radical under Fenton reaction conditions. A) ESI-MS/MS spectrum of the ion at *m/z* 481 ($[M-H+O]^+$); B) ESI-MS/MS spectrum of the ion at *m/z* 495 ($[M-H+2O-2Da]^+$); C) ESI-MS/MS spectrum of the ion at *m/z* 493 ($[M-H+2O-4Da]^+$); D) ESI-MS/MS spectrum of ion at *m/z* 226.

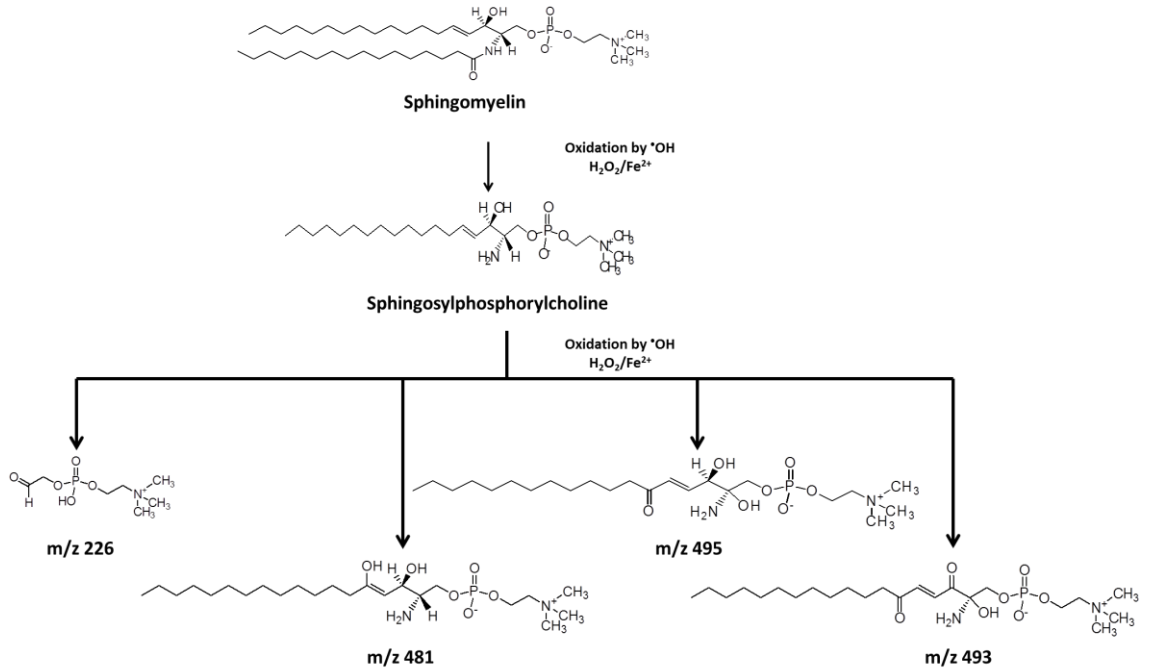

Scheme 2. Structure of oxidation products of SM and SPC by hydroxyl radical under Fenton reaction conditions.

Conclusions

The purpose of the current study was to determine the changes in sphingolipids molecular structure under oxidative stress conditions. This study has shown that SPC is more susceptible to oxidative modification compared to SM. No oxidation products were observed from ceramide. Also, we have shown that oxidation of SM involves the sphingosine backbone and elimination of the acyl chain and we have identified several oxidation products. These findings enhance our understanding of sphingolipids oxidation, although more research is needed to better understand its biological relevance.

Acknowledgments

Thanks are due to Fundação para a Ciência e a Tecnologia and COMPTE for funding to REDE/1504/REM/2005 (that concerns the Portuguese Mass Spectrometry Network), QOPNA (Research Unit 62/94) and Research Unit in Vila Real (POCTI-SFA-3-616).

CHAPTER III

Lipidomic approach of the biological activity of tacrine and two tacrine-analogues on rat non-synaptic brain mitochondria

Lipidomic approach of the biological activity of tacrine and two tacrine-analogues on rat non-synaptic brain mitochondria

Tânia Melo[a], Romeu A. Videira[b], M. Manuel Oliveira[c], Sónia André[b], A.M. Oliveira-Campos[d], Lígia M. Rodrigues[d], Maria R.M. Domingues[a*] and Francisco Peixoto[b]

[a]Mass Spectrometry Centre, Chemistry Department, University of Aveiro, 3810-193 Aveiro, Portugal

[b]CECAV, Chemistry Department, University of Trás-os-Montes e Alto Douro, 5001-801 Vila Real, Portugal

[c]CQ-VR, Chemistry Department, University of Trás-os-Montes e Alto Douro, 5001-801 Vila Real, Portugal

[d]CQ, Chemistry Department, University of Minho, Campus de Gualtar, 4710-057 Braga, Portugal

* Author to whom correspondence should be addressed:

M.Rosário M. Domingues

e-mail: mrd@ua.pt

Phone:+351 234 370 698

Fax:+ 351 234 370 084

Abstract

Alzheimer's disease is a neurodegenerative disorder characterized by progressive impairments in memory and cognition. Recently, the development and progression of Alzheimer's disease was also associated with increased neuronal oxidative stress and mitochondrial dysfunction, which contributes to increasing the oxidative processes at the neuronal level, affecting multiple cellular components, including phospholipids. Tacrine is a cholinesterase inhibitor used to improve neuronal communication by inhibiting the degradation of a signaling molecule called acetylcholine. Unfortunately there is some evidence for toxicity of tacrine. However, the search for tacrine analogues, with less toxicological effects, is still of interest. In this study, mass spectrometry coupled with separation techniques was used to identify alteration in the profile of phospholipids from non-synaptic mitochondria of rat brain treated with tacrine and two proposed analogues T1 and T2. Bioenergetics assays was used to evaluate the activity of non-synaptic mitochondrial respiratory complexes isolated from rats treated with tacrine, T1 and T2 analogues. Tacrine induced some significant changes in mitochondrial phospholipid profile, namely in PC, PI, PE and CL content, seems to increase the susceptibility of PS to undergo oxidation, and affects the activity of mitochondrial enzymes. T1 and T2 analogues also induce some of these changes but in a less expressive way comparing with tacrine.

Key-words (4): phospholipids, mass spectrometry, mitochondria, tacrine

Introduction

Alzheimer's disease (AD) is the generic name for a process of progressive dementia characterized in the early stages by a profound inability to form new memories. The prevalence of this disease in developed countries has increased substantially with the increase in life expectancy. Thus, age is considered the main risk factor supporting the hypothesis that oxidative stress should play an important role in disease pathogenesis [136]. Even knowing that, the molecular mechanisms underlying the onset of disease as well as various aspects related to its progression still remain unclear, and no effective therapy for AD is available yet. However, experimental evidences show that the pathological hall-marks of AD are the extracellular accumulation of senile plaques (mostly formed by deposition of amyloid-beta peptide) and the intracellular formation of neurofibrillary tangles composed by hyperphosphorylated tau protein [137]. Additionally, clinical and laboratory analyses of AD suggests the involvement of early synaptic dysfunction followed by a progressive synaptic loss, formation of neurofibrillary tangles and finally neuronal death [138]. Considering that cholinergic dysfunction and neuronal loss in brain regions involved in learning and memory contribute to the cognitive deficit in AD [139] as well as the fact that acetylcholinesterase (AChE) activity is increased around senile plaques [140], the therapeutic strategies to treat this disease have mainly focused on drugs to increase cholinergic transmission by blocking the Acetylcholine hydrolysis. In this context, tacrine, a reversible AChE inhibitor partly competitive with the substrate acetylcholine [141], was the first molecule approved for the clinical treatment of AD. Unfortunately, the clinical use of this molecule has been demonstrated to induce side effects, including hepatotoxicity as indicated by an increase in transaminase levels [142]. Although the molecular mechanisms of hepatotoxicity are still not understood, experimental studies suggest that the toxic tacrine-metabolites [142,143], oxidative stress [144,145], biophysical changes in cell membrane organization [22,146,147] and mitochondria impairment [8] play an important role in tacrine toxicity. Despite the toxic effects caused by tacrine have limited its therapeutic use in AD, they have also stimulated research in order to design tacrine-related compounds with improved efficiency and

biological selectivity [148]. However, the attributes of neuroprotection assigned to tacrine as well as to several tacrine-analogues cannot be accounted exclusively through their action on AChE.

For example, tacrine inhibits the axonal-potassium efflux increasing the duration of the action potentials [149]. In addition, the uptake of noradrelalina, dopamine and seronotina by storage vesicles is also inhibited by tacrine, suggesting widespread effects on the monoaminergic system [150].

The above results suggest that the biological effects of the cholinesterase inhibitor tacrine congeners are membrane connected as consequence of changes in organization and/or lipid composition, as is also postulated for others protonatable lipophilic amines [147,151]. An interaction favoured by lipophilic and amphipatic character of these compounds.

On the other hand, the mitochondrium is an organelle with high relevance to the eukaryotic cells, since they are responsible for the synthesis of more than 90% of the ATP used by the cell [152]. Changes in mitochondria functionality, which are dependent of specific lipid membrane composition [15], have a relevant importance to clarify the mechanism underlying xenobiotics toxicity [152]. The mitochondria-phospholipid composition influence the cell susceptibility to apoptosis and/or necrosis, since it reflect the redox state of cell and modulate the cytochrome *c* release [153,154].

Thus, the aim of the present work is to evaluate the effects induced by a single dose of tacrine or two novel tacrine analogues (figure 1) on lipid profile of non-synaptic rat brain mitochondria and how these putatively changes are reflected on mitochondrial bioenergetics.

Additionally, the effects of those compounds on brain AChE activity were also evaluated. The Phospholipids profile was evaluated by mass spectrometry, using a lipidomic approach [155]. The different Phospholipids classes were initially separated by TLC and further analyzed by ESI-MS and by tandem mass spectrometry (ESI-MS/MS), allowing the identification of the detailed structural, namely PL polar head and fatty acyl composition.

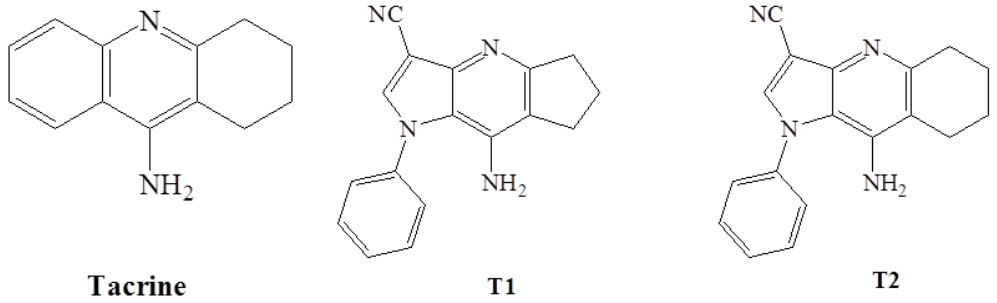

Figure 1. Chemical structure of Tacrine and analogues. Tacrine - 1,2,3,4-tetrahydroacridin-9-amine; T1 -8-Amino-1,5,6,7-tetrahydro-1-phenylcyclopenta[e]pyrrolo[3,2-b]pyridine-3-carbonitrile; T2 -9-Amino-5,6,7,8-tetrahydro-1-phenyl-1H-pyrrolo[3,2-b]quinoline-3-carbonitrile.

Main PLs identified in non-synaptic mitochondria included phosphatidylcholines (PC), phosphatidylethanolamines (PE), phosphatidylinositols (PI), phosphatidylserines (PS), cardiolipins (CL), and small amounts of sphingomyelin (SM). Therefore, the characterization the brain mitochondrial lipid changes connected with tacrine or with tacrine analogues are important to understand the mechanism underlying chemical toxicity and/or positive biomedical benefits of these AChE inhibits.

Experimental

Material

Biological Samples

As biological material we used non-synaptic mitochondria from brain cortex of male Wistar rats non-treated (control) and treated with tacrine and two analogues (T1 and T2). Male Wistar rats were purchased from Charles River (Spain, Barcelona).

Cholinesterase Assay

Acetylthiocholine iodide (ATCI) and 5,5'-dithiobis-(2-nitrobenzoic acid) (DNTB) were purchased from Sigma-Aldrich (Madrid, Spain).

Thin Layer Chromatography (TLC) and Silica Extraction

For TLC were used the TLC silica gel 60 plates with concentrating zone 2.5x20cm, (Merck, Germany) and reagents: boric acid (DHB chemicals), absolute ethanol (Panreac, Spain), triethylamine (Merck, Germany), primuline and acetone (Sigma-Aldrich, Spain), chloroform (HPLC grade), methanol (HPLC grade), purified milli-Q water (Millipore, USA).

The phosphatidic acid (PA), phosphatidylcholine (PC), phosphatidylethanolamines (PE), phosphatidylinositol (PI), phosphatidylserine (PS), sphingomyelin (SM), ceramide and cardiolipin (CL) standards were purchased from Avanti Polar Lipids, Inc (Alabama, USA).

All standards and reagents were used without further purification.

Quantification

For quantification were used perchloric acid 70 % (Panreac, Spain), ammonium molibdate (Riedel-de Haën, Germany), ascorbic acid (VWR BDH Prolabo, UK), chloroform (HPLC grade) and sodium dihydrogenphosphate dihydrated, $NaH_2PO_4.2H_2O$ (Riedel-de Haën, Germany). All reagents were used without further purification.

Animal Care

The experiments were carried out in accordance with the National (DL 129/92; DL 197/96; P 1131/97) and European Convention for the Protection of Animals used for Experimental and Other Scientific Purposes and related European Legislation (OJ L 222, 24.8.1999). Male Wistar rats, purchased from Charles River (Spain, Barcelona) were acclimatized to standard laboratory conditions (temperature 24±2ºC, relative humidity 55±5% and a 12 hour photoperiod) in polycarbonate cages (five rats per cage) for 1 week prior to the beginning of the experiment. During the entire period of the study, the mice were fed both water and supplemented standardized diet *ad libitum*.

Drug Treatment

Twenty male Wistar rats, weighing between 250 and 300 g, were randomly assigned to four experimental groups, with five animals in each. In the Control group, rats were intraperitoneally injected with a single dose of DMSO (the solvent used to solubilise the

three drugs); In the Tacrine treatment group, the animals were injected intraperitoneally with a single dose of tacrine (15 mg/Kg); In T1 and T2 experimental groups, the tacrine analogues were also administered intraperitoneally at single dose of 30 mg/Kg, which is, in terms of molar concentration, equivalent to the dose of tacrine. Eighteen hours after treatment, control and treated animals were sacrificed by cervical displacement and the cerebral cortex was dissected and used to isolate non-synaptic brain mitochondria and to determine brain Acetylcholinesterase activity.

Cholinesterase Assay

Rat brain AChE activity was determined colorimetrically by Ellman's Method, with slightly modifications [156]. Samples of cerebral cortex of the control and treated rats were diced and homogenized (1:10 w/v) in cold buffer containing 160 mM sucrose, 10 mM Tris-HCl, pH 7.2. The homogenates were centrifuged at 10 000 *g* for 10 min, at 4ºC. The pellet was discharged and the supernatant used for the enzymatic assays. The protein concentration of the supernatants was determined by biuret method using bovine serum albumin as a standard [157]. Afterwards, 10 µL of brain homogenate was placed in quartz cuvettes containing 2 ml of the phosphate buffer (0.1 M KH_2PO_4, pH 7.4) and 10 µL of Ellman's reagent (0.15 mM of DTNB (5,5'-Dithio-bis(2-nitrobenzoic acid) in 0.1 M phosphate buffer pH 7.4). After pre-incubation for 2 minutes, the reaction was initiated by adding acetylthiocholine (ACTI), as substrate. The catalytic activity is measured by following the increase of the absorbance at 412 nm (i.e., the yellow anion 5-thio-2-nitrobenzoate produced from thiocholine when it reacts with DTNB) for 3 minutes, using a Cary 50 UV-Vis spectrophotometer, at 25ºC. The AChE activity was evaluated as a function of substrate concentration, using seven concentrations of ACTI ranging from 28 to 3000 µM, to determine the Michaelis-Menten kinetic parameters K_m (Michaelis constant) and V_{max} (maximal velocity).

Non-synaptic brain mitochondrial isolation and purification

Non-synaptic rat brain mitochondria were isolated combining differential centrifugation and discontinuous ficoll and sucrose density gradients centrifugation. First, the non-synaptic mitochondria fraction was obtained with a ficoll gradient, and then purified using a sucrose discontinuous gradient to yield highly enriched mitochondria populations free of miyelin contamination, as previously described [15]. Briefly, the cerebral cortex obtained from control and treated animals were homogenized with a Potter–Elvehjem in a medium (MIB) containing 0.32 M sucrose, 10 mM Tris–HCl, and 1 mM ethylenediaminetetraacetic (EDTA), pH 7.4. Mitochondria isolation was performed at 4ºC without delay using differential centrifugation. The homogenate was differentially centrifuged at 1000 *g* for 5 min. Supernatant was collected and the pellet was washed twice by centrifugation at 1000 g for 5 min, collecting the supernatants each time. The collected supernatant was then spun at 14 000 g for 15 min. Supernatant was discarded and the pellet, which contained primarily non-synaptic mitochondria, synaptosomes, and myelin, was resuspended in MIB and was layered on a 7.5/12% discontinuous Ficoll gradient, made from a 20% Ficoll stock with MIB. The gradient was centrifuged at 73 000 *g* for 36 min (4ºC) in a Beckman L5-75B ultracentrifuge, rotor type 75 TI. The Ficoll gradient purified non-synaptic mitochondria were collected as a pellet below 12% Ficoll. The pellet, containing non-synaptic mitochondria was resuspended in MIB containing 0.5 mg/mL bovine serum albumin (BSA) and centrifuged at 12 000 *g* for 15 min. The resulting pellet was collected and resuspended in MIB. The resuspended pellet was layered on a discontinuous sucrose gradient containing 0.8/1.0/1.3/1.6 M sucrose. The gradients were made from a 1.6 M sucrose stock containing 1 mM EDTA-K and 10 mM Tris–HCl, pH 7.4. The discontinuous sucrose gradient was centrifuged at 50 000 *g* for 2 h (4ºC) in a Beckman L5-75B ultracentrifuge, rotor type 75 TI. Purified NS mitochondria were collected at the interface of 1.3 and 1.6 M sucrose and resuspended in (1:3, v/v) Tris-EDTA buffer (1 mM EDTA-K and 10 mM Tris–HCl, pH 7.4) containing 0.5 mg/mL BSA and centrifuged at 18 000 *g* for 15 min. The pellet was then resuspended in MIB and centrifuged at 12 000 g for 10 min. The pellet was again resuspended in MIB and

centrifuged at 8200 *g* for 10 min. The final concentration of the mitochondrial protein was determined by the biuret method [157], using BSA as standard.

Determination of mitochondrial enzyme activity

Complex I – The activity of this enzyme complex was evaluated spectrofluorometry, monitoring the decrease in fluorescence at 450 nm caused by NADH oxidation, as previously described [158]. The non-synaptic mitochondria obtained by differential centrifugation were submitted to three cycles of freezing/thawing. Afterwards, a volume of the mitochondrial fraction corresponding to 0.5 mg of protein was placed in quartz cuvettes containing 2 ml of the buffer solution (KH_2PO_4 25 mM, $MgCl_2$ 10 mM; pH 7.4) and KCN 1 mM. The reaction was initiated by the addition of NADH 50 µM. The fluorescence intensity was monitored as a function of time in a Varian Eclipse fluorescence spectrophotometer equipped with a thermostated cell holder, at 30ºC. The fluorescence intensity of NADH was measured at 450 nm with an excitation at 366 nm. The bandpass was 3 nm for excitation and emission beams. After to NADH fluorescence emission peak was reached, dodecylubiquinone 162.5 µM was added, with a consequent fall in fluorescence emission, graphically expressed by a line whose slope allowed the determination of mitochondrial complex I activity. In the final of each assay, a specific complex I inhibitor (rotenone 3.8 µM) was added, in order to guarantee that the rate of fluorescence decay were indeed complex I enzyme activity. Enzyme activity was the difference between the slopes of the lines before and after rotenone addition, determined with the software provided with the spectrofluorimeter. This value is expressed in arbitrary units.

Complex IV – The complex IV enzyme activity was evaluated by O_2 consumption associated with cytochrome c oxidation, in the presence of rotenone (specific inhibitor of complex I) and antimycin A (inhibitor of complexes II–III) [159]. The oxygen uptake was measured by the polarography technique using a Clark type oxygen electrode (Hansatech) coupled to a computer. Chamber volume adjustable from 1 to 2 ml is thermo stated at 30ºC. Mitochondrial homogenate (0.5 mg) was resuspended in 1 ml of standard reaction

medium (130 mM sucrose, 50 mM KCl, 5 mM MgCl2, 5 mM KH2PO4, and 5 mM Hepes, pH 7.2) supplemented with 3 µM rotenone, 0.1 µM antimycin A and 15 µM cytochrome c. The reaction was initiated with 10 µL of Ascorbate 500 mM/TMPD 250 mM, and O_2 consumption was was monitored for 5 min. KCN (2 mM) was used to inhibit complex IV activity. The difference between O_2 uptake before and after KCN addition was used to determine complex IV enzyme activity, expressed in nmol O_2/min/mg protein.

F_oF_1-ATPase – The activity of the F_oF_1-ATPase of non-synaptic brain mitochondria was determined by an electrometric technique (pH electrode), as previously described [160]. The cleavage of ATP releases protons. Thus, the kinetic of the reaction can be evaluated recording the continuous pH changes in reaction medium with pH electrode. The reaction occurred, at 30ºC, in open reaction thermostated chamber with permanent magnetic stirring in 2 ml of reaction medium (130 mM sucrose, 60 mM KCl, 0.5 mM Hepes and 2.5 mM MgCl 2, pH 7.0). The reaction medium was supplemented with rotenone 3 µM and 0.5 mg of mitochondrial protein and the reactions were initiated by the addition of 2 mM ATP-Mg. The release of protons was followed continuously with a Crison pH evaluation system consisting of a glass electrode connected to a Kipp and Zonen recorder. The addition of oligomycin (1 µg) to the medium completely abolished the production of protons. At the end of the reaction, pH titration was performed, using a standard HCl solution, for system calibration.

Extraction of phospholipids

The total lipids were extracted from of each mitochondrial extract according to the method of Bligh and Dyer [83]. We added 3.75 mL of $CHCl_3$:MeOH (1:2 v/v) to each 1 mL of mitochondrial extract, vortexed well and incubated on ice for 30 min. Then, an additional volume of 1.25 ml chloroform and 1.25 ml dH2O were added and finally, following vigorous vortex, samples were centrifuged at 1000 *g* for 5 min at room temperature, using a Mixtasel Centrifuge (Selecta), to obtain a two-phase system: aqueous upper phase and organic bottom phase which lipids were obtained. These extracts were dried with a nitrogen flow and stored at -20ºC for further analysis.

Separation of phospholipids classes by Thin Layer Chromatography (TLC)

PL classes from the total lipid extract were separated by thin layer chromatography (TLC) using silica gel 60 with concentrating zone 2.5x20cm. Prior to separation, plates were pre washed with $CHCl_3$:MeOH (1:1 v/v) and then were left in the *hotte* to dry for 15 min. After being dried, plates were sprayed with a solution of boric acid in ethanol (2.3% w/v) and placed in an oven at 100ºC for 15 min. Then, plates were left in the *hotte* to cool for subsequent application of lipid extracts. In each spot was applied 20 µL of phospholipid solution in chloroform (with a concentration of 150 µg of phospholipid per 100 µl). To control, we applied three spots with a mixture of phospholipids standards, including phosphatidylcholine, phosphatidylethanolamine and ceramide; sphingomyelin, phosphatidylserine and cardiolipin; phosphatidylinositol and phosphatidic acid.

The plates were dried in nitrogen flow and developed in solvent mixture chloroform/ethanol/water/triethylamine (30:35:7:35, v/v/v/v), in a chromatographic chamber. After complete elution, plates were left in the *hotte* until complete eluent evaporation. For phospholipids spots development, TLC plates were sprinkled with a primuline solution (50 µg/100 mL acetone: water, 80:20, v/v) and left to dry in the *hotte*. Then, we identified the different spots with UV light (λ = 254 nm). After identification of spots by comparison with phospholipid standards, spots were scraped off from the plates to glasses tubes. The different phospholipid classes were further quantified using the phosphorus assay, or were extracted from the silica with $CHCl_3$:MeOH (2:1) and analyzed by mass spectrometry in positive and negative modes, after dilution with methanol.

Quantification of phospholipids

In order to determine the phospholipid content of each lipid extract and compare the lipid content in each phospholipid class obtained by TLC, a phosphorus assay was performed according to Bartlett and Lewis [161].

For TLC samples, the silica spots were scraped off from the plates to glasses tubes for posterior quantification. In case of lipid extracts, 10 µL of sample were previously transferred to a glass tube and left to dry under a nitrogen flow until complete evaporation. Then, 650 µL of perchloric acid 70% were added to tubes, which were then

incubated for 45 min at 180ºC in the heating block (Stuart, U. K.); then were left to cool. To all tubes were added 3.3 mL of H_2O and vortexed well, 0.5 ml of ammonium molybdate (2.5 g ammonium molybdate/ 100 mL H_2O) and vortexed well and 0.5 mL of ascorbic acid (10 g ascorbic acid/ 100 mL H_2O) and vortexed well, followed by incubation for 10 min at 100ºC in a water bath. We also prepared several tubes for phosphate standards at concentrations of 0.1; 0.2; 0.4; 0.8; 1.6 and 2 µg of phosphorus from a phosphate standard solution of $NaH_2PO_4.2H_2O$ (100 µg/ mL of P), and underwent the same treatment of samples. After cool, 1 mL of samples being from TLC was transferred to an eppendorf and centrifuged at 4000 rpm for 5 min, in a Mini Spin Plus (Eppendorf) in order to remove silica from phospholipid; colored solution were removed and used to following read the absorvance. Finally, 200 µL of each standard and sample were added to each spot plate and were measured at 800 nm in a plate reader (Multiscan 90, ThermoScientific).

The amount of phosphorus present in each sample was calculated by linear regression through the graph which relates the amount of phosphorus present in the patterns (X-axis) and absorbance obtained from duplicates of various concentrations (Y-axis). The amount of phospholipid was directly calculated by multiplying the amount of result phosphorus by 25. The percentage of each phospholipid class refers to the total percentage of phospholipid phosphorus recovered from TLC, and was calculated by relating the amount of phosphorus in each spot to the total amount of phosphorus in the sample, thus giving the relative abundance of each PL class.

Silica Extraction

In order to analyze the different phospholipid classes by mass spectrometry, TLC spots corresponding to all identified classes were scraped off from the plates with the help of a spatula to a piece of aluminum paper, and then transferred to a glass tube. To all tubes were added 450 µL of $CHCl_3$, vortex well and left to stand for 5 min, in order to be able to extract the phospholipids from the silica. Then, samples, one by one, were filtered under vacuum with a sand plate funnel; 450 µL of $CHCl_3$/MeOH (1:1 v:v) were added to the tubes, vortex well and then filtered again. In order to remove some vestiges of silica

which might still exist, all samples were filtered again using a syringe (Hamilton GASTIGHT 1 mL, Sigma-Aldrich, Spain) containing filters (Syringe Driver Filter 0.22 µm, Millipore-Millex, USA). In order to recover some vestiges of sample, after filtration of samples the syringe was washed twice with 200 µL of chloroform. After each sample filtration, syringe and filter was thoroughly washed with methanol, and filter was changed every two filtered samples. The filtered samples were dried under nitrogen flow and were re-suspended in 100 µL of $CHCl_3$ to mass spectrometry analysis, or stored at -4ºC for further analysis.

Instrumentation

Extracts of each class of phospholipids were analyzed by mass spectrometry mass using electrospray ionization, using two different mass spectrometers: an electrospray linear ion trap and a triple quadrupole instrument.

The LQX linear ion trap mass spectrometer (ThermoFinnigan, San Jose, CA) was used in positive mode, with the following electrospray conditions: electrospray voltage of 5 kV, capillary temperature of 275ºC, gas flow of 25 units. In negative mode were used the same conditions by changing only: electrospray voltage of 4.7 kV. Isolation with of 0.5 Da was used with a 30 ms activation time for MS/MS experiments. Full scan MS spectra and MS/MS spectra were acquired with a 50 ms and 200 ms maximum ionization time, respectively. Normalized collision energy^{TM} (CE) was varied between 15 and 30 of arbitrary units for MS/MS performed on ions of interest. Data acquisition and treatment of results was performed using the Xcalibur data system (V2.0).

The triple quadruple instrument (Micromass, Manchester, UK) was used in positive mode for parent scan experiments, with the following electrospray conditions: electrospray voltage was 3.5 kV, capillary temperature of 300ºC, gas flow of 32 units. An isolation width of 0.5 Da was used with a 30 ms activation time for MS/MS experiments. Full scan MS spectra and MS/MS spectra were acquired with a 50 ms and 200 ms maximum ionization time, respectively. Normalized collision energy^{TM} (CE) was varied

between 20 and 30 for MS/MS. Data acquisition was carried out with a Mass Lynx data system (V4.0).

Statistical analysis

Results are presented as means ± standard error (raw data or expressed as percentage of control), for the number of results indicated. Results were analysed using the one way ANOVA test. The level of significance used was $P < 0.05$.

Results and Discussion

Acetylcholinesterase (AchE) activity

In order to confirm the biological effects of tacrine and its two proposed analogues we tested their capacity to inhibit AchE activity. Similar to tacrine, T1 and T2 analogues show inhibitory capacity for AchE, though tacrine T1 analogue was shown to be the most efficient in inhibiting AchE (figure 2). These results also confirm that as tacrine, T1 and T2 analogues can cross the blood brain barrier.

By analysis of Michaelis-Menten kinetic parameters (K_m and V_{max}) of brain acetylcholinesterase of control and treated groups we can conclude that inhibition exerted by tacrine and its analogues is non-competitive since increasing in Ach concentration, the degradation rate stops.

Electron Transport Chain (ECT) activities

Electron transport chain activities have been used to determine the effects of tacrine and its analogues in brain mitochondrial bioenergetics. The activities of Complexes I, IV, and V were significantly decreased for tacrine treated mitochondria. T1 analogue affects the activity of mitochondrial Complexes I and IV. In T2 analogue treated mitochondria the activity of Complex I was also decreased (figure 3).

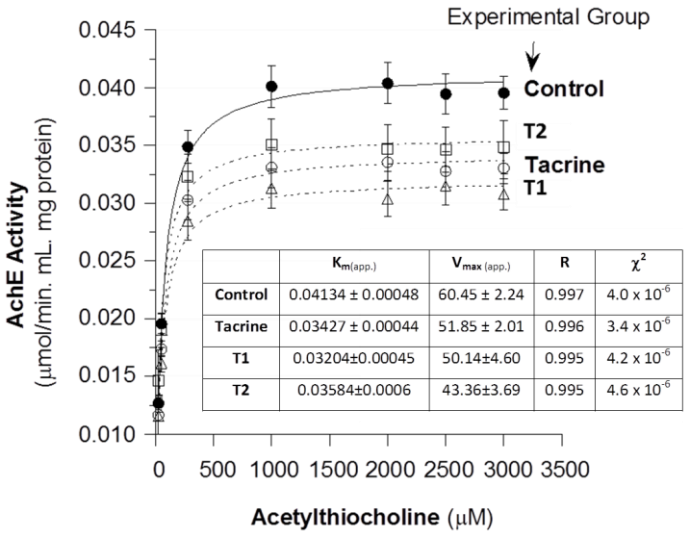

	$K_{m(app.)}$	$V_{max\ (app.)}$	R	χ^2
Control	0.04134 ± 0.00048	60.45 ± 2.24	0.997	4.0×10^{-6}
Tacrine	0.03427 ± 0.00044	51.85 ± 2.01	0.996	3.4×10^{-6}
T1	0.03204±0.00045	50.14±4.60	0.995	4.2×10^{-6}
T2	0.03584±0.0006	43.36±3.69	0.995	4.6×10^{-6}

Figure 2. Comparison of the values of the brain Acetylcholinesterase activity (AchE) of the four experimental groups (control, tacrine, T1 and T2 tacrine analogues). Data were fit to a Michaelis-Menten kinetic equation using the error minimization procedure of the KaleidaGraph software with a χ^2between successive iterations less than 0.001%. Insert - Apparent Michaelis-Menten kinetic parameters of brain acetylcholinesterase of control and the animal groups treated with tacrine and with its analogues (T1 and T2).

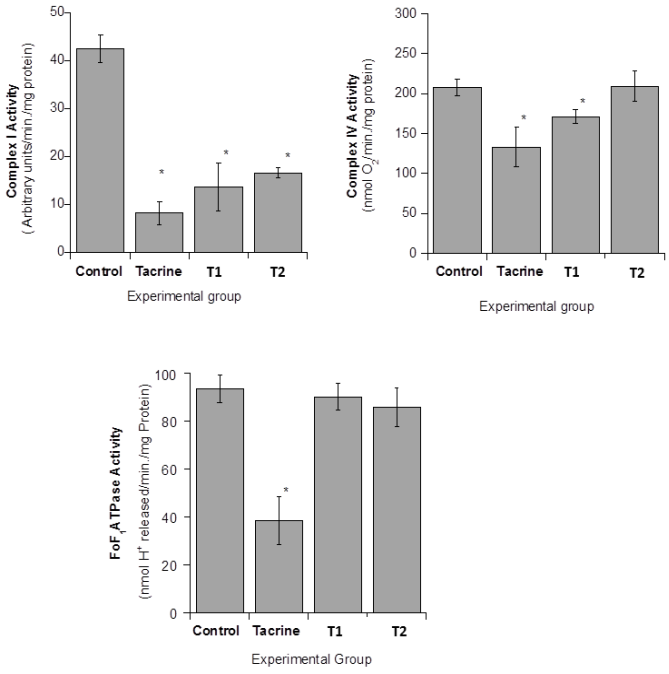

Figure 3. Comparison of the values of the enzyme activity of non-synaptic brain mitochondria of the four experimental groups (control, tacrine, T1, T2) for each of the complexes studied (I, IV and ATPase, in the presence of the substrate of each complex (NADH, ascorbate/TMPD or ADP, respectivelly). *Significantly different from control group ($P < 0.05$).

Lipidomic analysis of phospholipid profile of rat brain non-synaptic mitochondria

Lipidomics analysis of phospholipid profile of rat brain mitochondria was studied to evaluate the effect of treatment with tacrine and other synthetic analogues (T1 and T2) in phospholipid profile. This study was performed by analysis by ESI-MS in positive and negative modes of different classes of phospholipids, phosphatidylcholine (PC), phosphatidylethanolamine (PE), phosphatidylinositol (PI), phosphatidylserine (PS), sphingomyelin (SM), and cardiolipin (CL), after preliminary separation by Thin Layer Chromatography (TLC). Molecular characterization and fatty acyl composition within each class was assessed by ESI-MS and ESI-MS/MS. The different classes of phospholipids were also quantified using phosphorus assay [160].

Separation by Thin layer Chromatography (TLC) and phospholipid classes content

Phospholipid classes were fractionated by TLC and each class was identified by comparison with standards applied and subsequently confirmed by ESI-MS and ESI-MS/MS**.** A typical TLC profile of major phospholipid classes from the rat brain mitochondria are shown in figure 4. Different phospholipid spots were visualized using a primuline spray.

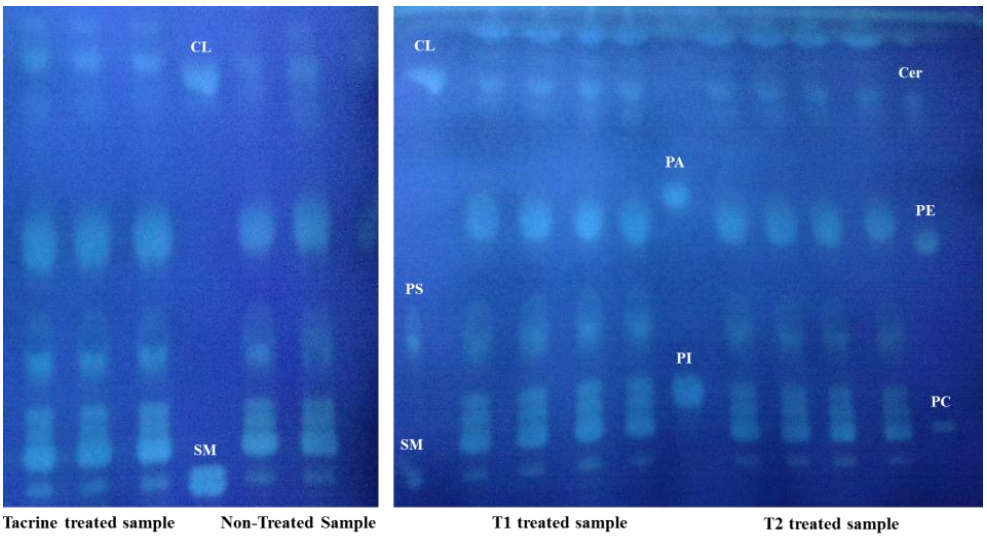

Figure 4. TLC of total lipid extract from rat brain non-synaptic mitochondria before (non-treated sample - control) and after tacrina and its analogues (T1 and T2) treatment. SM – sphingomyelin, PA – Phosphatidic Acid, PC– phosphatidylcholine, PI – phosphatidylinositol, PS – phosphatidylserine, PE – phosphatidylethanolamine, CL– cardiolipin, Cer-1P – Ceramide 1-Phosphate.

To evaluate the variation of phospholipid content each spot was quantified using phosphorous assay and the results are shown in figure 5. This analysis was performed in triplicate for each sample and different samples obtained in different days in order to confirmed the reproducibility.

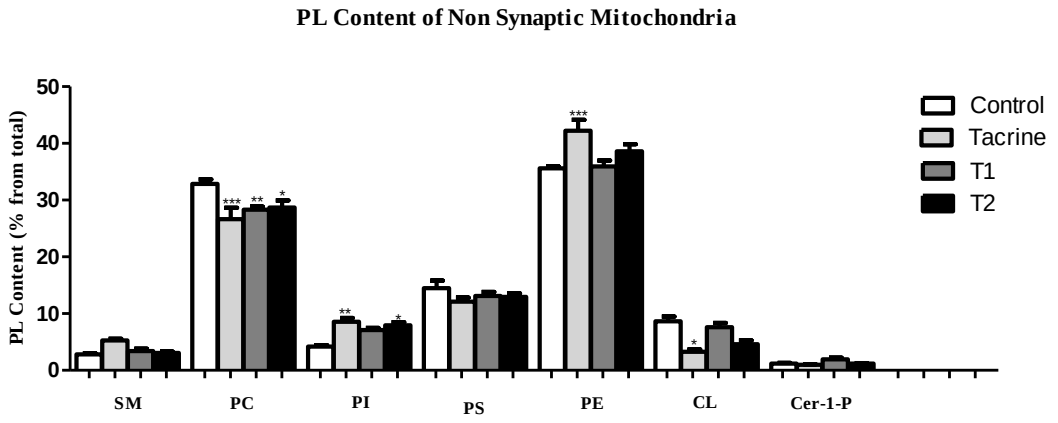

Figure 5. Phospholipid (PL) content of rat brain mitochondria non-treated and treated with tacrina and their analogues. SM – sphingomyelin, PC – phosphatidylcholine, PI – phosphatidylinositol, PS – phosphatidylserine, PE – phosphatidylethanolamine, CL– cardiolipin, Cer-1P – Ceramide 1-Phosphate. PL content, % from total refers to the percentage of phospholipid phosphorus recovered from respective TLC. * $p < 0,05$ versus non-treated, ** $p < 0,01$ versus non-treated, *** $p < 0,001$ versus non-treated, n=3 independent experiments.

In all samples, PC and PE represented the two dominant phospholipid classes of the total phospholipids, and this is in accordance with the results obtained by Kiebish and collaborators (2008) [15], that studied the lipid content of mitochondria from rat brain. Additionally other phospholipids in the order of their abundance – PS > PI > SM > CL > Cer-1P – in tacrine treated mitochondria; PS > CL > PI > SM > Cer-1P – in non-treated and tacrine T1 analogue treated mitochondria; and PS > PI > CL > SM > Cer-1P – in tacrine T2 analogue treated mitochondria were detected on the plates. No significant variation was observed for PS content. SM was increased in rat mitochondria treated with tacrina although not in a statistically significant way. PC were significantly decreased in all treated mitochondria while CL were significantly decreased only in Tacrina and T2 analogue treated mitochondria; PI levels were statistically increased in tacrina and T2 analogues

treated mitochondria; PE levels were statistically increased only in tacrina treated mitochondria comparing with non-treated mitochondria.

To evaluated if changes in content occur also with variation in the profile of the PL in each class, each spot was analysed by MS.

Analysis by MS

The characterization of molecular species included in each class was performed after extraction of silica and analyzed by MS in a positive mode for PC and SM and negative for PS, PI, PE and CL.

PE is one of the most abundant PLs in the membrane bilayers cell. The molecular species of PE were analyzed in negative mode, showing the $[M-H]^-$. The species identified from PE spot included two groups of molecular species: diacyl-PE (*m/z* 690, 714, 718, 744, 762, 764, 766, 768, 790, 794) and alkenyl-PE (*m/z* 726, 728, 750, 774, 776, 778) as resumed in table 1, and as shown in figure 6. All these ions were induced fragmentation by collision with a gas and the MS/MS spectrum obtained allowed the confirmation of these species, their composition in fatty acyl residues of both diacyl-PE and alkenyl-PE, and proposed localization along the glycerol backbone (table 1). For example, MS/MS spectra of diacyl PE at *m/z* 790, which dominated among other PE molecular species in all samples, show two abundant ions at *m/z* 283 and *m/z* 327, that correspond to stearic (C18:0) and docosahexaenoic (C22:6) acid fatty acyl residues, respectively (table 1). This approach was applied to all PE species allowing the confirmation of fatty acyl residues composition.

Analysis of table 1 indicates a predominance of unsaturated fatty acid namely oleic acid (C18:1), linoleic acid (C18:2), eicosatrienoic acid (C20:3), eicosatetraenoic acid (C20:4), , adrenic acid (22:4) and docosahexaenoic acid (C22:6).

Curiously in tacrine treated mitochondria some ions detected in this spot show fragmentation pathways distinct from PE. This fragmentation correspond a neutral loss 58 Da, which were identified recently to be typical of phospholipids with a terminal acetic acid in the polar head [135]. Interesting this modified phospholipids were formed during

PS *in vitro* oxidation. These species also contain oxygen atoms insertion in PS fatty acyl chains. Their composition was also confirmed by MS/MS as shown in figure 7.

Table 1. Major PE molecular species from rat brain non-synaptic mitochondria.

Class	$[M-H]^-$ *m/z*	Fatty Acyl Chains			
	(C:N)	Control	Tacrine	T1	T2
PE					
Diacyl species	690 (32:0)	16:0/16:0	16:0/16:0	16:0/16:0	16:0/16:0
	714 (34:2)	16:0/18:2	16:0/18:2	16:0/18:2	16:0/18:2
	718 (34:0)	16:0/18:0	16:0/18:0	16:0/18:0	16:0/18:0
	744 (36:1)	18:0/18:1	18:0/18:1	18:0/18:1	18:0/18:1
	745 (34:2)	-----	16:0/18:1+O-2Da	-----	-----
	747 (34:1)	-----	16:0/18:1+O	16:0/18:1+O	16:0/18:1+O
	762 (38:6)	16:0/22:6	16:0/22:6	16:0/22:6	16:0/22:6
	764 (38:5)	18:1/20:4	18:1/20:4	18:1/20:4	18:1/20:4
	766 (38:4)	18:0/20:4	18:0/20:4	18:0/20:4	18:0/20:4
	768 (38:3)	18:0/20:3	18:0/20:3	18:0/20:3	18:0/20:3
	768 (38:3)	20:1/18:2	20:1/18:2	20:1/18:2	20:1/18:2
	790 (40:6)	18:0/22:6	18:0/22:6	18:0/22:6	18:0/22:6
	794 (40:4)	18:0/22:4	18:0/22:4	18:0/22:4	18:0/22:4
	794 (40:4)	20:0/20:4	20:0/20:4	20:0/20:4	20:0/20:4
	794 (40:4)	20:3/20:1	20:3/20:1	20:3/20:1	20:3/20:1
PE					
Alkenyl-acyl species	726 (36:2)	18:1p/18:1	18:1p/18:1	18:1p/18:1	18:1p/18:1
	728 (36:1)	18:0p/18:1	18:0p/18:1	18:0p/18:1	18:0p/18:1
	728 (36:1)	16:0p/20:1	16:0p/20:1	16:0p/20:1	16:0p/20:1
	750 (38:4)	18:0p/20:4	18:0p/20:4	18:0p/20:4	18:0p/20:4
	750 (38:4)	16:0p/22:4	16:0p/22:4	16:0p/22:4	16:0p/22:4
	774 (40:6)	18:0p/22:6	18:0p/22:6	18:0p/22:6	18:0p/22:6
	776 (40:5)	18:1p/22:4	18:1p/22:4	18:1p/22:4	18:1p/22:4
	778 (40:4)	18:0p/22:4	18:0p/22:4	18:0p/22:4	18:0p/22:4

Phospholipids are designated as follows: diacyl 38:6 PE, where 38 indicates the summed number of carbon atoms at both the *sn*-1, *sn*-2, positions and 6 designates the summed number of double bonds at both positions. +O corresponds to molecular species of PS containing one hydroxyl group and +O-2Da corresponds to molecular species of PS containing one keto group. These m/z values indicate ratios of mass to charge for singly charged $[M-H]^-$ ions; p - an *sn*-1 vinyl ether (alkenyl- or plasmalogen) linkage.

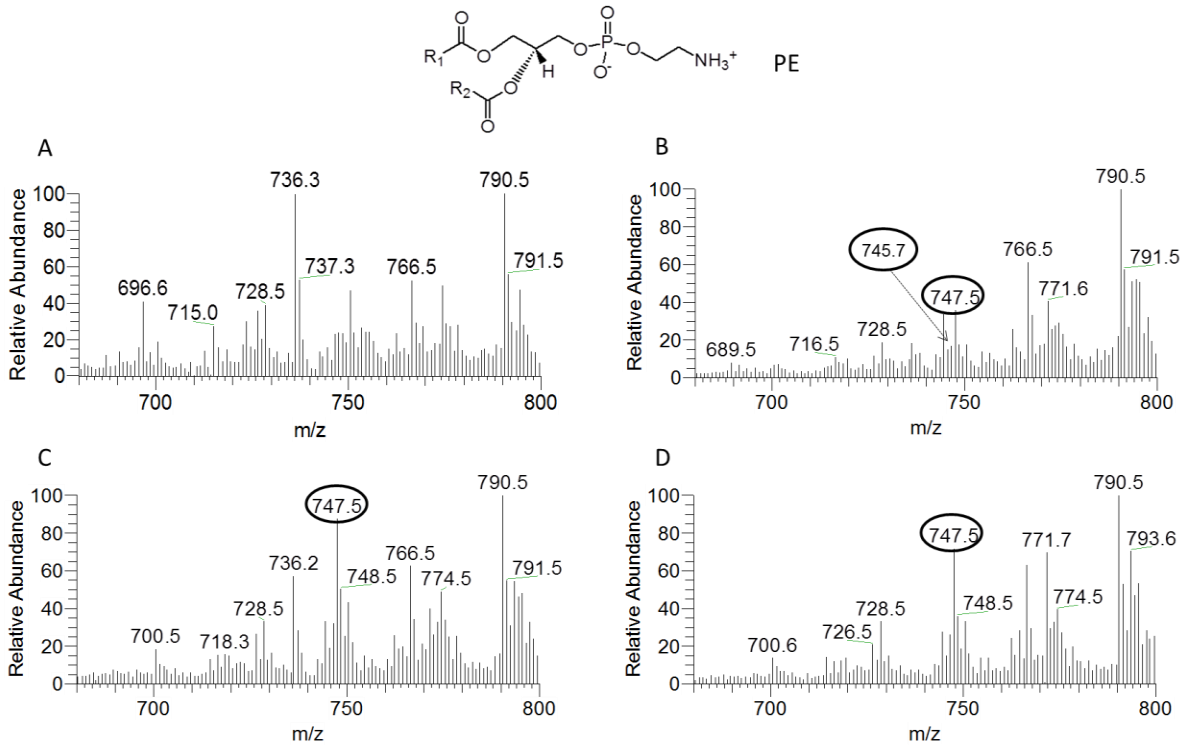

Figure 6. General PE structure; Negative ESI-MS spectra of PE molecular species from non-treated (A), tacrina (B), T1 (C) and T2 tacrine analogues (D) treated samples from rat brain non-synaptic mitochondria after their separation by TLC.

The typical PS neutral loss of 87 Da [162], is not observed for these ions but instead, is observed a neutral loss of 58 Da thus indicating that these products are formed from oxidative modification in PS polar head due to the loss of 58 Da (87-29) [135]. Ions with *m/z* 745 and 747 corresponds to $[760\text{-H+O-2Da-29}]^-$ and $[760\text{-H+O-29}]^-$ (figure 7). Ion at *m/z* 747 is also present in tacrine analogues treated mitochondria. The presence of oxidized species of PS which co-eluted in PE spot may suggest that the increase in PE content observed for tacrine and T2 analogue treated mitochondria (figure 5) may be due to the presence of these oxidized species instead of an increase in PE synthesis.

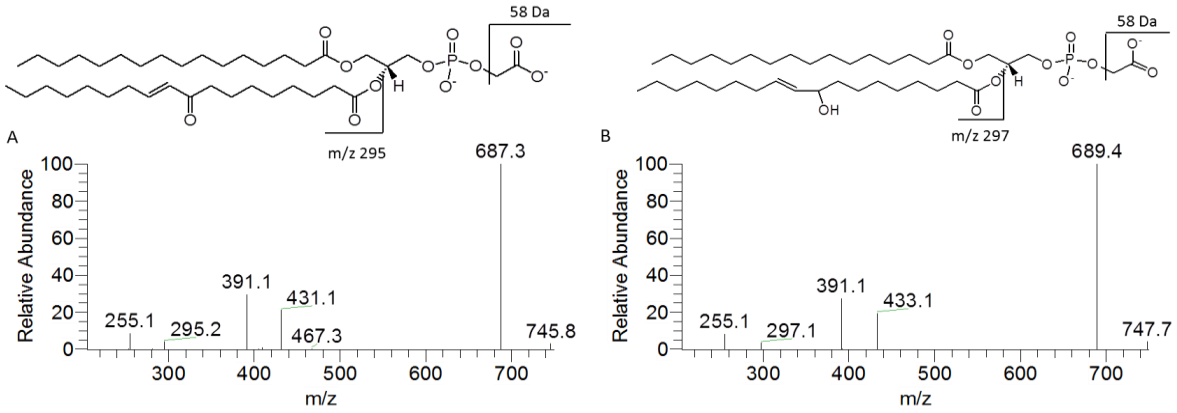

Figure 7. The MS/MS spectra of the $[M-H+O-2Da-29]^-$ (A) and $[M-H+O-29]^-$ (B) ions obtained by oxidation of PS (16:0/18:1) and the structures proposed [135].

Analysis of PS revealed molecular species at *m/z* 760, 788, 790, 806, 810, 834, 838, 842, 844, 862 and 864 (figure 8, table 2). The major ion for treated samples was observed at *m/z* 834 containing C18:0 (stearic acid) and C22:6 (docosahexaenoic acid) fatty acyl residues, while the non-treated mitochondria shows several abundant PS species being the ion at *m/z* 806, containing C18:2 (linoleic acid) and C20:4 (arachidonic acid) fatty acyl residues, the most abundant. MS spectrum of tacrine treated mitochondria (figure 8 B) shows an increase in relative abundance of ion at *m/z* 788 and a decrease in ions at *m/z* 806 and 862, by comparison with non-treated mitochondria (figure 8 A).

ESI-MS and MS/MS spectra of PS from tacrina and analogues treated mitochondria revealed some oxidized products corresponding to insertion of oxygen atoms in PS fatty acyl chains. This oxidation products were identified as PS hydroxide ($[M-H+O]^-$), keto ($[M-H+O-2Da]^-$) and peroxide ($[M-H+2O]^-$) derivatives, as have already been reported to be formed for PS under oxidative conditions, and were already studied by others groups [106,107]. Ions at *m/z* 774, 776 and 792 corresponds to $[760-H+O-2Da]^-$, $[760-H+O]^-$, and $[760-H+2O]^-$, respectively (table 2 and 3). These oxidized products are not present in non-treated mitochondria suggesting that tacrina increase the susceptibility to oxidation of mitochondrial PS. In tacrine analogues treated mitochondria these oxidation products are present in much lower abundance, which may suggest that tacrine analogues are less capable to increase the susceptibility to oxidation of mitochondrial PS.

Some PS oxidized products detected in PS spot correspond to oxidized species with a neutral loss 57 Da and 58 Da, which were identified recently to be typical of phospholipids with a terminal acetamide and acetic acid, respectively, in the polar head [135]. The typical PS neutral loss of 87 Da [162], is not observed for these ions but instead, is observed a neutral loss of 58 and 57 Da, respectively thus indicating that these products are formed from oxidative modification in PS polar head due to the loss of 58 Da (87-29) and 57 (87-30) [135]. Their composition was also confirmed by MS/MS as shown in figure 9. Ions at *m/z* 730 and 731 corresponds to $[760\text{-H-30}]^-$ and $[760\text{-H-29}]^-$, respectively. Ion at *m/z* 730 was also detected in tacrine analogues treated mitochondria but in much lower abundance.

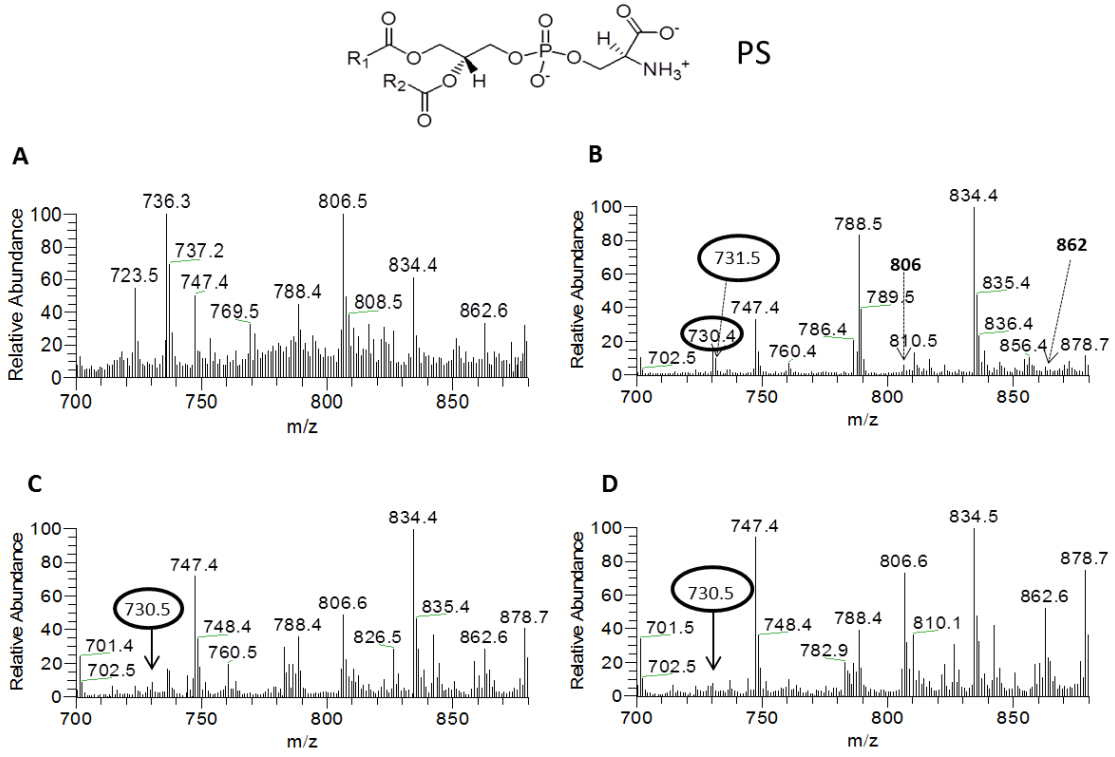

Figure 8. General PS structure; Negative ESI-MS spectra of PS molecular species from non-treated (A), tacrina (B), T1 (C) and T2 tacrine analogues (D) treated samples from rat brain non-synaptic mitochondria after their separation by TLC.

Table 2. Major PS molecular species from rat brain non-synaptic mitochondria.

Class	$[M-H]^-$ *m/z*	Fatty Acyl Chains			
	(C:N)	Control	Tacrine	T1	T2
PS					
Diacyl species	730 (34:1)	-----	16:0/18:1	16:0/18:1	16:0/18:1
	731 (34:1)	-----	16:0/18:1	-----	-----
	760 (34:1)	16:0/18:1	16:0/18:1	16:0/18:1	16:0/18:1
	774 (34:2)	-----	16:0/18:1+O-2Da	16:0/18:1+O-2Da	16:0/18:1+O-2Da
	776 (34:1)	-----	16:0/18:1+O	16:0/18:1+O	16:0/18:1+O
	788 (36:1)	18:0/18:1	18:0/18:1	18:0/18:1	18:0/18:1
	790 (36:0)	18:0/18:0	18:0/18:0	18:0/18:0	18:0/18:0
	792 (34:1)	-----	16:0/18:1+OO	16:0/18:1+OO	16:0/18:1+OO
	806 (38:6)	18:2/20:4	18:2/20:4	18:2/20:4	18:2/20:4
	810 (38:4)	18:0/20:4	18:0/20:4	18:0/20:4	18:0/20:4
	834 (40:6)	18:0/22:6	18:0/22:6	18:0/22:6	18:0/22:6
	838 (40:4)	18:0/22:4	18:0/22:4	18:0/22:4	18:0/22:4
	842 (40:2)	18:0/22:2	18:0/22:2	18:0/22:2	18:0/22:2
	844 (40:1)	18:0/22:1	18:0/22:1	18:0/22:1	18:0/22:1
	862 (42:10)	20:4/22:6	20:4/22:6	20:4/22:6	20:4/22:6
	864 (42:4)	20:0/22:4	20:0/22:4	20:0/22:4	20:0/22:4

Phospholipids are designated as follows: diacyl 40:6 PS, where 40 indicates the summed number of carbon atoms at both the *sn*-1, *sn*-2, positions and 6 designates the summed number of double bonds at both positions; +O corresponds to molecular species of PS containing one hydroxyl group, +O-2Da corresponds to molecular species of PS containing one keto group, and +OO correspond to molecular species of PS containing one peroxy group. These m/z values indicate ratios of mass to charge for singly charged $[M-H]^-$ ions.

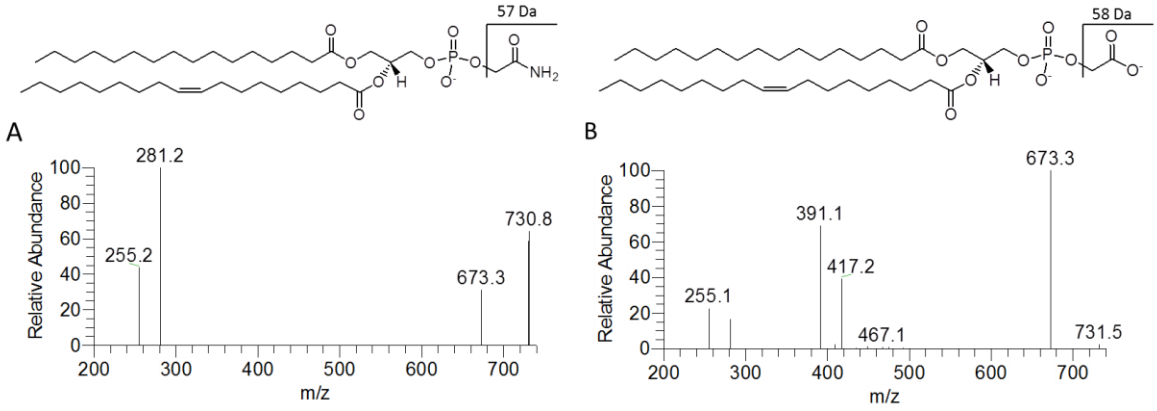

Figure 9. The M/MS spectra of the $[M-H-30]^-$ (A) and $[M-H-29]^-$ (B) ions obtained by oxidation of PS (16:0/18:1) head and the structures proposed [135].

Table 3. Major PS oxidized products from rat brain non-synaptic mitochondria due to tacrine and T1 and T2 analogues treatment.

Class	$[M-H]^-$ *m/z* (C:N)	Fatty Acyl Chains	Oxidation products			
			$[M-H+16]^-$	$[M-H-29]^-$	$[M-H-30]^-$	$[M-H-32]^-$
PS	760 (34:1)	16:0/18:1	776	731	730	792
	774 (34:2)	16:0/18:1+O-2Da	-----	745	-----	-----
	776 (34:1)	16:0/18:1+O	-----	747	-----	-----
	792(34:1)	16:0/18:1+OO	-----	763	-----	-----

Phospholipids are designated as follows: diacyl 34:1 PS, where 34 indicates the summed number of carbon atoms at both the *sn*-1, *sn*-2, positions and 1 designates the summed number of double bonds at both positions; +O correspond to molecular species of PS containing 1 hydroxy group ($[M-H+16]^-$), and +OO correspond to molecular species of PS containing 1 peroxy group ($[M-H+32]^-$). $[M-H+29]^-$ correspond to molecular species of polar head oxidized PS with loss of 58 Da and $[M-H+30]^-$ correspond to molecular species of polar head oxidized PS with loss of 57 Da. These m/z values indicate ratios of mass to charge for singly charged $[M-H]^-$ ions.

Analysis of PI in negative mode by ESI-MS revealed a predominant $[M-H]^-$ ion at *m/z* 885 (figure 10 A), identified as PI C18:0 (stearic acid) and C20:4 (arachidonic acid).

The other PIs identified are presented in table 5. Characteristic fragments characterizing the polar head group of PI, at *m/z* 241 identified as inositolphosphate with loss of water molecule and *m/z* 97 as $[H_2PO_4]^{2-}$ anion was also identified [49]. Although PI class increased with treatment with tacrine and analogues, the PI composition doesn't change, since MS is similar for both PI spot, and representative spectra of PI are shown in figure 10 A.

Tacrine is a lipophilic drug able to crosses the mitochondrial membrane [8], probably by interaction with phospholipids. Tacrine has an amine group positively charged at physiological pH that allows its insertion in membranes, increasing membrane positive charge. Probably, the observed increase in PI content in tacrine treated mitochondria may occur to balance the charges in mitochondrial membrane surface. Since PI classes are important signaling molecules, as described previously [60], this increase may suggest that signaling processes which involves these lipids are altered. Increase in PI content may

be also related with toxicological mechanism of this drug, since is described that tacrine preferentially binds to acidic-phospholipid containing membrane [22]. So these changes in PI content may allow the insertion of tacrine in mitochondrial membrane and probably allows it to crosses to membrane.

CL is located almost exclusively in the mitochondrial inner membrane where it constitutes about 20% of the total lipid composition. It is associated with several mitochondrial proteins and is essential for the optimal function of numerous enzymes that are involved in mitochondrial energy metabolism and has been implicated in the process of apoptosis. This phospholipid has a dimeric structure, corresponding at two phosphatidylglycerols connect with a glycerol backbone in the center [99]. So it has four alkyl groups and potentially possesses two negative charges resulting in either singly charged $[M-H]^-$ or doubly charged $[M-2H]^{2-}$ ions observable in the MS spectra [98]. Singly charged ions of CL in negative mode were represented by at least 7 different molecular clusters with *m/z* 1427, 1455, 1477, 1499, 1525, 1553 and 1575 with a variety of fatty acid residues (from C16:0 to C22:6). Typical ions formed during fragmentation process of CL (a, b, a+56, or b+136) were identified in MS^2 spectra as described by Hsu and co-authors [98] and are resumed in table 4. CL composition doesn't change between samples, since MS is similar for both CL spots, and representative spectra of CL are shown in figure 10 B.

Decrease in CL content due to tacrine and T2 analogue treatment (figure 5) may be due to a decrease in its production which could be related to increase in PI content, since they are produced from same precursor (scheme 1). This preference for increase PI content instead CL content may be related to toxicity mechanism of these drugs. CL is a phospholipid essential for normal mitochondrial function and bioenergetics due to its interaction with complexes III and IV, and also forms a complex with cytochrome c which plays a regulatory role in apoptosis. Analysis of figure 3 shows that in tacrine treated mitochondria the activity of mitochondrial complexes I, IV and V are significantly decreased which may be related with this decrease in CL content.

Decreases in CL content may be also related with changes in PS content. By analysis of table 3 is possible to observe that at least seven species of oxidized PS were derived from PS 16:0/18:1. So decreases in CL content may be due to remodeling of CL species with C16:0 and C18:1 as fatty acyl chains in order to restore PS 16:0/18:1 levels.

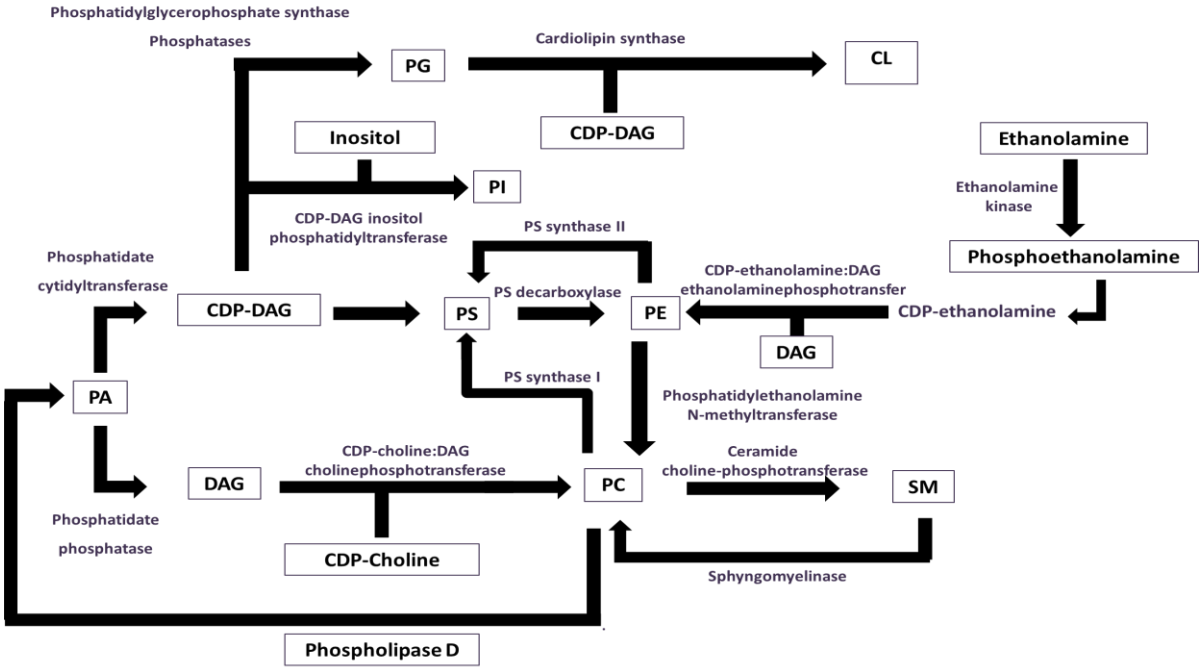

Scheme 1. Phospholipid biosynthetic pathways. CDP-choline – cytidine diphosphate, DAG – Diacylglycerol, CDP-DAG – cytidine diphosphate diacylglycerol. PA – Phosphatidic Acid, PC – phosphatidylcholine, PE – phosphatidylethanolamine, PG – Phosphatidylglycerol, PI – phosphatidylinositol, PS – phosphatidylserine, CL– cardiolipin, SM – sphingomyelin.

PC is one of the most abundant PLs in the cell, and the most important structural PL in the membrane. PC ionize in positive mode as $[M+H]^+$ and the typical MS/MS spectra show a major ion correspondent to the choline phosphate fragment ion at *m/z* 184 [60]. Since in the MS spectra it is also observed the $[M+Na]^+$ ions that can lead to some misinterpretations and in order to obtain exclusively the $[M+H]^+$ ions, parent scan of the *m/z* 184 was performed (figure 10 D) and demonstrated the presence of the major PC molecular species as $[M+H]^+$ ions at *m/z* 734, 746, 760, 782, 788, 806, 810 and 834.

However, ions regarding structural information are of low abundance. We performed MS/MS analysis of all these ions to obtain the confirmation of fatty acyl residues composition of both diacyl-PC and alkenyl-PC and their location along the glycerol backbone (table 6).

On the other hand the MS/MS spectra of the alkenyl-acyl show only the $R_2C=C=O$, and considering the molecular weight it allows to identify the composition of alkenyl chain. This approach was applied to all PC species allowing the confirmation of fatty acid composition. Although PC class content decreases by treatment with tacrine and analogues (figure 5), the PC composition doesn't change, since MS is similar for both PC spots, and representative spectra of PC are shown in figure 10 D.

Decrease in PC content may be related to increase in SM content verified for all conditions as shown in figure 5, since the precursors and synthesis pathways of these two lipids are related (scheme 1). On the other hand, decreases in PC content may be also related with PS content alterations. By analysis of figure 10 D is possible to observe that the major PC molecular specie is at *m/z* 760, which corresponds to 16:0/18:1 (table 6), and by analysis of table 3 is possible to observe that at least seven species of oxidized PS were derived from PS 16:0/18:1. So decreases in PC content by be due to remodeling of polar head by phospholipase D of PC species with C16:0 and C18:1 as fatty acyl chains in order to restore PS 16:0/18:1 levels.

It is also important refer that this decrease in PC content may also be associated with the toxicological mechanism of this drug, because may contribute to alterations in mitochondrial membrane integrity and properties.

SM has important functions in the cytoplasmic membrane structure and cell signaling. As PC, SM species ionize in positive mode as $[M+H]^+$ forming a typical choline phosphate fragment ion at *m/z* 184 as the common abundant fragment ion [60]. SM identification was obtained by parent scan of the ion *m/z* 184 similar as performed for PC, but they can be easily discriminated since PC appear at even *m/z* values, whereas protonated molecules of SM exhibit odd *m/z* values due to the presence of an additional nitrogen atom in SM (figure 10 C) [49]. The major SM molecular species identified are resumed in

table 6, and corresponds at *m/z* 703 and 731, which correspond to SM containing a C16:0 (palmitic acid) and C18:0 (stearic acid) fatty acyl chains, respectively. MS spectrum of SM from all spots is similar, and representative spectra of SM are shown in figure 10 C.

The increase in SM content (figure 5) may suggest that the signaling processes which involve these lipids are altered.

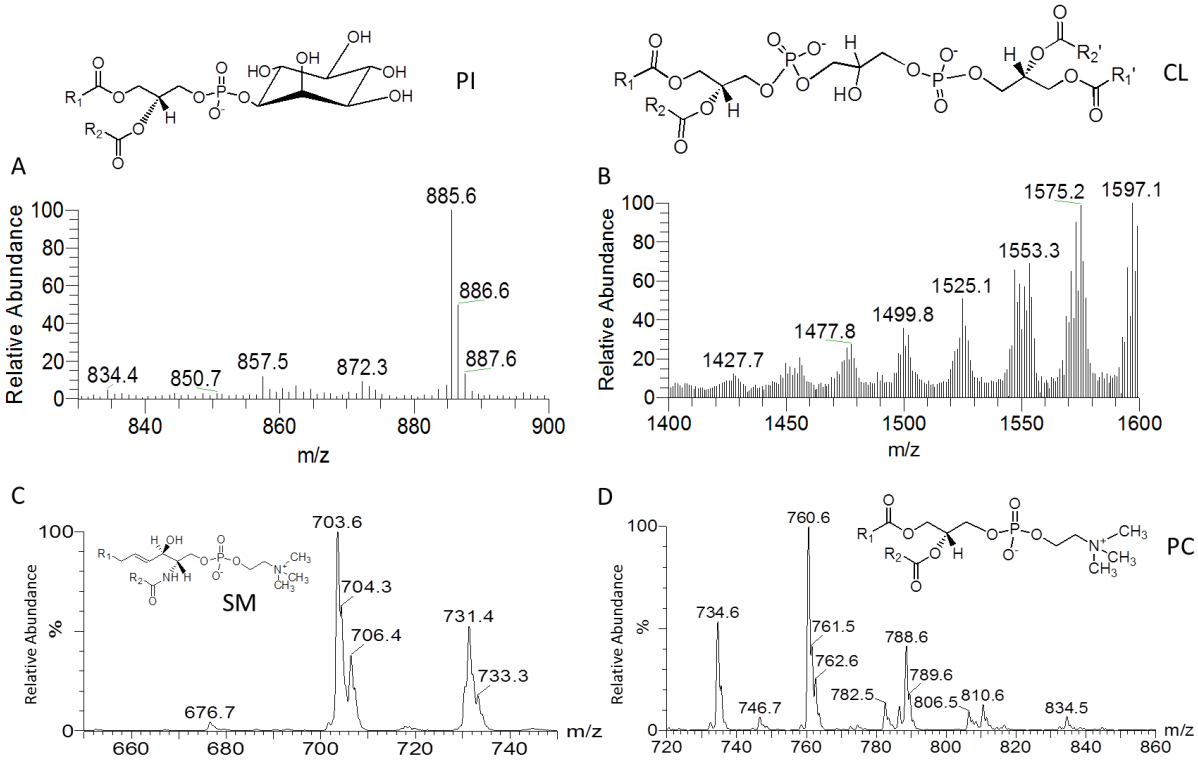

Figure 10. Representative ESI-MS spectrum in negative mode of PI (A) and CL (B) molecular species, and parent scan of SM (C) and PC (D) molecular species obtained for all samples from rat brain non-synaptic mitochondria and general structure of each class.

Table 4. Major CL molecular species from rat brain non-synaptic mitochondria.

CL		Diacyl species
$[M-2H]^{2-}$ m/z	$[M-H]^{-}$ *m/z*	Fatty Acyl Chains
701.5	1402.8 (68:2)	16:1/16:0/18:1/18:0; 18:1/18:1/16:0/16:0; 18:2/18:0/16:0/16:0
710.5	1421.7 (70:7)	16:1/$(18:2)_3$; 20:4/18:1/16:1/16:1; 20:4/18:2/16:1/16:0
711.5	1423.7 (70:6)	16:1/18:1/$(18:2)_2$; 20:4/18:1/16:1/16:0
712.5	1425.7(70:5)	16:1/18:2/$(18:1)_2$; 16:2/$(18:1)_3$;18:2/18:1/18:0/16:2; 16:1/18:0/$(18:2)_2$
713.5	1427.7 (70:4)	16:1/$(18:1)_3$; 18:2/$(18:1)_2$/16:0
716.5	1432.9 (70:2)	$(18:0)_2$/16:1/18:1; 18:0/$(18:1)_2$/16:0
722.5	1446.8(72:9)	16:1/16:0/18:3/22:5; 16:1/18:1/18:3/20:4; $(20:4)_2$/16:1/16:0; 20:4/$(18:2)_2$/16:1
723.5	1447.8 (72:8)	$(18:2)_4$; 16:1/18:1/18:2/20:4; 16:0/18:1/18:3/20:4
724.5	1449.7 (72:7)	16:1/18:1/18:2/20:3; 18:1/$(18:2)_3$; 20:4$(18:1)_2$/16:1; 20:4/18:2/18:1/16:0
725.4	1451.7 (72:6)	$(18:1)_2$/$(18:2)_2$; 16:1/$(18:1)_2$/20:3; 20:4/$(18:1)_2$/16:0
726.5	1453.8 (72:5)	16:0/$(18:1)_2$/20:3; $(18:1)_3$/18:2
727.5	1455.8 (72:4)	$(18:1)_4$; 16:0/$(18:1)_2$/20:2
736.4	1473.7 (74:9)	18:1/$(18:2)_2$/20:4; $(20:4)_2$/18:1/16:0; 16:1/18:1/18:1/22:6; 16:0/18:1/18:2/22:6
737.5	1475.8 (74:8)	16:1/$(18:1)_2$/22:5; 16:1/18:2/20:3/20:2; 16:0/$(18:1)_2$/22:6 ;16:0/18:1/20:4/20:3; 20:4/18:2/$(18:1)_2$
738.5	1477.8 (74:7)	$(18:1)_3$/20:4; 16:1/18:2/20:3/20:1
739.5	1479.8 (74:6)	$(18:1)_2$/18:0/20:4; 16:0/18:1/20:4/22:4; 16:0/18:0/20:4/22:5; 20:3/$(18:1)_3$
746.5	1493.7 (76:13)	16:1/18:2/20:4/22:6; 22:6/18:3/$(18:2)_2$
747.5	1495.7 (76:12)	16:1/18:2/20:3/22:6; $(20:4)_2$/$(18:2)_2$; $(20:4)_3$/16:0/22:6/20:4/18:1/16:1; $(22:6)_2$/$(16:0)_2$; 22:6/$(18:2)_3$
748.5	1497.6 (76:11)	18:1/18:2/$(20:4)_2$
749.5	1499.8 (76:10)	$(18:1)_2$/$(20:4)_2$; 18:0/$(18:2)_2$/22:6
750.5	1501.8 (76:9)	20:4/20:3/$(18:1)_2$; 22:6/$(18:1)_3$
751.5	1503.8 (76:8)	18:1/18:2/20:3/20:2; 16:0/18:2/20:2/22:4; 22:6/$(18:1)_2$/18:0
752.5	1505.8 (76:7)	16:0/18:1/20:3/22:3; 16:0/18:0/20:1/22:6/ 20:4/20:2/18:1/18:0; 20:4/20:1/$(18:1)_2$
758.5	1517.9 (78:15)	16:1/18:2/$(22:6)_2$; 22:6/$(20:4)_2$/16:1
759.5	1519.9 (78:14)	$(18:2)_1$/$(20:4)_3$
760.5	1521.9 (78:13)	$(18:1)_1$/$(20:4)_3$; 18:1/18:2/20:4/22:6
761.5	1523.8 (78:12)	$(18:1)_2$/20:4/22:6
762.5	1525.1 (78:11)	$(18:1)_2$/20:3/22:6; 22:6/20:4/18:1/18:0
765.5	1532.1 (78:8)	16:1/18:1/20:3/22:3; 22:3/18:1/20:0/22:6
772.5	1545.1 (80:15)	18:1/$(20:4)_2$/22:6
773.5	1547.1 (80:14)	18:0/$(20:4)_2$/22:6; $(22:6)_2$/$(18:1)_2$; 22:6/20:4/20:3/18:1

Table 4. Continued.

CL		Diacyl species
$[M-2H]^{2-}$ m/z	$[M-H]^{-}$ *m/z*	Fatty Acyl Chains
774.5	1549.2 (80:13)	18:1/18:0/$(22:6)_2$; $(18:1)_2$/22:5/22:6; 18:0/$(20:4)_2$/22:5; 16:0/20:3/$(22:5)_2$; 18:2/$(20:3)_2$/22:5; 18:0/20:3/20:4/22:6
776.5	1553.3 (80:11)	$(18:1)_2$/22:5/22:4; 18:1/18:0/22:4/22:6
784.5	1569.1 (80:17)	18:1/20:4/$(22:6)_2$; 22:6/$(20:4)_2$/20:3
785.5	1571.2 (80:16)	18:1/20:3/$(22:6)_2$
790.5	1582.3 (82:11)	20:4/20:0/20:2/22:4

Phospholipids are designated as follows: tetra-acyl 78:8 CL, where 78 indicates the summed number of carbon atoms at both *sn*-1, *sn*-2, *sn*-1' and *sn*-2' positions and 8 designates the summed number of double bonds at both the *sn*-1, *sn*-2, and *sn*-1' and *sn*-2' positions. These m/z values indicate ratios of mass to charge for singly charged $[M-H]^{-}$ ions and doubly charged ions $[M-2H]^{2-}$.

While TLC analysis not allowed the separation of phosphatidic acid (PA) class since it eluted in the spot of PE, we were able to identify, based on MS/MS analysis, the two major species of PA at *m/z* 673 corresponding to PA C16:0 (palmitic acid) and C18:1 (oleic acid) and at *m/z* 701 corresponding to PA C18:0 (stearic acid) and C18:1 (oleic acid) (table 5).

Table 5. Major PI and PA molecular species from rat brain non-synaptic mitochondria.

Class	$[M-H]^{-}$ *m/z*	Fatty Acyl Chains
PI		
Diacyl species	857 (36:4)	16:0/20:4
	859 (36:3)	18:2/18:2
	885 (38:4)	18:0/20:4
	887 (38:3)	18:0/20:3
PA		
Diacyl species	673 (34:1)	16:0/18:1
	701 (36:1)	18:0/18:1

Phospholipids are designated as follows: diacyl 38:4 PI, where 38 indicates the summed number of carbon atoms at both the *sn*-1, *sn*-2, positions and 4 designates the summed number of double bonds at both positions; diacyl 34:1 PA, where 34 indicates the summed number of carbon atoms at both the *sn*-1, *sn*-2, positions and 1 designates the summed number of double bonds at both positions. These m/z values indicate ratios of mass to charge for singly charged $[M-H]^{-}$ ions.

Ceramides are key elements in the metabolism of sphingolipids and important messengers for various cellular processes, including apoptosis [114]. By analysis of figure 5 there are no significant alterations in ceramide 1-phosphate levels, between samples. Due to its low abundance in samples, ceramide couldn't be analyzed by MS.

Table 6. Major PC and SM molecular species from rat brain non-synaptic mitochondria.

Class	$[M+H]^+$ *m/z*	Fatty Acyl Chains
PC		
Diacyl species	734 (32:0)	16:0/16:0
	734 (32:0)	14:0/18:0
	760 (34:1)	16:0/18:1
	760 (34:1)	18:0/16:1
	782 (36:4)	16:0/20:4
	782 (36:4)	18:1/18:3
	788 (36:1)	18:0/18:1
	788 (36:1)	16:0/20:1
	806 (38:6)	16:0/22:6
	806 (38:6)	18:4/20:2
	810 (38:4)	18:0/20:4
	810 (38:4)	18:1/20:3
	810 (38:4)	16:0/22:4
	810 (38:4)	18:3/20:1
	810 (38:4)	20:0/18:4
	834 (40:6)	18:1/22:5
	834 (40:6)	18:0/22:6
	834 (40:6)	20:2/20:4
	834 (40:6)	16:0/24:6
PC		
Alkenyl-acyl species	746 (34:0)	18:0p/18:0
SM		
	703 (16:0)	d18:1/16:0
	731 (18:0)	d18:1/18:0

Phospholipids are designated as follows: diacyl 40:6 PC, where 40 indicates the summed number of carbon atoms at both the *sn*-1, *sn*-2, positions and 6 designates the summed number of double bonds at both positions. d18:1/16:0 SM, where d18:1 indicates the sphingosine chain and 16:0 indicates the fatty acyl residue. These m/z values indicate ratios of mass to charge for singly charged $[M+H]^+$ ion.

Conclusions

Biological effects of tacrine and its analogues were evaluated by AchE assay. Similarly with tacrine, two tacrine analogues show inhibitory capacity for AchE but tacrine T1 analogue was shown to be the most efficient in inhibiting AchE, being a promising alternative to tacrine for treatment of AD disease.

Mass spectrometry was used to evaluate the effects of tacrine and analogues treatment in phospholipid profile of non-synaptic mitochondria. Tacrine induced some significant changes in mitochondrial phospholipid profile, namely in PC, PI, PE and CL content, and seems to increase the susceptibility of PS to undergo oxidation. Treatment with tacrine analogues, T1 and T2, also induce changes in phospholipid content, seems to increase the susceptibility of PS to undergo oxidation but in a less expressive way than tacrine.

Both tacrine and analogues affects the activity of mitochondrial complexes activities and consequently the mitochondrial bioenergetics and cellular function, but once again the effects of analogues were less expressive than tacrine. Alterations in CL content and occurrence of oxidized PS products could be the result of mitochondrial increased ROS promoted by tacrine and analogues, namely due to incorporation on mitochondrial membrane, and in the other hand may also contribute to decrease on mitochondrial respiratory complexes. These results may suggest that changes in phospholipids and in mitochondrial bioenergetics are involved in neuronal side effects of these drugs, similarly as observed for hepatotoxic effect which were related with changes in mitochondrial bioenergetics.

These findings may suggest that proposed tacrine T1 analogue could be an alternative to tacrine in the therapy of AD, probably presenting less side effects.

Acknowledgments

Thanks are due to FCT/SAU-NMC/115865/2009, Funded under the Programme Operacional Temático Factores de Competitividade (COMPETE) and Shared by the Fundo Comunitário Europeu (FEDER).

CHAPTER IV

Discussion

Since Alzheimer disease is associated with an increase in cellular oxidative stress and deregulation in sphingolipids metabolism, we performed a study of SM, SPC and Cer oxidation *in vitro*, in order to evaluate the molecular changes induced to its sphingolipids when subjected to oxidative stress conditions.

Sphingolipids are involved in several biological processes, namely inflammation and apoptosis which have been associated with oxidative stress conditions. SM, SPC and Cer were oxidized by the hydroxyl radical, generated under Fenton reaction conditions, and the oxidation reaction was monitored by ESI-MS in positive mode. Analysis of mass spectra data after oxidation allows detecting oxidation products in the ESI-MS spectra of SPC and SM, while no oxidation products were observed in the case of ceramide.

The oxidations products detected in ESI-MS spectrum of oxidized SPC correspond to the oxidation products formed by insertion of 1 or 2 oxygen atoms, as ketene groups, and from cleavage of sphingosine backbone. In the oxidized SM spectrum were present ions corresponding to SPC and their oxidation products which indicate that oxidation of SM involve the sphingosine backbone and elimination of acyl chain. The faster oxidation of SPC, in comparison with SM, suggests that SPC is more prone to oxidation which may be involved in the SPC induced ROS generation observed previously [124].

Tacrine was used as AChE inhibitor approved for AD treatment. In order to evaluate the effects of tacrine and its analogues in brain, we performed an enzymatic assay of acetilcholinesterase activity. Tacrine reduced the AchE activity; T2 analogue was shown to be less efficient than tacrine in its inhibitory capacity, and T1 analogue was shown to be the more efficient of all.

In this work we have also study the effects of tacrine, and its two analogues (T1 and T2), in phospholipid profile of rat brain mitochondria and in mitochondrial bioenergetics. Previous studies have demonstrated that tacrine treatment has proven to be hepatotoxic [6,7,20], contribute to mitochondrial dysfunction [8,9], ROS production, lipid peroxidation [10,17] and apoptosis [20]. However, there are no studies that relate the effects of tacrine treatment with alterations in mitochondrial bioenergetics and phospholipid content in brain.

Mitochondrial complexes activities were measured to determine the effects of tacrine and analogues in brain mitochondrial bioenergetics, and try to correlate these effects with changes in mitochondrial phospholipid profile due to these compounds treatment.

In order to achieve the aims of this work we performed a lipidomics analysis of phospholipid profile of rat brain mitochondria for evaluate the effect of tacrine and two proposed analogues, T1 and T2. The first approach performed in lipidomics analysis consisted in separation of phospholipid classes by TLC, followed by quantification using phosphorus assay. Tacrine treatment induces significant changes in content of PI and CL comparing with a control. Tacrine is a lipophilic molecule with an amine group positively charged at physiological pH that allows its insertion in membranes, increasing membrane positive charge. Probably, the observed increase in PI content in tacrine treated mitochondria may occur to balance the charges in mitochondrial membrane surface. Decrease in PC content may occurs to reduce the excess of positive charge in membrane surface, or on the other hand may be related with PS content changes: PC 16:0/18:1 may suffer remodeling in polar head in order to restore PS 16:0/18:1 levels because at least seven species of oxidized PS were derived from this molecular specie. However, this decrease in PC content may also contribute to alterations in mitochondrial membrane properties. Tacrine T2 analogue also affects significantly the PC and PI content, while T1 analogue only affects significantly the content of PC. No apparent change occurs in PS content despite this also be a negatively charged phospholipid. PE content increases in treated mitochondria, but this alteration occurs due to presence of oxidation products of PS that co-eluted with PE class. The increment of global negative charge of PS by formation of oxidized species could be related to the metabolic changes resulting from tacrine incorporation on mitochondrial membrane. The occurrence of oxidized PS products could be the result of mitochondrial increased ROS promoted by tacrine and analogues, namely due to incorporation on mitochondrial membrane, and in the other and may also contribute to decrease on activity of mitochondrial respiratory complexes.

Both tacrine and analogues treated mitochondria showed significant decreased in activity of complex I (NADH quinone oxidoreductase), and tacrine and T1 analogue also affect significantly the complex IV (cytochrome c oxidase) activity. It has been shown that

cytochrome c oxidase and F_oF_1 ATPase have a specific requirement for CL [111]. Since tacrine treatment affects significantly the CL levels, the cytochrome oxidase and F_oF_1 ATPase activity was significantly reduced in samples treated with tacrine comparing with a control, as we expected. For tacrine analogues, the activity of these complexes was also reduced. Alterations in CL content due to tacrine and T2 analogue treatment may be due to a decrease in its production which could be related to increase in PI content, since they are produced from same precursor, or may occur as result of remodeling of CL species with C16:0 and C18:1 as fatty acyl chains in order to restore the PS 16:0/18:1 levels.

ESI-MS and ESI-MS/MS analysis in positive and negative modes of different phospholipid classes was performed in order achieve the molecular characterization and fatty acyl chain composition within each class. Although significant changes in content of some phospholipids classes (PC, PI, PE, CL), no significant changes in mitochondrial phospholipid profile of PC, SM, PI, and CL were verify between samples.

ESI-MS and MS/MS analysis of tacrine treated mitochondria revealed the formation of PS oxidation products, due to oxidative modification in PS polar head (neutral loss of 57 and 58 Da) or oxidized products corresponding to insertion of oxygen atoms in PS fatty acyl chains. Oxidized products due to polar head PS modifications were also detected in PE spot and correspond to a neutral loss of 58 Da, which were identified recently to be typical of phospholipids with a terminal acetic acid in the polar head. These oxidized products are not present in non-treated mitochondria suggesting that tacrina increase the susceptibility to oxidation of mitochondrial PS. In tacrine analogue treated mitochondria these oxidation products are also present but in much lower abundance, which may suggest that tacrine analogues are less capable to increase the susceptibility to oxidation of mitochondrial PS.

CHAPTER V

Conclusion

The oxidation products, formed during *in vitro* reaction of the hydroxyl radical with selected spingolipids, SPC, SM and Cer, were identified by Electrospray Mass Spectrometry (ESI-MS) and Electrospray Tandem Mass Spectrometry (ESI-MS/MS). Oxidation products formed by addition of 1 and 2 oxygen atoms, as kete groups, to SPC were characterized by ESI-MS/MS. SM oxidation involves the formation of SPC and their oxidation products. Ceramide does not prone oxidation in the used experimental conditions.

These findings may allow to a better understanding of the behavior of some sphingolipids under oxidative stress, and the biological roles of the oxidized lipids.

The effect of tacrine and its two proposed analogues as therapeutic agents for Alzheimer disease in non-synaptic mitochondria phospholipid profile were analyzed by Electrospray Mass Spectrometry (ESI-MS) and Electrospray Tandem Mass Spectrometry (ESI-MS/MS). Acetylcholinesterase activity and mitochondrial respiratory complexes activity were also determined.

Similarly with tacrine, two tacrine analogues show inhibitory capacity for AchE but tacrine T1 analogue was shown to be the most efficient in inhibiting AchE, being a promising alternative to tacrine for treatment of AD disease.

Tacrine induced significant changes in mitochondrial phospholipid profile, namely in PC, PE, PI and CL content, seems to increase the susceptibility of PS to undergo oxidation, and affects the activity of mitochondrial complexes and consequently the mitochondrial bioenergetics and cellular function. T1 and T2 tacrine analogues treatment, also induce changes in phospholipid content, seems to increase the susceptibility of PS to undergo oxidation, and affects the activity of mitochondrial complexes, but in a less expressive way than tacrine. These results may suggest that changes in phospholipids profile and in mitochondrial bioenergetics are involved in neuronal side effects of these drugs, similarly as observed for hepatotoxic effect, which were related with changes in mitochondrial bioenergetics.

These findings may suggest that proposed tacrine T1 analogue affects mitochondrial phospholipid profile and mitochondrial function in a less significant way, and has a greater inhibitory capacity comparing with tacrine and T2 analogue, thus indicating that

this analogue could be an alternative to tacrine in the therapy of AD, probably presenting less side effects.

This work contributes to a better understanding of the biological and toxicological effects of tacrine in brain mitochondrial function, and to research of new tacrine analogues with more inhibitory efficiency and with lower toxicological effects.

CHAPTER VI

References

References

[1] Kung, H. F.; Lee, C. W.; Zhuang, Z. P.; Kung, M. P.; Hou, C. and Plössl, K. (**2001**) *Novel stilbenes as probes for amyloid plaques*. Journal of the American Chemical Society, **123**(50):12740-12741.

[2] Förstl, H. and Kurz, A. (**1999**) *Clinical features of Alzheimer's disease*. European Archives of Psychiatry and Clinical Neuroscience, **249**(6):288-290.

[3] Sivaprakasam, K. (**2006**) *Towards a unifying hypothesis of Alzheimer's disease: cholinergic system linked to plaques, tangles and neuroinflammation.* Current Medicinal Chemistry, **13**(18):2179-2188.

[4] Tabet, N. (**2006**) *Acetyl cholinesterase inhibitors for Alzheimer's disease: anti-inflammatories in acetylcholine clothing*. Age Ageing, **35**(4):336-338.

[5] De Ferrari, G. V.; von Bernhardi, R.; Calderón, F. H:; Luza, S. C. and Inestrosa, N. C. (**1998**) *Responses induced by tacrine in neuronal and non-neuronal cell lines.* Journal of Neuroscience Research, **52**(4):435-444.

[6] O'brien, J. T.; Eagger, S. and Levy, R. (**1991**) *Effects of tetrahydroaminoacridine on liver function in patients with Alzheimer's disease.* Age Ageing, **20**(2):129-131.

[7] Summers, W. K.; Koehler, A. L.; Marsh, G. M.; Tachiki, K. and Kling, A. (**1989**) *Long-term hepatotoxicity of tacrine*. Lancet, **1**(8640):729.

[8] Berson, A.; Renault, S.; Letteron, P.; Robin, M. A.; Fromenty, B.; Fau, D.; Le Bot, M. A.; Riche, C.; Durand-Schneider, A. M.; Feldmann, G. and Pessayre, D. (**1996**) *Uncoupling of rat and human mitochondria: A possible explanation for tacrine-induced liver dysfunction.* Gastroenterology, **110**(6):1878-1890.

[9] Robertson, D. G.; Braden, T. K.; Urda, E. R.; Lalwani, N. D. and de la Iglesia, F. A. (**1998**) *Elucidation of mitochondrial effects by tetrahydroaminoacridine (tacrine) in rat, dog, monkey and human hepatic parenchymal cells.* Archives of Toxicology, **72**(6):362-371.

[10] Lagadic-Gossmann, D.; Rissel, M.; Le Bot, M. A. and Guillouzo, A. (**1998**) *Toxic effects of tacrine on primary hepatocytes and liver epithelial cells in culture.* Cell Biology and Toxicology, **14**(5):361-373.

[11] Gangoiti, P.; Camacho, L.; Arana, L.; Ouro, A.; Granado, M. H.; Brizuela, L.; Casas, J.; Fabriás, G:; Abad, J. L.; Delgado, A. and Gómez-Muñoz, A. (**2010**) *Controlo f metabolismo and signaling of simple bioactive sphingolipids: implications in disease*. Progress in Lipid Research, **49**(4):316-334.

[12] Valko, M.; Rhodes, C. J.; Moncol, J.; Izakovic, M. and Mazur, M. (**2006**) *Free radical, metals and antioxidant in oxidative stress-induced cancer.* Chemico-Biological Interactions, **160**(1):1-40.

[13] Halliwell, B. and Gutteridge, J. M. C. (**1999**) *Oxidative stress: adaptation, damage, repair and death.* Free Radicals in Biology and Medicine. 3rd ed., Oxford: Oxford University Press, cap.4, 246-350.

[14] Lai, J. C. K. and Clark, J. B. (**1989**) *Isolation and characterization of synaptic and nonsynaptic mitochondria from mammalian brain.* Neuromethods, **11**:43-98.

[15] Kiebish, M. A.; Han, X.; Cheng, H.; Lunceford, A.; Clarke, C. F.; Moon, H.; Chuang, J. H. And Seyfried, T. N. (**2008**) *Lipidomic analysis and electron transport chain activities in C57BL/6J mouse brain mitohondria.* Journal of Neurochemistry, **106**(1):299-312.

[16] Morishima-Kawashima, M. and Ihara, Y. (2002) *Alzheimer's disease: beta-Amyloid protein and tau*. Journal of Neuroscience Research, **70**(3):392-401.

[17] Giacobini E. (**1998**) *Invited review: Cholinesterase inhibitors for Alzheimer's disease therapy: from tacrine to future applications.* Neurochemistry International, **32**(5-6):413-419.

[18] Ezoulin, M.J.; Dong, C. Z.; Liu, Z.; Chen, H. Z.; Heymans, F.; Lelièvre, L.; Ombetta, J. E.; Massicot, F. (**2006**) *Study of PMS777, a new type of acetylcholinesterase inhibitor, in human HeCL cells. Comparison with tacrine and galanthamine on oxidative stress and mitochondrial impairment.* Toxicology In Vitro, **20**(6):824-831.

[19] Stachlewitz, R. F.; Arteel, G. E.; Raleigh, J. A.; Connor, H. D.; Mason, R. P. and Thurman, R. G. (**1997**) *Development and characterization of a new model of tacrine-induced hepatotoxicity: role of the sympathetic nervous system and hypoxia-reoxygenation.* Journal of Pharmacology and Experimental Therapeutics, **282**(3):1591-1599.

[20] Polinsky, R. J. (**1998**) *Clinical pharmacology of rivastigmine: a new-generation acetylcholinesterase inhibitor for the treatment of Alzheimer's disease.* Clinical Therapeutics, **20**(4):634-647.

[21] Salaheldin, A. M.; Oliveira-Campos, A. M. F.; Parpot, P.; Rodrigues, L. M.; Oliveira, M. M. and Peixoto, F. P. (**2010**) *Synthesis of New Tacrine Analogues from 4-Amino-1H-pyrrole-3-carbonitrile.* Helvetica Chimica Acta, **93**(2):242-248.

[22] Lehtonen, J. Y.; Rytömaa, M. and Kinnunen, P. K. (**1996**) *Characteristics of the binding of tacrine to acidic phospholipids.* Biophysical Journal, **70**(5):2185-2194.

[23] Su, B.; Wang, X.; Zheng, L.; Perry, G.; Smith, M. A. and Zhu, X. (**2010**) *Abnormal mitochondrial dynamics and neurodegenerative diseases*. Biochimica et Biophysica Acta, **1802**(1):135-142.

[24] Frazier, A. E.; Kiu, C.; Stojanovski, D.;Hoogenraad, N. J. and Ryan, M. T. (**2006**) *Mitochondrial morphology and distribution in mammalian cells*. Bilogical Chemistry, **387**(12):1551-1558.

[25] Kann, O. and Kovacs, R. (**2007**) *Mitochondria and neuronal activity. American Journal of Physiology*. Cell Physiology, **292**(2):641-657.

[26] Moreira, P. I.; Santos, M. S.; seiça, R. and oliveira, C. R. (**2007**) *Brain mitochondrial dysfunction as a link between Alzheimer's disease and diabetes*. Journal of Neurological Sciences, **257**(1-2):206-214.

[27] Mattson, M. P. and Chan, S. L. (**2003**) *Neuronal and glial calcium signaling in Alzheimer's disease.* Cell Calcium, **34**(4-5):385-397.

[28] Rego, A.C. and Oliveira, C. R. (**2003**) *Mitochondrial dysfunction and relative oxygen species in excitotoxicity and apoptosis: implications for the pathogenesis of neuroidegenerative diseases.* Neurochemical Research, **28**(10):1563-1574.

[29] Spät, A.; Szanda, G.; Csordás, G. and Hajnóczky, G. (**2008**) *High- and low-calcium-dependent mechanisms of mitochondrial calcium signaling.* Cell Calcium, **44**(1):51-63.

[30] Hirai, K.; Aliev, G.; Nunomura, A.; Fujioka, H.; Russell, R. L.; Atwood, C. S.; Johnson, A. B.; Kress, Y.; Vinters, H. V.; Tabaton, M.; Shimohama, S.; Cash, A. D.; Siedlak, S. L.; Harris, P. L. R.; Jones, P. K.; Petersen, R. B.; Perry, G. And Smith, M. A. (**2001**) *Mitochondrial abnormalities in Alzheimer's disease*. Journal of Neurocience, **21**(9):3017-3023.

[31] Wallace, D. C. (**2005**) *A mitochondrial paradigm of metabolic and degenerative diseases, aging, and cancer: a dawn for evolutionary medicine.* Annual Review of genetics, **39**:359-407.

[32] Jones, D. P.; Lemasters, J. j.; Han, D.; boelsteril, U. A. and Kaplowitz, N. (**2010**) *Mechanisms of pathogenesis in drug hepatotoxicity putting the stress on mitochondria*. Molecular Interventions, **10**(2):98-111.

[33] Moreira, P. I.; Zhu, X.; Wang, X.; Lee, H. G.; Nunomura, A.; Petersen, R. B.; Perry, G. and Smith, M. A. (**2010**) *Mitochondria: a therapeutic target in neurodegeneration.* Biochimica et Biophysica Acta, **1802**(1):212-220.

[34] Valko, M.; Leibfritz, D.; Moncol, J.; Cronin, M. T. D.; Mazur, M.; Telser, J. (**2007**) *Free radicals and antioxidants in normal physiological functions and human disease.* The International Journal of Biochemistry & Cell Biology, **39**(1)44-84.

[35] Floyd, R. A (**1999**) *Antioxidants, oxidative stress, and degenerative neurological disorders.* Proceedings of the Society for Experimental Biology and Medicine, **222**(3):236-245.

[36] Niki, E.; Yoshida, Y.; Satio, Y. and Noguchi, N. (**2005**) *Lipid peroxidation: mechanisms, inhibition, and biological effects.* Biochemical and Biophysical Research Communications, **338**(1):668-676.

[37] Patricò, D. (**2002**) *Oxidative imbalance and lipid peroxidation in Alzheimer's disease.* Drug Development Research, **56**(3):446-451.

[38] Domingues, M. R. M.; Reis, A. and Domingues, P. (**2008**) *Mass spectrometry analysis of oxidized phospholipids.* Chemistry and Physics of Lipids, **156**(1-2):1-12.

[39] Catalá, A. (**2006**) *An overviewof lipid peroxidationwith emphasis in outer segments of photoreceptors and the chemiluminescence assay.* International Journal of Biochemistry & Cell Biology, **38**(9):1482-1495.

[40] Niki, E. (**2009**) *Lipid Peroxidation: physiological levels and dual biological effects.* Free Radical Biology & Medicine, **47**(5):469-484.

[41] Fruhwirth, G. O.; Loidl, A. and hermetter, A. (**2007**) *Oxidized phospholipids: from molecular properties to disease.* Biochimica et Biophysica Acta, **1772**(7):718-736.

[42] Hu, C.; van der Heijden R.; Wang, M.; van der Greef, J.; Hankemeier, T. and Xu, G. (**2009**) *Analytical strategies in lipidomics and applications in disease biomarker discovery.* Journal of Chromatography B, Analytical Technologies in the Biomedical and Life Sciences, **877**(26):2836-2846.

[43] Han, X. and Gross, R. W. (**2005**) *Shotgun lipidomics: Electrospray ionization mass spectrometric analysis and quantitation of the cellular lipidomes directly from crude extracts of biological samples.* Mass Spectrometry Reviews, **24**(3):367-412.

[44] Wassall, S. R. and Stillwell, W. (**2008**) *Docosahexaenoic acid domains: the ultimate non-raft membrane domain.* Chemistry and Physics of Lipids, **153**(1):57-63.

[45] McDonald, J. G.; Thompson, B. M.; McCrum, E.C.; Russell, D.W. (**2007**) *Extraction and analysis of sterols in biological matrices by high performance liquid chromatography electrospray ionization mass spectrometry.* Methods in Enzymology, **432**:145-170.

[46] Milne, S.; Ivanova, P.; Forrester, J. and Alex Brown, H. (**2006**) *Lipidomics: an analysis of cellular lipids by ESI-MS*. Methods, **39**(2):92-103.

[47] Peretó, J.; López-García, P. and Moreira, D. (**2004**) *Ancestral lipid biosynthesis and early membrane evolution.* Trends in Biochemical Sciences, **29**(9):469-477.

[48] Hein, E. M.; Blank, L. M.; Heyland, J.; Baumbach, J. I.; Schmid, A. and Hayen, H. (**2009**) *Glycerophospholipid profiling by high-performance liquid chromatography/mass spectrometric fragmentation experiments in parallel.* Rapid Communications in Mass Spectrometry, **23**(11):1636-1646.

[49] Schlame, D. R. and Greenberg, M. L. (**2000**) *The biosynthesis and functional role of cardioloipin*. Progress in Lipid Research, **39**(3):257-288.

[50] Allegrini, P. R.; Pluschke, G. and Seelig, J. (**1984**) *Cardiolipin conformation and dynamics in bilayer-membranes as seen by deuterium magnetic-resonance*. Biochemistry, **23**(26):6452-6458.

[51] Won, J. S. and Singh, I. (**2006**) *Sphingolipid signaling and redox regulation.* Free Radical Biology & Medicine, **40**(11):1875-1888.

[52] Merrill Jr, A. H:, Sullards, M. C.; Allegood, J. C.; Kelly, S. and Wang, E. (**2005**) *Sphingolipidomics: high-throughput, structure-specific, and quantitative analysis of sphingolipids by liquid chromatrography tandem mass spectrometry*. Methods, **36**(2):207-224.

[53] Sparvero, L. J.; Amoscato, A. A.; Kochanek, P. M.; Pitt, B. R.; Kagan, V. E. and Bayir, H. (**2010**) *Mass-spectrometry based oxidative lipidomics and lipid imaging: applications in traumatic brain injury.* Journal of Neurochemistry, **115**(6):1322-1336.

[54] Han, X. (**2007**) *Neurolipidomics: challenges and developments*. Frontiers in Bioscience, **12**:2601-2615.

[55] Mielke, M. M. and Lyketsos, C. G. (**2006**) *Lipids and the pathogenesis of Alzheimer's disease: is there a link?* International Review of Psychiatry, **18**(2):173-186.

[56] Fahy, E.; Subramaniam, S.; Brown, H. A.; Glass, C. K.; Merrill, A. H. Jr.; Murphy, R. C.; Raetz, C. R.; Russell, D. W.; Seyama, Y.; Shaw, W. Shimizu, T.; Spener, F.; van Meer, G.;

VanNieuwenhze, M.S.; White, S.H.; Witztum, J. and Dennis, E.A. (**2005**) *A comprehensive classification system for lipids.* Journal of Lipid Research, **46**(5):839-862.

[57] Fahy, E.; Subramaniam, S.; Murphy, R. C.; Nishijima, M.; Raetz, C. R. H.; Shimizu, T.; Spener, F.; van Meer, G.; Wakelam, M. J. O. and Dennis, E. A. (**2009**) *Update of the LIPID MAPS comprehensive classification system for lipids.* Journal of Lipid research, **50**(9-14):9-14.

[58] Hiren, R. M.; Surendra, S. K. and Minal, A. P. (**2008**) *Ageing-induced alterations in lipid/phospholipid Profiles of rat brain and liver mitochondria: implications for mitochondrial energy-linked functions.* Journal of Membrane Biology, **221**(1):51-60.

[59] Zinser, E.; Sperka-Gottlieb, C. D.; Fasch, E. V.; Kohlwein, S. D.; Paltauf, F. and Daum G. (**1991**) *Phospholipid synthesis and lipid composition of subcellular membranes in the unicellular eukaryote Saccharomyces cerevisiae.* The Journal of Bacteriology, **173**(6):2026-34.

[60] Pulfer, M. and Murphy, R. C. (**2003**) *Electrospray mass spectrometry of phospholipids.* Mass Spectrometry Reviews, 22(5):332-364.

[61] Kiefer, S.; Rogger, J.; Melone, A.; Mertz, A. C.; Koryakina, A.; Hamburger, M. and Küenzi, P. (**2010**) *Separation and detection of all phosphoinositoide isomers by ESI-MS.* Journalk of Pharmaceutical and Biomedical Analysis, **53**(3):552-558.

[62] Pope, S.; Land, J. M. and Heales, S. J. (**2008**) *Oxidative stress and mitochondrial dysfunction in neurodegeneration; cardiolipin a critical target?* Biochimica et Biophysica Acta, **1777**(7-8):794-799.

[63] Bayir, H.; Tyurin, V.A.; Tyurina, Y. Y.; Viner, R.; Ritov, V.; Amoscato, A. A.; Zhao, Q.; Zhang, X. J.; Janesko-Feldman, K. L.; Alexander, H.; Basova, L. V.; Clark, R.S.; Kochanek, P. M. and Kagan, V. E. (**2007**) *Selective early cardiolipin peroxidation after traumatic brain injury: an oxidative lipidomics analysis.* Annals of Neurology, **62**(2):154-169.

[64] Chicco, A. J. and Sparagna, G. C. (**2007**) *Role of cardiolipin alterationsin mitochondrial dysfunction and disease.* American Journal of Physiology-Cell Physiology, **292**(1):C33-44.

[65] Beyer, K. and Nuscher, B. (**1996**) *Specific cardiolipin binding interferes with labeling of sulfhydryl residues in the adenosine diphosphate/adenosine triphosphate carrier protein from beef heart mitochondria.* Biochemistry, **35**(49):15784-15790.

[66] Joshi, A. S.; Zhou, J.; Gohil, V. M.; Chen, S. and Greenberg, M. L. (**2009**) *Cellular functions of cardiolipin in yeast.* Biochimica et Biophysica Acta, **1793**(1):212-218.

[67] Zhang, M.; Mileykovskaya, E. and Dowhan,W. (**2002**) *Gluing the respiratory chain together. Cardiolipin is required for supercomplex formation in the inner mitochondrial membrane.* The Journal of Biological Chemistry, **277**(46):43553-43556.

[68] Tuominem, E. K. J.; Wallace, C. J. A. and Kinnunen, P. K. J (**2002**) *Phospholipid-cytochrome c interaction-Evidence for the extended lipid anchorage.* Journal of Biological Chemistry, **277**(11):8822-8826.

[69] Kagan, V. E.; Tyurina, Y. Y.; Bayir, H.; Chu, C. T.; Kapralov, A. A.; Vlasova, I. I.; Belikova, N. A.; Tyurin, V. A.; Amoscato, A.; Epperly, M.; Greenberger, J.; DeKosky, S.; Shvedova, A. A. And Jiang, J. (**2006**) *The "pro-apoptotic genies" get out of mitochondria: oxidative lipidomics and redox activity of cytochrome c/cardiolipin complexes.* Chemico-Biological Interactions, **163**(1–2):15-28.

[70] Belikova N. A., Vladimirov Y. A., Osipov A. N. et al. (**2006**) *Peroxidase activity and structural transitions of cytochrome C bound to cardiolipin-containing membranes*. Biochemistry, **45**(15):4998-5009.

[71] Belikova, N. A.; Jiang, J.; Tyurina, Y. Y.; Zhao, Q.; Epperly, M. W.; Greenberger, J. and Kagan, V. E. (**2007**) *Cardiolipin-specific peroxidase reactions of cytochrome C in mitochondria during irradiation-induced* apoptosis. International Journal of Radiation Oncology Biology Physics, **69**(1):176-186.

[72] Nitsch, R. M.; Blusztajn, J. K.; Pittas, A. G.; Slack, B. E.; Growdon, J. H. and Wurtman, R. J. (**1992**) *Evidence for a membrane defect in Alzheimer disease brain.* Proceedings of the National Academy of Sciences, **89**(5):1671-1675.

[73] Han, X.; Holtzman, D. M. and McKeel, D. W. Jr. (**2001**) *Plasmalogen deficiency in early Alzheimer's disease subjects and in animal models: molecular characterization using electrospray ionization mass spectrometry.* Journal of Neurochemistry, **77**(4):1168-80.

[74] Tully, A. M.; Roche, H. M.; Doyle, R.; Fallon, C.; Bruce, I.; Lawlor, B.; Coakley, D. and Gibney, M. J. (**2003**) *Low serum cholesteryl ester-docosahexaenoic acid levels in Alzheimer's disease: a case-control study.* British Journal of Nutrition, **89**(4):483-489.

[75] Grimm, M. O.; Grimm, H. S.; Patzold, A. J.; Zinser, E. G.; Halonen, R.; Duering, M.; Tschape, J. A.; De Strooper, B.; Muller, U.; Shen, J. And Hartmann, T. (**2005**) *Regulation of cholesterol and sphingomyelin metabolism by amyloid-beta and presenilin.* Nature Cell Biology, **7**(11):1118-1123.

[76] Zha, Q.; Ruan, Y.; Hartmann, T.; Beyreuther, K. and Zhang, D. (**2004**) *GM1 ganglioside regulates the proteolysis of amyloid precursor protein.* Molecular Psychiatry, **9**(10):946-952.

[77] Lightle, S. A.; Oakley, J. I. and Nikolova-Karakashian, M. N. (**2000**). *Activation of sphingolipid turnover and chronic generation of ceramide and sphingosine in liver during aging.* Mechanisms of Ageing and Development, **120**(1-3):111-125.

[78] Birbes, H.; Bawab, S. E.; Obeid, L. M. and Hannun, Y. A. (**2002**) *Mitochondria and ceramide: intertwined roles in regulation of apoptosis*. Advances in Enzyme Regulation, **42**:113-129.

[79] Ruvolo, P. P. (**2003**). *Intracellular signal transduction pathways activated by ceramide and its metabolites.* Pharmacological Research, **47**(5):383-392.

[80] Han, X.; Holtzman, D. M.; McKeel Jr., D. W.; Kelley, J. And Morris, J. C. (**2002**) *Substantial sulfatide deficiency and ceramide elevation in very early Alzheimer's disease: Potential role in disease pathogenesis.* Journal of Neurochemistry, **82**(4):809-818.

[81] Watson, A. D. (**2006**) *Thematic review series: systems biology approaches to metabolic and cardiovascular disorders. Lipidomics: a global approach to lipid analysis in biological systems.* Journal of Lipid Research, **47**(10):2101-2111.

[82] Lagarde, M.; Geloen, A.; Record, M.; Vance, D. and Spencer, F. (**2003**) *Lipidomics is emerging*. Biochemistry. Biochimica et Biophysica Acta, **1634**(3):61.

[83] Bligh, E. G. and Dyer, W. J. (**1959**) *A rapid method of total lipid extraction and purification*. Canadian Journal of Biochemistry and Physiology, **37**(8): 911-917.

[84] Wolf, C. and Quinn, P. J. (**2008**) *Lipidomics: Practical aspects and applications*. Progress in Lipid Research, **47**(1): 15-36.

[85] Fuchs, B.; Süß, R.; Teuber, K.; Eibisch, M. and Schiller, J. (**2011**) *Lipid analysis by thin-layer chromatography – A review of the current state*. Journal of Chromatography A, **1218**(19):2754-2774.

[86] Peterson, B. L. and Cummings, B. S. (**2006**) *A review of chromatographic methods for the assessment of phospholipids in biological samples*. Biomedical Chromatography, **20**(3): 227-243.

[87] Carrasco-Pancorbo, A.; Navas-iglesias, N. and Cuadros-rodrigues, L. (**2009**) *From lipid analysis towards lipidomics, a new challange for the analytical chemistry of the 21st century. Part 1: Modern lipid analysis.* Trends in Analytical Chemistry, **28**(3):263-278.

[88] Bele, A. A. and Khale, A. (**2011**) *An overview on thin layer chromatography.* International Journal of Pharmaceutical Sciences and Research, **2**(2): 256-267.

[89] Schiller, J.; Süß, R.; Arnhold, J.; Fuchs, B.; Leßig, J.; Müller, M.; Petković, M.; Spalteholz, H.; Zschörnig, O. and Arnold, K. (**2004**) *Matrix-assisted laser desorption and ionization time-of-flight (MALDI-TOF) mass spectrometry in lipid and phospholipid research.* Progress in Lipid Research, **43**(5):449-488.

[90] Adibhatla, R. M.; Hatcher, J. F. and Dempsey, R. J. (**2006**) *Lipids and lipidomics in brain injury and diseases*. Journal of the American Association of Pharmaceutical Scientists, **8**(2):314-321.

[91] Han, X. and Gross, R. W. (**2003**) *Global analyses of cellular lipidomes directly from crude extracts of biological samples by ESI mass spectrometry: a bridge to lipidomics*. Journal of Lipid Research, **44**(6):1071-1079.

[92] Cole, R.B. (**2000**) *Some tenets pertaining to electrospray ionization mass spectrometry.* Journal of Mass Spectrometry, **35**(7):763-772.

[93] Douglas, D. J.; Frank, A. J. and Mao, D. M. (**2005**) *Linear ion traps in mass spectrometry.* Mass Spectrometry Reviews, **24**(1):1-29.

[94] Cui, Z. and Thomas, M. J. (**2009**) *Phospholipid profiling by tandem mass spectrometry.* The Journal of Chromatography B: Analytical Technologies in the Biomedical and Life Sciences, **877**(26):2709-2715.

[95] Zehethofer, N. and D. M. Pinto (**2008**). *Recent developments in tandem mass spectrometry for lipidomic analysis.* Analytica Chimica Acta, **627**(1): 62-70.

[96] Taguchi, R.; Houjou, T.; Nakanishi, H.; Yamazaki, T.; Ishida, M.; Imagawa, M. And Shimizu, T. (**2005**) *Focused lipidomics by tandem mass spectrometry*. Journal of Chromatography, **823**(1):26-36.

[97] Hsu, F.-F. and Turk, J. (**2009***) Electrospray ionization with low-energy collisionally activated dissociation tandem mass spectrometry of glycerophospholipids: mechanisms of fragmentation and structural characterization. Journal of Chromatograpgy B.* Analytical technologies in the Biomedical and Life Sciences, **877**(26):2673-2695.

[98] Brügger, B.; Erben, G.; Sandhoff, R.; Wieland, F. T. and Lehmann, W. D. (**1997**) *Quantitative znalysis of biological membrane lipids at the low picomole level by nano-electrospray ionization tandem mass spectrometry*. Proceedings of the National Academy of Sciences, **94**(6):2339-2344.

[99] Hsu, F.- F.; Turk, J.; Rhoades, E. R.; Russell, D. G.; Shi, Y. and Groisman, E. A. (**2005**) *Structural characterization of cardiolipin by tandem quadrupole and multiple-stage quadrupole ion-trapmass spectrometrywith electrospray ionization*. Journal of American Society of Mass Spectrometry, **16**(4):491-504.

[100] Hsu, F.-F. and Turk, J. (**2002**) *Characterization of ceramides by low energy collisional-activated dissociation tandem mass spectrometry with negative-ion electrospray ionization*. Journal of American Society of Mass Spectrometry, **13**(5):558-570.

[101] Guan, Z. (**2009**) *Discovering novel brain lipids by liquid chromatography/tandem mass spectrometry.* Journal of Chromatography B, **877**(26):2814-2821.

[102] Wang, H. Y.; Liu, C. B.; Wu, H. W. and Kuo, J. S. (**2010**) *Direct profiling of phospholipids and lysophospholipids in rat brain sections after ischemic stroke*. Rapid Communications in Mass Spectrometry, **24**(14):2057-2064.

[103] Aaltonen, N.; Laitinen, J. T. and Lehtonen, M. (2010) *Quantification of lysophosphatidic acids in rat brain tissue by liquid chromatography-electrospray tandem mass spectrometry*. Journal of Chromatography B, **878**(15-16):1145-1152.

[104] Khaselev, N. and Murphy, R. C. (**1999**) *Susceptibility of plasmenyl glycerophosphoethanolamine lipids containing arachidonate to oxidative degradation*. Free Radical Biology & Medicine, **26**(3-4):275-284.

[105] Maskrey, B. H.; Bermúdez-Fajardo, A.; Morgan, A. H.; Stewart-Jones, E.; Dioszeghy,V.; Taylor, G. W.; Baker, P. R. S.; Coles, B.; Coffey, M. J.; Kühn, H. and O'Donnell,V.B. (**2007**) *Activated platelets and monocytes generate four hydroxyphosphatidylethanolamines via lipoxygenase.* Journal of Biological Chemistry, **282**(28):20151-20163.

[106] Tyurina, Y. Y.; Tyurin, V. A.; Epperly, M. W.; Greenberger, J. S. and Kagan, V. E. (**2008**) *Oxidative lipidomics of gamma-irradiation-induced intestinal injury*. Free Radical Biology & Medicine, **44**(3):299-314.

[107] Tyurin, V. A.; Tyurina, Y. Y.; Feng, W.; Mnuskin, A.; Jiang, J.; Tang, M.; Zhang, X.; Zhao, Q.; Kochanek, P. M.; Clark, R. S.; Bayir, H. and Kagan, V. E. (**2008**) *Mass-spectrometric characterization of phospholipids and their primary peroxidation*

products in rat cortical neurons during staurosporine-induced apoptosis. Journal of Neurochemistry, **107**(6), 1614-1633.

[108] Tyurin, V. A.; Tyurina, Y.; Jung, M. Y.; Tungekar, M. A.; Wasserloos, K. J.; Bayir, H.; Greenberger, J. S.; Kochanek, P. M.; Shvedova, A. A.; Pitt, B. and Kagan, V. E. (**2009**) *Mass-spectrometric analysis of hydroperoxy- and hydroxy-derivatives of cardiolipin and phosphatidylserine in cells and tissues induced by pro-apoptotic and pro-inflammatory stimuli*. Journal of Chromatography B. Analytical Technologies in the Biomedical and Life Sciences, **877**(26):2863-2872.

[109] Tyurina, Y. Y.; Tyurin, V. A.; Zhao, Q.; Djukic, M.; Quinn, P. J.; Pitt, B. R. and Kagan, V. E. (**2004**). *Oxidation of phosphatidylserine: a mechanism for plasma membrane phospholipid scrambling during apoptosis?* Biochemical and Biophysical Research Communications, **324**(3):1059-1064.

[110] Shadyro, O.; Yurkova, I.; Kisel, M.; Brede, O. and Arnhold, J. (**2004**) *Formation of phosphatidic acid, ceramide, and diglyceride on radiolysis of lipids: Identification by MALDI-TOF mass spectrometry.* Free Radical Biology & Medicine, **36**(12):1612-1624.

[111] Yurkova, R.; Huster, D. and Arnhold, J. (**2009**) *Free radical fragmentation of cardiolipin by cytochrome c.* Chemistry and Physics of Lipids, **158**(1):16-21.

[112] Hannun, Y. A. and Luberto, C. (**2000**) *Ceramide in the eukaryotic stress response*. Trends in Cell Biology, **10**(2):73-80.

[113] Kolesnick, R. N. and Krönke, M. (**1998**) *Regulation of ceramide production and apoptosis*. Annual Review of Physiology, **60**:643-465.

[114] Okazaki, T.; Kondo, T.; Kitano, T. and Tashima, M. (**1998**) *Diversity and complexity of ceramide signalling in apoptosis*. Cell Signalling, **10**(10):685-692.

[115] Obeid, L. M. and Hannun, Y. A. (**1995**) *Ceramide: a stress signal and mediator of growth suppression and apoptosis*. Journal of Cellular Biochemistry, **58**(2):191-198.

[116] Fishbein, J. D.; Dobrowsky, R. T.; Bielawska, A.; Garrett, S. and Hannun Y. A. (**1993**) *Ceramide-mediated growth inhibition and CAPP are conserved in Saccharomyces cerevisiae*. Journal of Cellular Biochemistry**, 268**(13):9255-9261.

[117] Venable, M. E.; Lee, J. Y.; Smyth, M. J.; Bielawska, A. and Obeid, L. M. (**1995**) *Role of ceramide in cellular senescence*. Journal of Cellular Biochemistry, **270**(51):30701-30708.

[118] Chao, M. V. (**1995**) *Ceramide: a potential second messenger in the nervous system*. Molecular and Cellular Neuroscience, **6**(2):91-96.

[119] El Alwani, M.; Wu, B. X.; Obeid, L. M. and Hannun, Y. A. (**2006**) *Bioactive sphingolipids in the modulation of the inflammatory response*. Pharmacology and Therapeutics, **112**(1):171-183.

[120] Meyer zu Heringdorf, D.; Himmel, H. M. and Jakobs, K. H. (**2002**) *Sphingosylphosphorylcholine-biological functions and mechanisms of action*. Biochimica et Biophysica Acta, **1582**(1-3):178-189.

[121] Desai, N. N.; Carlson, R. O.; Mattie, M. E.; Olivera, A.; Buckley, N. E.; Seki, T.; Brooker, G. and Spiegel, S. (**1993**) *Signaling pathways for sphingosylphosphorylcholine-mediated mitogenesis in Swiss 3T3 fibroblasts*. Journal of Cell Biology, **121**(6):1385-1395.

[122] Boguslawski, G.; Lyons, D.; Harvery, K. A. and English, D. (**2000**) *Sphingosylphosphorylcholine induces endothelial cell migration and morphogenesis.* Biochemical and Biophysical Research Communications, **272**(2):603-609.

[123] Wirrig, C.; Hunter, I.; Mathieson, F. A. and Nixon, G. F. (**2011**) *Sphingosylphosphorylcholine is a proinflammatory mediator in cerebral arteries*. Journal of Cerebral Blood Flow and Metabolism, **31**(1)212-221.

[124] Joen, E. S.; Lee, M. J.; Sung, S. M. and Kim, J. H. (**2007**) *Sphingosylphosphorylcholine induces apoptosis of endothelial cells through reactive oxygen species-mediated activation of ERK*. Journal of Cellular Biochemistry, **100**(6):1536-1547.

[125] Merrill, A. H. Jr (**1991**) *Cell regulation by sphingosine and more complex sphingolipids*. Journal of Bioenergetics and Biomembranes, **23**(1):83-104.

[126] Kolesnick, R. N. and Hemer, M. R. (**1990**) *Characterization of a ceramide kinase activity from human leukemia (HL-60) cells. Separation from diacylglycerol kinase activity*. Journal of Biologycal Chemistry, **265**(31):18803-18808.

[127] Bochkov, V. N.; Oskolkova, O. V.; Birukov, K. G.; Levonen, A. L.; Binder, C. J. and Stöckl, J. (**2010**) *Generation and biological activities of oxidized phospholipids*. Antioxidants and Redox Signaling, **12**(8):1009-1059.

[128] Maciel, E.; Domingues, P. and Domingues, M. R. (**2011**) *Liquid chromatography/tandem mass spectrometry analysis of long-chain oxidation products of cardiolipin induced by the hydroxyl radical.* Rapid Communications in Mass Spectrometry, **25**(2):316-326.

[129] Nusshold, C.; Kollroser, M.; Köfeler, H.; Rechberger, G.; Reicher, H.; Ullen, A.; Bernhart, E.; Waltl, S.; Kratzer, I.; Hermetter, A.; Hackl, H.; Trajnoski, Z.; Hrzenjak, A.; Malle, E. and Sattler, W. (**2010**) *Hypochlorite modification of sphingomyelin generates chlorinated lipid species that induce apoptosis and proteome alterations in dopaminergic PC12 neurons in vitro*. Free Radical Biology and Medicine, **48**(12):1588-1600.

[130] Reis, A.; Domingues, P.; Ferrer-Correia, A. J. and Domingues, M. R. (**2004**) *Tandem mass spectrometry of intact oxidation products of diacylphosphatidylcholines: evidence for the occurrence of the oxidation of the phosphocholine head and differentiation of isomers*. Journal of Mass Spectrometry, **39**(12):1513-1522.

[131] Wheelan, P.; Zirrolli, J. A. and Murphy, R. C. (**1995**) *Analysis of hydroxy fatty acids as pentafluorobenzyl ester, trimethylsilyl ether derivatives by electron ionization gas chromatography/mass spectrometry*. Journal of The American Society for Mass Spectrometry, **6**(1):40-51.

[132] Domingues, M. R.; Simões, C.; da Costa, J. P.; Reis, A. and Domingues, P. (**2009**) *Identification of 1-palmitoyl-2-linoleoyl-phosphatidylethanolamine modifications under oxidative stress conditions by LC-MS/MS.* Biomedical Chromatography, **23**(6):588-601.

[133] Davies, M. J. (**1996**) *Protein and peptide alkoxyl radicals can give rise to C-terminal decarboxylation and backbone cleavage*. Archives of Biochemistry and Biophysics, **336**(1):163-172

[134] Xu, G. and Chance, M. R. (**2007**) *Hydroxyl radical-mediated modification of proteins as probes for structural proteomics*. Chemical Reviews, **107**(8):3514-3543.

[135] Maciel, E.; da Silva, R. N.; Simões, S.; Domingues, P. and Domingues, M. R. (**2011**) *Phosphatidylserine Oxidation by Fenton Reaction: Recognition of Oxidation of Serine Polar Head by TLC and Mass Spectrometry*. Journal of The American Society for Mass Spectrometry, accepted for publication.

[136] Smith, C. D.; Carney, J. M.; Starke-Reed, P. E.; Oliver, C. N.; Stadtman, E. R.; Floyd, R. A. and Markesbery, W. R. (**1991**) *Excess brain protein oxidation and enzyme dysfunction in normal aging and Alzheimer disease*. Proceedings of the National Academy of Sciences USA, **88**(23): 10540-10543.

[137] Selkoe, D. J. (**1994**) *Alzheimer's disease: a central role for amyloid*. Journal of Neuropathology and Experimental Neurology, **53**(5):438-447.

[138] Terry, R. D. (**2000**) *Cell death or synaptic loss in Alzheimer disease*. Journal of Neuropathology and Experimental Neurology, **59**(12):1118-1119.

[139] Walsh, D. M. and Selkoe, D. J. (**2004**) D*eciphering the molecular basis of memory failure in Alzheimer's disease.* Neuron, **44**(1):181-193.

[140] Talesa, V. N. (**2001**) *Acetylcholinesterase in Alzheimer's disease*. Mechanisms of Ageing and Development, **122**(16):1961-1969.

[141] Heilbronn, E. (**1961**) *Inhibition of cholinesterase by tetrahydroaminoacric*. Acta Chemica Scandinavica, **15**:1386-1390.

[142] Watkins, P. B.; Zimmerman, H. J.; Knapp, M. J.; Gracon, S. I. and Lewis, K. W. (**1994**) Hepatotoxic effects of tacrine administration in patients with Alzheimer's disease. Journal of the American Medical Association, **271**(13):992-998.

[143] Spaldin, V.; Madden, S.; Pool, W. F.; Woolf, T. F. and Park, B. K. (**1994**) *The effect of enzyme inhibition on the metabolism and activation of tacrine by human liver microsomes.* British Journal of Clinical Pharmacology, **38**(1):15-22.

[144] Meng, Q.; Ru, J.; Zhang, G.; Shen, C.; Schmitmeier, S. and Bader, A. (**2007**) *Re-evaluation of tacrine hepatotoxicity using gel entrapped hepatocytes.* Toxicology Letters, **168**(2):140-147.

[145] Osseni, R. A.; Debbasch, C.; Christen, M. O.; Rat, P. and Warnet, J. M. (**1999**) *Tacrine-induced reactive oxygen species in a human liver cell line: the role of anethole dithiolethione as a scavenger*. Toxicology In Vitro, **13**(4-5):683-688.

[146] Galisteo, M.; Rissel, M.; Sergent, O.; Chevanne, M.; Cillard, J.; Guillouzo, A. and Lagadic-Gossmann, D. (**2000**) *Hepatotoxicity of tacrine: occurrence of membrane*

fluidity alterations without involvement of lipid peroxidation. Journal of Pharmacology and Experimental Therapeutics, **294**(1):160-167.

[147] Sergent, O.; Ekroos, K.; Lefeuvre-Orfila, L.; Rissel, M.; Forsberg, G. -B.; Oscarsson, J.; Andersson, T. B. and Lagadic-Gossmann, D. (**2009**) *Ximelagatran increases membrane fluidity and changes membrane lipid composition in primary human hepatocytes*. Toxicology In Vitro**, 23**(7):1305-1310.

[148] Kozurkova, M.; Hamulakova, S.; Gazova, Z.; Paulikova, H. and Kristian, P. (**2011**) *Neuroactive Multifunctional Tacrine Congeners with Cholinesterase, Anti-Amyloid Aggregation and Neuroprotective Properties*. Pharmaceuticals, **4**(2):382-418.

[149] Hallivel, J. V. and Grove, E. A. (**1989**) *9-Amino-1,2,3,4-tetrahydroacridine (THA) blocks agonist-induced potassium conductance in rat hippocampal neurones*. European Journal of Pharmacology, **163**(2-3):369-372.

[150] Drukarch, B.; Leysen, J. E. and Stoof, J. C. (**1988**) *Further analysis of the neuropharmacological profile of 9-amino-1,2,3,4-tetrahydroacridine (THA), an alleged drug in the treatment of Alzheimer's disease*. Life Sciences, **42**(9):1011-1017.

[151] Antunes-Madeira, M. C.; Videira, R. A.; Klüppel, M. L. W. and Madeira, V. M. C. (**1995**) *Amiodarone effects on membrane organization evaluated by fluorescence polarization*. International Journal of Cardiology, **48**(3):211-218.

[152] Wallace, D. C. (**1999**) *Mitochondrial diseases in man and mouse*. Science, **283**(5407):1482-1488.

[153] Kagan, V. E.; Borisenko, G. G.; Tyurina, Y. Y.; Tyurin, V. A.; Jiang, J.; Potapovich, A. I.; Amoscato, A. A. and Fujji, Y. (**2004**) *Oxidative lipidomics of apoptosis: redox catalytic interations of cytochrome c with cardiolipin and phosphatidylserine*. Free Radical Biology and Medicine, **37**(12):1963-1985.

[154] Petrosillo, G.; Casanova, G.; Matera, M.; Ruggiero, F. M. and Paradies. G. (**2006**) *Interaction of peroxidized cardiolipin with rat-heart mitochondrial membranes: induction of permeability transition and cytochrome c release*. FEBS Letters, **580**(27):6311-6316.

[155] Maciel, E.; Domingues, P.; Marques, D.; Simoes, C.; Reis, A.; Oliveira, M. M.; Videira, R. A.; Peixoto, F. and Domingues, M. R. M. (**2011**) *Cardiolipin and oxidative stress: Identification of new short chain oxidation products of cardiolipin in in vitro analysis and in nephrotoxic drug-induced disturbances in rat kidney tissue*. International Journal of Mass Spectrometry, **301**(1-3):62-73.

[156] Ellman, G. L.; Courtney, K. D.; Andres, B. Jr. and Featherstone, R. M. (**1961**) *A new and rapid colorimetric determination of acetylcholinesterase activity*. Biochemical Pharmacology, **7**:88-95.

[157] Gornall, A. G.; Bardawill, C. and David, M. M. (**1949**). *Determination of serum proteins by means of the biuret reaction*. Journal of Biological Chemistry, **177**(2):751-756.

[158] Monteiro, P.; Duarte, A. I.; Moreno, A.; Gonçalves, L. M. and Providência, L. A. (**2003**) *Carvedilol improves energy production during acute global myocardial ischaemia*. European Journal of Pharmacology, **482**(1-3):245-253.

[159] Vilela, S. M. F.; Santos, D. J. S. L.; Felix, L.; Almeida, J. M.; Antunes, L. and Peixoto, F. (**2009**) *Are fentanyl and remifentanil safe opioids for rat brain mitochondrial bioenergetics?* Mitochondrion, **9**(4):247-253.

[160] Madeira, V. M. C.; Antunes-Madeira, M. C. and Carvalho, A. P. (**1974**) *Activation energies of the ATPase activity of sarcoplasmic reticulum*. Biochemical and Biophysical Research Communications, **58**(4):897-904.

[161] Bartlett, M. E. and Lewis, D. H. (**1970**) *Spectrophotometric determination of phosphate esters in the presence and absence of orthophosphate*. Analytical Biochemistry, **36**(1):159-167.

[162] Hsu, F. -F. and Turk, J. (**2005**) *Studies on Phosphatidylserine by Tandem Quadrupole and Multiple Stage Quadrupole Ion-Trap Mass Spectrometry with Electrospray Ionization: Structural Characterization and the Fragmentation Processes*. Journal of the American Society for Mass Spectrometry, **16**(9):1510-1522.